This is to certify that the

dissertation entitled

Measuring and Modeling the Effect of Time and Temperature on Removal Torque and Sealing Force of a Continuous Thread Closure

presented by

Supachai Pisuchpen

has been accepted towards fulfillment
of the requirements for

Ph.D. degree in Packaging

Hugh E. Lockhart
Major professor

Date January 2, 2003

MEASURING AND MODELING THE EFFECT OF TIME AND TEMPERATURE ON REMOVAL TORQUE AND SEALING FORCE OF A CONTINUOUS THREAD CLOSURE

By

Supachai Pisuchpen

A DISSERTATION

Submitted to
Michigan State University
in partial fulfillment of the requirements
for the degree of

DOCTOR OF PHILOSOPHY

School of Packaging

2002

ABSTRACT

MEASURING AND MODELING THE EFFECT OF TIME AND TEMPERATURE ON REMOVAL TORQUE AND SEALING FORCE OF A CONTINUOUS THREAD CLOSURE

By

Supachai Pisuchpen

A new technique for measuring the sealing force of a container-closure system was developed by employing a strain gage based transducer. The sealing force is considered a direct indicator for monitoring the mechanical seal integrity of the container-closure systems. A sealing force measuring device and a torque meter were used to investigate the effect of environmental conditions on the relaxation behavior of a 28-400 closure system. The responses from both devices during storage over time were transformed to the percent (%) force retention (FRT) and percent (%) torque retention (TRT) and used to analyze the effect. The high temperature and relative humidity of tropical conditions showed significant effect on the relaxation of the systems studied. It was found that the % TRT over time data were less consistent than the % FRT due to the nature of torque measurement and effect of environmental conditions. The % TRT data were higher than the % FRT indicating less relaxation of torque than of force. Therefore, using the removal torque or % TRT may be misleading in the interpretation of the seal integrity of the container-closure systems. The apparent

seal integrity is less when measured by force retention. Mathematical modeling of the relaxation behavior of the systems revealed that the theoretical models derived from spring and dashpot are not applicable. Empirical models using the curve fitting techniques were then applied and excellent agreement with the experimental data was found. The mathematical models developed were extended to long-term prediction for 3 years; the predicted values of the % FRT and % TRT were in the acceptable range for agreement among the models.

ACKNOWLEDGMENTS

I would like to express my appreciation to my research guidance committee: Dr. Hugh Lockhart, my major advisor, for his support, advice and guidance throughout my graduate program. He is the model for students in teaching and researching. His help in providing financial support and giving me the opportunities to work in many projects are a major contribution to my success. I thank Dr. Gary Burgess for his valuable advice and support. He always comes up with thoughtful solutions for students all the time. I am grateful to Dr. Gary Cloud for his great help and guidance in introducing me to the area of experimental mechanics. I also thank Dr. Robert Clarke for his encouragement, guidance, and constant greeting which is a resource of comfort during my study in the School of Packaging.

I thank Bob Hurwitz, a best friend, who always inspires me and supports me. Your friendship will always be with me and my family.

I would like to acknowledge the Thai government for the scholarship and support given throughout my study at Michigan State University.

I heartily thank my parents for their support and encouragement toward education.

Finally and most importantly, my beloved wife: Wariya, a special thanks is given to her, for her strength, support, understanding, and friendship. She is always there with me during hard times. The appreciation is beyond words and will never fade away.

TABLE OF CONTENTS

LIST OF TABLES

LIST OF FIGURES

LIST OF ABBREVIATIONS

TIP	=	Torque Inch Pounds
AT	=	Application Torque
RT	=	Removal Torque
% FRT	=	Percent Force Retention
% TRT	=	Percent Torque Retention
PE	=	Polyethylene
PET	=	Polyethylene Terephthalate
HDPE	=	High-Density Polyethylene
PP	=	Polypropylene
Tg	=	Glass Transition Temperature

1. INTRODUCTION

The seal integrity of a container-closure system is important, not only for packaging appearance but for consumer satisfaction and safety as well. Today, consumers expect effective packaging as well as product quality. The expectations of container-closure systems especially for pharmaceuticals focus on functional performance of the seal. The consumer would avoid buying products having an improper seal. Indications of an improper seal can be shown in detectable leakage, tampering, contamination, and ergonomic factors such as ease of opening and closing. Therefore, finding ways to maintain and monitor the seal integrity of the container-closure systems is necessary.

The use of plastics in container-closure systems has become the predominant choice in packaging applications because of inherent advantages over other materials. Plastics offer good barrier and mechanical properties, flexibility in forming different shapes and an economical advantage. A major drawback is that plastic material properties are highly dependent on time and temperature. This strong time and temperature sensitivity of plastic properties is a consequence of the viscoelastic nature of polymeric materials. This implies that plastics exhibit combined viscous and elastic behavior. A good example of these properties is that if a weight is suspended from a piece of plastic, the strain or elongation will not be constant but will increase slowly with time. In a container-closure system, the effect of viscoelastic properties shows in the stress relaxation behavior which is primarily suspected as a major cause of loss of seal integrity. Numerous studies have been conducted to research this behavior by

using the removal torque as the indicator but the reliability of removal torque for indicating loss of seal integrity has not been established. One reason is that the characteristics of removal torque are fairly complex; variation from one measure to another is usually large. There are other factors involved not related to the seal integrity, such as adhesion, threads and dimensions mismatch, closure misalignment and human factor. However, a positive aspect of the removal torque testing is that it is inexpensive, easy and quick. This method is well known and commonly used as the mechanical seal indicator throughout industry.

The removal torque can be precisely defined as the unscrewing moment needed to start the various surfaces in the system sliding against friction forces (Figure 1).

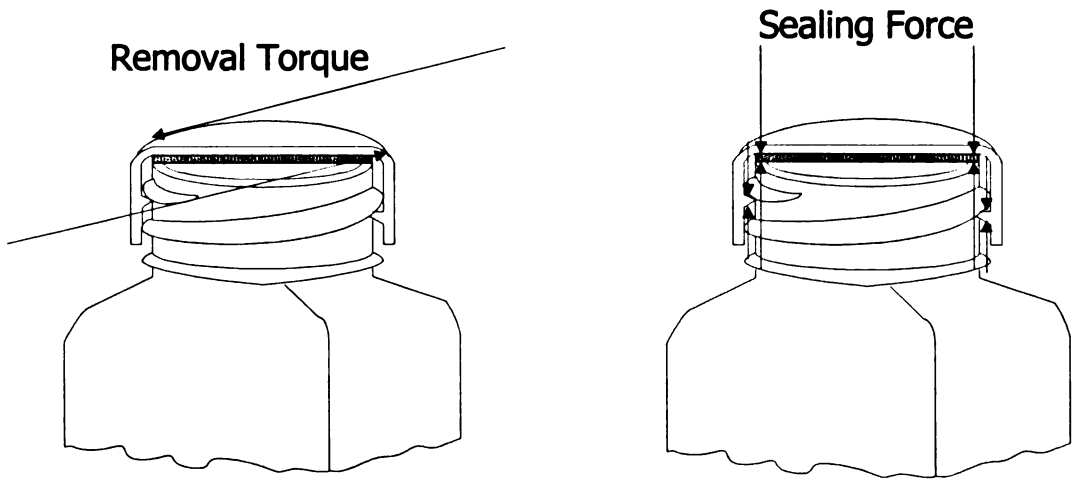

Figure 1 Comparison Between Removal Torque and Sealing Force

A previous study (Pisuchpen, 2000) explained how the seal mechanism in the container-closure system works. Torque applied to a container-closure system is actually translated to a sealing force which is the compression force or axial force acting at the liner and thread interface. The radial force that is

generated from factors not related to the seal integrity is excluded from the system. Therefore, the sealing force keeping all interfaces in contact can be considered as a direct indicator for seal integrity of a container-closure system. Assessing and comparing both indicators through the relaxation behavior of the container-closure system offer a better understanding of the seal integrity of the system. Although the sealing force seems to be an alternative indicator, there is no easy way to measure this force directly in the system yet (Pisuchpen, 2000). This indicates that research in this area is needed. In addition, consideration should be given to the prediction of relaxation behavior of container-closure systems as well since the sealing force associated with the viscoelastic properties is a function of time. The economical way to predict this long-term behavior of the system is by using mathematical modeling.

Objectives

One objective of this research was to develop a technique for measuring the sealing force of container-closure system. This will provide another way to verify and monitor the seal integrity of the system other than using the removal torque. A second objective was to apply a technique developed by this research to investigate the effect of time and temperature on the relaxation behavior of container-closure systems. The final objective was to establish mathematical models for long-term prediction of the relaxation behavior of container-closure systems.

2. LITERATURE REVIEW

The research began with surveying literature in this area in order to gather the information for experimental design. The concept of sealing force is certainly not new. In 1956, Robert V. McCarthy (McCarthy, 1956) conducted research in determining performance of plastic screw thread caps on glass bottles. He developed a measuring device using a strain gage to determine the sealing force of glass bottle-plastic closure systems over a short period of time (20 min.) at room temperature. Typical relaxation curves were found by using his measuring device. One limitation of his research is that the measuring device was not designed to account for the relaxation behavior of the liner which is one of the most important factors in providing the seal integrity of the system. The empirical model for sealing force decay was also developed from various exponential relationships; the calculated values from the model compared favorably with the experimental data. After 1956, there is no published research conducted in the sealing force area. One reason is that other researches followed the ASTM D3198 test method which recommends using the removal torque as a guideline for measurement. In 1992, Dr. Hugh E. Lockhart (Lockhart, 1992) studied the torque loss over time for a 28 mm metal closure on plastic bottle which was subjected to various temperatures (5°C, 23°C and 43°C) for 12 weeks. He concluded that temperature, time and application torque all have a statistically significant effect on the level of removal torque. However, these effects are of little practical importance except for the torque losses at 43°C. This study

indicates that high temperature significantly increases the torque loss of the system through the relaxation behavior. The next publication in the relaxation of container-closure system is in 1993 by Dr. Gerald Greenway (Greenway, 1993). He conducted a short-term study (10 days) of closure torque decay for 24 mm HDPE closures with paper pulp liner on PET bottles. The container-closure systems were stored at room temperature and tested for ten days. He concluded that the removal torque decay process is a logarithmic function. It decreases initially at a very rapid rate and continues to gradually decrease at slower and slower rates. A plot of removal torque vs log of time shows a good linear relationship. This study shows a typical relaxation curve obtained from using the removal torque and the semi log can be used to describe the relaxation behavior. The relaxation rate increases as the application toque increases. In 1999, Dr. Ching-Sung Lai and Dr. Gerald Greenway (Lai and Greenway, 1999) published a study on the effect of time on closure removal torque. A PP closure with vinyl liner on a PET bottle were studied at room temperature. It was found that a plot of removal torque vs log of time exhibits an "S" shape response. The removal torque first starts increasing until reaching the maximum level after around 10 days storage and then changes to slowly decrease over time. They believed that this phenomenon results from the interaction between the liner and the land area of the container, developing an adhesion effect. They said that the adhesion becomes stronger at the first period of storage time and then, as the storage time increases beyond 10 days, the adhesion becomes weaker causing a reduction of removal torque. This study is a good example of the uncertainty of using the

removal torque technique because the result suggests that the removal toque can be easily affected by other factors which, in turn, can affect the interpretation of the seal integrity. Adhesion is an uncontrolled factor which may or may not occur in the system. Therefore, the increase of the removal torque does not absolutely tell that the seal integrity is intact. In fact, the sealing force of the system initially decreases at a rapid rate and then continues to decrease at slower and slower rate. This is the actual relaxation behavior that could be obtained if using the sealing force as the indicator.

After surveying the experimental stress analysis techniques that can be applied to the research, it was found that the transducer strain gage technique is considered as the best tool for this research. The bonded resistance strain gage consists of a filament of very thin metallic foil mounted on plastic backing sheet (Figure 2). The filament material has a linear relation between the electronic resistance and the strain. The strain gage is widely used in measuring the strain on structural members for stress analysis. In addition to the direct determination of strain, the strain gage is employed as the sensing element for measuring load, force, torque, displacement and other physical variables. Good examples of the application are the electronic torque meter and the load cell of the Instron machine.

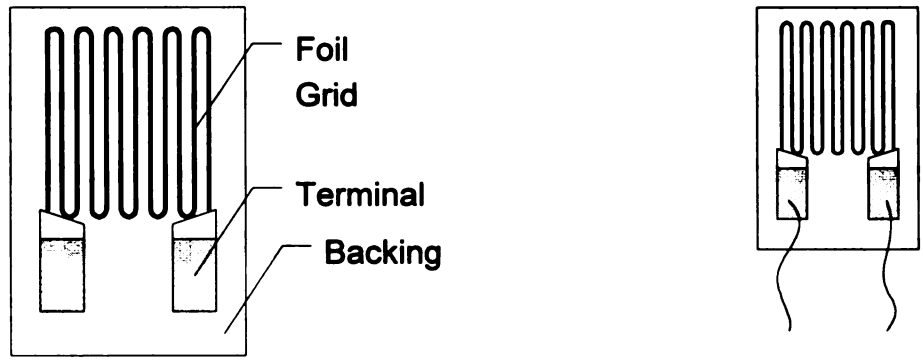

Figure 2 General Purpose Strain Gage

From simplicity, modeling the relaxation behavior of the container-closure system in this research is confined to the linear viscoelastic behavior, one-dimensional situation since non-linearity adds to the complexity of the problem. Such a linear viscoelastic behavior is sometimes a reasonable approximation for real materials, such as polymers, metals and ceramics at high temperatures (Dowling, 1993). The term linear refers to the mechanical response in which the ratio of the overall stress to strain is a function of time only and is independent of the magnitudes of the stress or strain. As a result of this situation, the stress-strain relationship for any given value of time is a straight line. The linear viscoelastic behavior of solid polymers can be observed under limited conditions which are homogeneous, isotropic, amorphous under small strains and at temperature close to or above Tg (Ferry, 1970). In spite of its limited use, the theory of linear viscoelasticity provides a useful starting point for numerous applications. To aid the analysis of viscoelastic response, mechanical models using spring and dashpot are usually introduced to represent the extremes of the mechanical response spectrum as shown in Figure 3 (Aklonis, 1972). The spring represents a linear elastic or Hookean solid. It responds instantaneously to

reach an equilibrium strain ε as long as the stress σ is maintained constant. Sudden removal of the stress causes in instantaneous recovery of the strain as well. It has a constant modulus that is independent of the strain rate or the speed of testing. Thus, the stress is a function of the strain only. In contrast to the spring, a linear viscous or Newtonian fluid is represented by a dashpot which is a piston moving in a cylinder of Newtonian fluid. A dashpot has no modulus but the shear stress is proportional to the speed of testing (strain rate $\dot{\gamma}$). In other words, the strain is a linear function of time at an applied external stress. Thus, the strain rate determines whether the deformation is elastic (spring) or viscous (dashpot). If a constant stress τ is suddenly applied to the dashpot, the strain γ increases linearly with time t as shown in Figure 3.

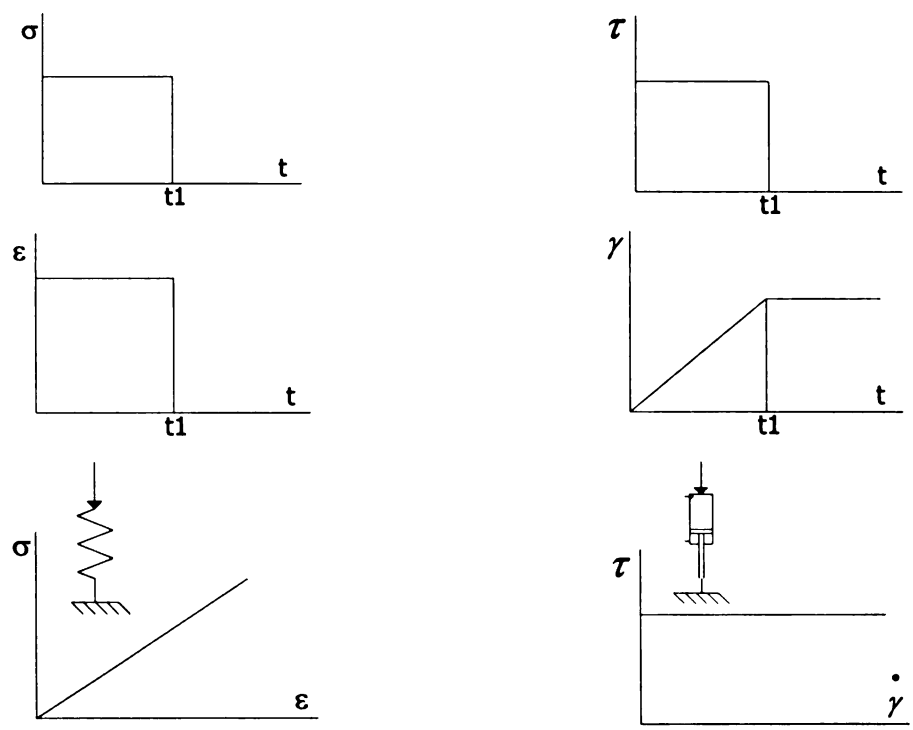

Figure 3 Pure Elastic Response (Spring) and Pure Viscous Response (Dashpot)

However, no real material shows either ideal elastic behavior or pure viscous flow. Viscoelastic materials such as polymers combine the characteristics of both elastic and viscous materials. In a polymer structure, the spring can be viewed as the contractile polymer chains and the dashpot is descriptive of the motion of chains caused by adjacent chains (Arridge, 1985). The mathematical expression used to describe the experimentally determined stress-strain response is known as the constitutive equation. Each constitutive equation is an idealization or mathematical abstraction of a measured stress-strain response of a real material. It is important to remember that each constitutive equation is only a model adopted to describe the most significant and idealized mechanical behavior of the material. It represents a simplification of the real stress-strain behavior of the specific material. It has significant restrictions and limitations for its general applicability. A simple constitutive relation for the behavior of a linear viscoelastic solid can be obtained by combining the Hookean solid (spring) and Newtonian fluid (dashpot). The mechanical response is described by Hooke's law ($\sigma_s = E.\varepsilon$) and the response of a fluid to a stress is given by $\sigma_d = \eta \frac{d\varepsilon}{dt}$. A possible formulation of linear viscoelastic behavior combines these equations; thus, the total stress supported by the parallel arrangement of the spring and dashpot is

$$\sigma_t = \sigma_s + \sigma_d = E.\varepsilon + \eta \frac{d\varepsilon}{dt} \qquad (1)$$

This makes the simplest possible assumption that the stresses related to the strain and strain rate are additive (Rosen, 1993). The equation represents

the Kelvin-Voight model, one of the simple models for linear viscoelastic behavior. The Kelvin-Voight model will be used as the basis model for relaxation behavior of the container-closure system. It represents the following characteristics of solid materials during loading. The spring and dashpot always remain parallel. This means that the strain in each element is the same. The total stress supported by the model is the sum of the stresses in the spring and dashpot. From Equation (1), if the strain is set to be constant, the solution for stress relaxation can be obtained. The viscoelastic behavior of material, in general, may be investigated by the use of mechanical models which consist of finite networks of springs and dashpots. Several springs and dahpots can be arranged in many ways; the application of the Boltzmann superposition principle which is of great use in linear viscoelasticity is recommended (Arridge, 1985).

3. THEORETICAL AND TECHNIQUE DEVELOPMENT

The relaxation behavior in a container-closure system reflects in the decay of sealing force over time that results from subjecting it to a constant strain. This can be measured through the instrumentation on the actual container-closure system. The basic concept for instrumentation is that the stress and strain are related to each other by a fundamental relation, the modulus of elasticity, for linearly elastic materials (Dally, 1993). The response by the instrumentation to an applied load is normally presented in strain. Strain is a fundamental physical quantity and stress or force (sealing force in this case) on the instrumentation is a derived quantity. Selection of an appropriate measuring technique for a particular application of the research is very important. Experimental stress analysis techniques: strain gage and photoelasticity were considered for this application. After careful consideration of complexity, physical size or shape limitations, operating environment, cost constraints and test limitations, the bonded resistance strain gage was finally selected to develop a sealing force measuring device. The strain gage is not used to measure strain, but it is to give a measurement of sealing force. In application the strain gage is called a transducer, which is an electromechanical device converting a mechanical change into an electrical signal. The basic concept of transducer design is a common principle. A spring element, which simply is a piece of suitable metal designed to deform elastically and linearly over the desired loading range, has strain gages mounted to it. The deformation on the spring element from the

applied load is then converted into strain output. It only needs an accurate calibration against the corresponding forces before use.

A sealing force measuring device using the transducer strain gage technique constructed according to the second design in this chapter was used in the preliminary study in order to compare the theoretical sealing force with an experimental sealing force. The purpose of the experiment was to evaluate the torque-friction model developed from a previous study and determine the potential of modification of the model to describe the relaxation behavior. The 28-400 HDPE containers and PP closures with PE foam liner were used in the preliminary study. The theoretical sealing force based on the torque-friction model (Equations (2) and (3)) assumes that the container-closure system is a rigid body. The torque-friction model was then developed from the equations of equilibrium for all forces acting on the system. The values of parameters (p, μ_t, μ_l, $\bar{r_t}$ and $\bar{r_l}$) used in equations below were taken from a previous study (Pisuchpen, 2000).

$$T = F_v . \left[\bar{r_t} \left[\frac{\cos\theta.p + 2.\pi.\mu_t.\bar{r_t}}{\cos\theta.2.\pi.\bar{r_t} - \mu_t.p} \right] + \mu_l.\bar{r_l} \right] \qquad (2)$$

$$T' = F_v . \left[\bar{r_t} \left[\frac{2.\pi.\mu_t.\bar{r_t} - \cos\theta.p}{\cos\theta.2.\pi.\bar{r_t} + \mu_t.p} \right] + \mu_l.\bar{r_l} \right] \qquad (3)$$

where T, T' = Application torque (TIP), Removal torque (TIP)

F_v = Sealing force (lb)

p = Thread pitch (inch) = 0.167 (6 threads/inch)

μ_t = Coefficient of friction at thread interface HDPE-PP = 0.17

μ_l = Coefficient of friction at liner interface HDPE-PE foam = 0.50

$\overline{r_t}$ and $\overline{r_l}$ = Mean radius of the thread contact (inch) = 0.5131" and liner contact = 0.4534"

θ = Contact angle between container threads and closure threads (degree) = 42.07°

There are 2 special cases in Equations (2) and (3) involving the design of a sealing force measuring device that should be considered.

1. $\mu_l \neq 0$. In this case, a liner is sliding on the bottle finish, while torque is applied to a closure. Thus, the static coefficient of friction at liner interface should be taken into the account. A closure in this case is considered as a glued attachment liner type, in which a liner is attached to the top panel of the closure by glue. The liner rotates with the closure when torque is applied. A system of HDPE-PP using PE foam liner is used as an example for this case and the solutions of Equations (2) and (3) are:

$$T = 0.3725 F_v \quad \text{or} \quad F_v = 2.6846\, T \tag{4}$$

$$T' = 0.3166\, F_v \quad \text{or} \quad F_v = 3.1586\, T' \tag{5}$$

If the application torque, T and the removal torque, T' are 14 and 8 TIP, the sealing forces will be 37.58 and 25.27 lb respectively.

2. $\mu_l = 0$. A liner is not sliding against a bottle finish but stays at the original position, while torque is applied to a closure. The static coefficient of friction at the liner interface is not involved in the equations in this case. It is assumed that

the friction generated between the center of the top panel of the closure and of the liner is negligible. This is a non-glued attachment liner type. The sealing force measuring device developed in this research is based on this case. A liner stays still on a container finish while the center of the shell is spinning against the lubricated "bump" disk. The static coefficient of friction at liner interface with the land area of container finish is therefore neglected. Only the coefficient of friction at thread interface is used in the equations. Therefore, when the rest of the parameters are substituted in Equations (2) and (3), the equations reduce to

$$T = 0.1458F_v \quad \text{or} \quad F_v = 6.8587T \tag{6}$$

$$T' = 0.090F_v \quad \text{or} \quad F_v = 11.11T' \tag{7}$$

Again, if the application torque, T and the removal torque, T' are 14 and 8 TIP, the sealing forces will be 96.02 and 88.88 lb respectively. Clearly, the sealing force increases 2.5-3.5 times compared with $\mu_l \neq 0$ case. This is due to the mechanical advantage; torque is efficiently translated into sealing force without loss from friction at the liner interface. Both special cases point out an interesting issue in the relationship among torque, sealing force and the static coefficient of friction at liner interface. Theoretically, the most effective way to achieve the highest sealing force is by approaching $\mu_l = 0$.

Equations (6) and (7) give a theoretical sealing force for a system which can be used to compare with the results from the experiment. The equations indicate a linear relationship between the application torque (removal torque) and the sealing force. To investigate the accuracy of Equations (6) and (7), a comparison between the experimental sealing force and theoretical sealing force

was conducted and the result is shown in Table 1. In the experiment, hand-applied application torque (T) of 14 TIP was used on the sealing force measuring device having PP closure and PE foam liner installed. The initial sealing force was recorded. The immediate removal torque (T') and the sealing force were then measured after storage for 15 min at room temperature. The application torque and removal torque were used to calculate the theoretical sealing force and the results were compared with the experimental sealing force from the sealing measuring device.

Table 1 Comparison between Experimental Sealing Force and Theoretical Sealing Force

Sample	Torque TIP	Experimental Sealing force, lb	Theoretical Sealing force, lb	% Difference (from experiment)
1	T= 14.0	110.0	96.0	13
	T'= 9.0	61.8	100.0	62
2	T= 13.9	107.1	95.3	11
	T'= 9.2	58.3	102.2	75

A comparison shows that Equation (6) for application torque estimates the sealing forces close to those experimentally measured, whereas the Equation (7) for removal torque gives a theoretical sealing force higher than the experimental results by about 70%. The difference between theoretical and experimental sealing force may result from the coefficient of friction at thread interface, which has a broad range of values used in models. A previous study found that the coefficient of friction for the container-closure systems can vary up to 35% (Pisuchpen, 2000); this can in turn cause the variation of the calculated sealing force. In addition, the mathematical model assumes that the container-closure

system is a rigid body; there is no deformation and change in the boundary condition of the system. The actual system, however, is made of plastic a non-rigid structure. It is a highly stressed system with a very complex shape and several stress concentrations. The basic deformation is usually elastic but there are always portions of the container-closure system that deform plastically; for example, a liner and the thread roots which can alter the geometry of the system. Moreover, the viscoelastic properties of the system made of plastic also add to the complexity of the system due to the time dependence of these properties. Therefore, the boundary condition of the system changes over time. This contributes to a large difference between the theoretical results from the removal torque and the experimental results.

Besides, from a work and energy concept, the torque-friction model (Equation (2) and (3)) only describes action and reaction force and torque on the system. It does not describe the various forms of heat and strain energy introduced to the system by the input work done on the system. The torque-friction model suggests that the input work ends up as friction loss but actually portions of the input work end up as liner and thread deformation also. The "true" relationship between the input torque and the sealing force, therefore, must take these outputs into account.

The serious limitation of the torque-friction model developed from previous research suggests that it is not applicable to use as a basic model for describing the relaxation behavior of the container-closure system. It is necessary to turn to

other theories that can be applied in the research to explain the viscoelastic properties of the system better.

3.1 Sealing Force Measuring Device Design

The development started with a simple design using two steel tubes having circular thin flat plate 1/32" thick at one end. The outer tube is hollow. One end is closed and the other end has circular thin flat plate. The inner tube having a radius end for low friction and the other end with circular thin flat plate is solid. A strain gage is attached at the middle of the outer tube in the axial direction which is the location of average strain. The assembly drawing of the design is shown in Figure 4. In use, both tubes are inserted into a plastic closure; the (upper) plate of the outer tube has a clearance of 1/32" from the (lower) plate of the inner tube. A liner is placed in between the lower plate and the land area of container finish. When torque is applied on a closure, torque is then translated into a sealing force by pushing the liner against the land area of the container finish. The reaction force from container finish transfers to a liner, lower plate of inner tube and radius end where inner tube and outer tube are in contact. This radius end then will push against the outer tube end in which the upper plate is restrained by compression of the closure top panel and the engagement of closure threads and container threads as a result of axial tension force on the outer tube. This axial tension force which is a sealing force will be computed from strain measured by the strain gage.

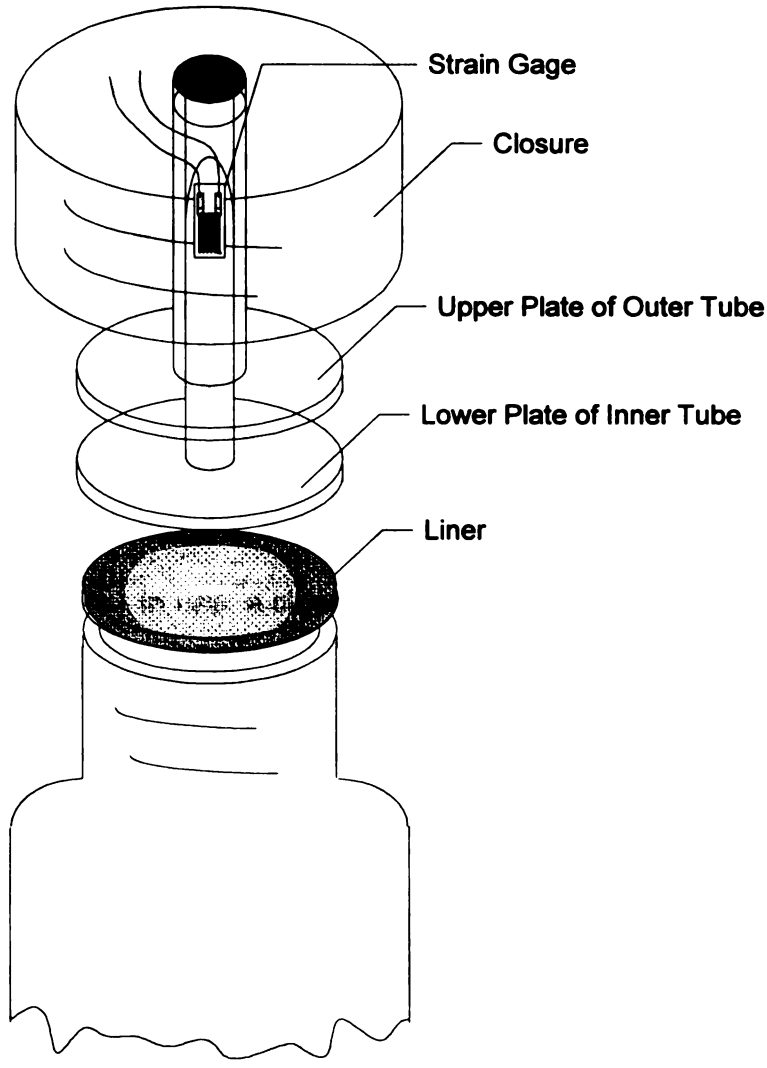

Figure 4 First Design of Sealing Force Measuring Device

It was found that this first design shows inconsistent measuring results; a tilting effect from improper thread engagement yielded a non-uniform sealing force around the contact area. It did not produce a typical relaxation curve. This is because the first design is limited by only small free headspace at the top panel of the closure. This free headspace controls the thread engagement of the system.

To solve a problem of limitation by the small headspace of closure, a second design was tried by assuming that dome bending near the periphery of the dome is small and can be neglected. Hence the top panel of the closure can be removed and this gives more space to work with. The second design consists of a tubular shell with one closed end, a circular flat disk 0.1" thick with a "bump" at the center and a retainer as shown in Figure 5. A circular flat disk is used as a mechanism to transfer a reaction force from the container-closure system to a strain gage which is installed at the center of the closed end shell where the average strain occurs. In use, a closure without its top panel is glued into the tubular shell and a removed top panel is glued on the flat surface side of a "bump" disk. A liner is inserted in between the disk and the land area of container finish. As torque is applied to the closure, the shell moving downward is pushed by a bump on the disk at the center of the closed end shell where the strain gage is mounted. The strain generated will be picked up by the strain gage and the reaction force which generates the strain is the sealing force of the container-closure system.

The next step is to estimate the thickness of the top panel of closed end shell needed to keep it in the elastic range when loaded. Thus, the strain generated at the center of the top panel of the tubular shell must be estimated. The assumption is that the closed end shell in circular shape stretches only when a force F is exerted at the center and the rim of the disk is completely restrained (boundary condition) (Figure 6a). Figure 6b shows that the same disk is pushed upward at the center by force F into a shape of spherical section while the base

is held at the original radius. Force F is applied by the "bump" disk as torque is applied.

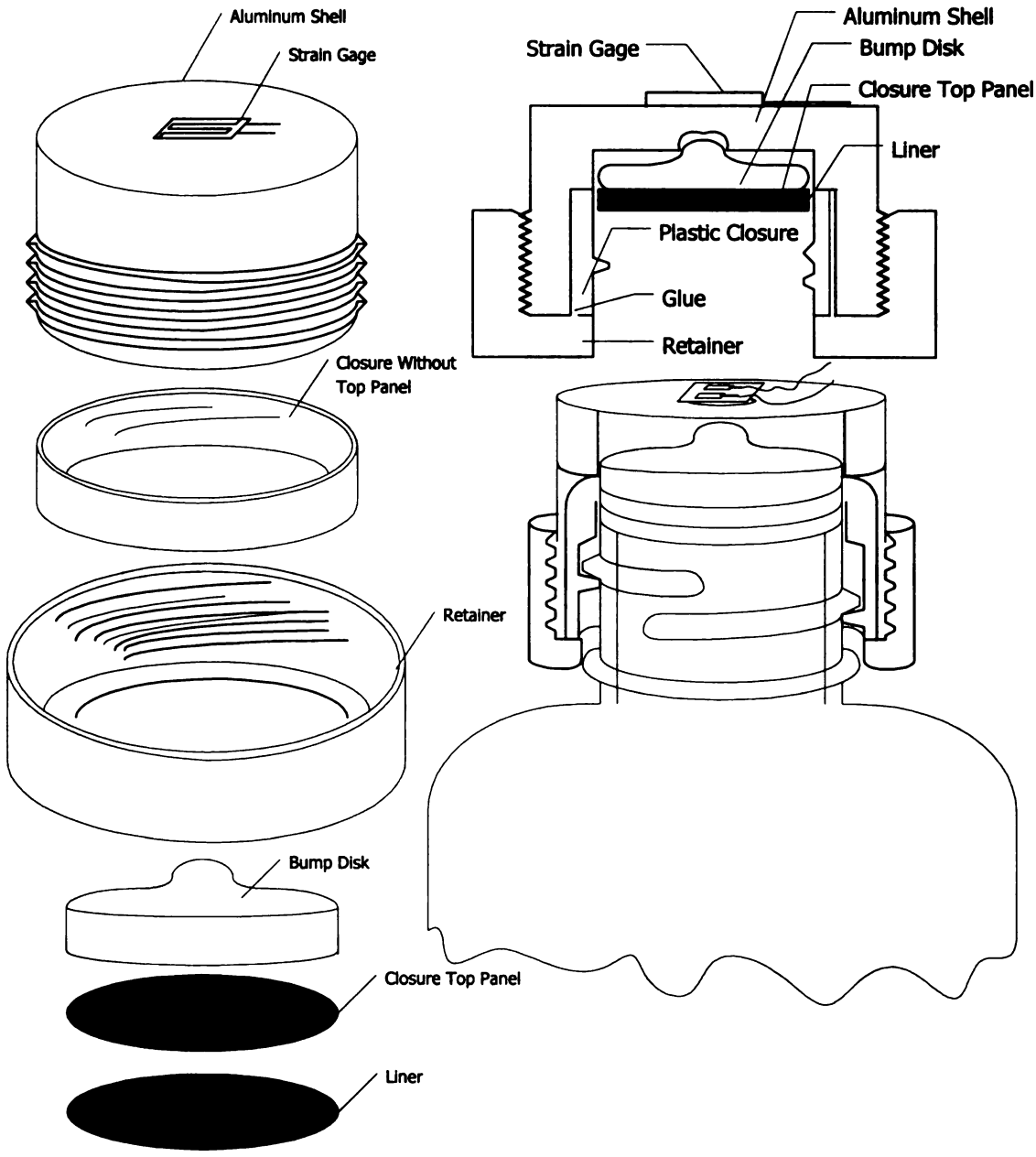

Figure 5 Second Design of Sealing Force Measuring Device

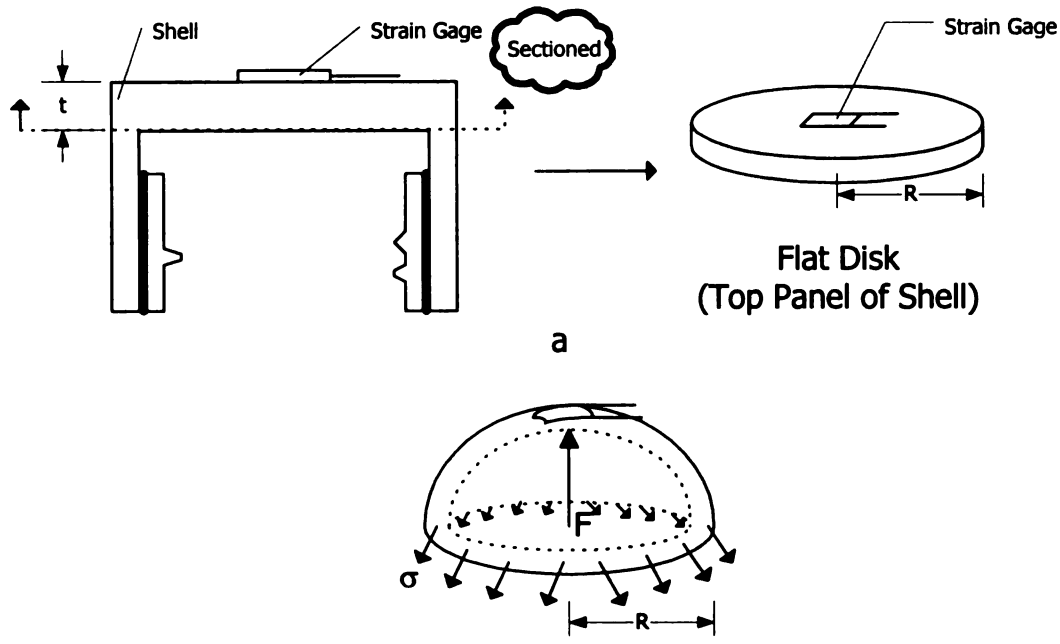

Figure 6 3D of Top Panel of Tubular Shell for Second Design

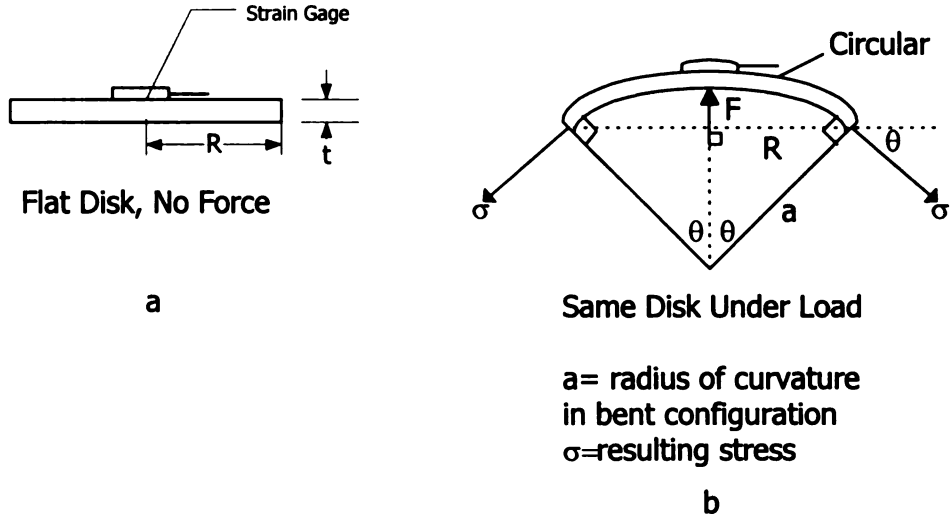

Figure 7 2D of Top Panel of Tubular Shell for Second Design

Figure 7 shows in two-dimensions the top panel of shell under loading. Because the perimeter of the disk is essentially held fixed by the shell part of the closure, the material stretches in the radial direction which goes from length 2R to length 2aθ. Thus, strain in the radial direction produces the equation.

$$\varepsilon = \frac{2a\theta - 2R}{2R} = \frac{a}{R}\theta - 1 \quad But \quad \sin\theta = \frac{R}{a} \tag{8}$$

$$\varepsilon = \frac{a}{R}\sin^{-1}\frac{R}{a} - 1 \tag{9}$$

From a series expansion, $\sin^{-1}x = x+x^3/6+3x^5/40+....$

So $$\varepsilon = \frac{a}{R}\left[\frac{R}{a} + \frac{R^3}{6a^3} + \frac{3}{40}\frac{R^5}{a^5} + ...\right] - 1 = \frac{R^2}{6a^2} + \frac{3}{40}\frac{R^4}{a^4} + ... \tag{10}$$

In Equation (9) "a" is large compared to R, so all higher order terms can be dropped as a result to give Equation (11)

$$\varepsilon = \frac{R^2}{6a^2} \tag{11}$$

Equation (11) is a resulting strain based on a geometric relationship. The next step is to get the equation based on material properties which can be obtained from the force balance in the vertical direction.

$$\sum F_{vertical} = 0, \qquad F = \sigma(2\pi Rt).\sin\theta \tag{12}$$

where $2\pi Rt$ = area of circular base edge

Therefore, $$\sigma = \frac{F}{2\pi Rt\ \sin\theta} = \frac{F}{2\pi Rt\left(\frac{R}{a}\right)} = \frac{Fa}{2\pi R^2 t} \tag{13}$$

Equation (13) is a resulting stress and in the elastic range, $\sigma = E\varepsilon$. Then, substitute this relation and geometry relation from Equation (11) into Equation (13).

$$\frac{Fa}{2\pi R^2 t} = E\frac{R^2}{6a^2} \tag{14}$$

Thus
$$a = \left(\frac{\pi}{3}\frac{ER^4 t}{F}\right)^{\frac{1}{3}} \tag{15}$$

"a" gives radius of curvature of bent shape due to force F.

Equation (11) is rearranged to get "a" which is then combined with Equation (15).

$$a = \left(\frac{\pi}{3}\frac{ER^4 t}{F}\right)^{\frac{1}{3}} = \left(\frac{R^2}{6\varepsilon}\right)^{\frac{1}{2}} \tag{16}$$

Therefore, Equation (16) can be rearranged to get F or ε in term of radius R, thickness t, Young's modulus E, and strain ε or force F.

$$F = \left(\frac{\pi}{3}6^{\frac{3}{2}}\right)ERt\varepsilon^{\frac{3}{2}} \quad \text{or} \quad \varepsilon = \left(\frac{1}{6}\left(\frac{3}{\pi}\right)^{\frac{2}{3}}\right)\left(\frac{F}{ER^t}\right)^{\frac{2}{3}} \tag{17}$$

Equation (17) is used to calculate the estimated strain developed in the top panel of the aluminum shell where a strain gage is located.

Design of top panel of aluminum shell

R = radius of top panel which is fixed at 0.5 in.

Maximum applied force F = 140 lb

E of 7075-T651 aluminum alloy = 10.3×10^6 psi (ASM, 1990)

Try thickness t = 0.1"

$$\varepsilon = \left(\frac{1}{6}\left(\frac{3}{\pi}\right)^{\frac{2}{3}}\right)\left(\frac{F}{ER^t}\right)^{\frac{2}{3}} = 0.162\left(\frac{100}{10.3x10^6 x0.5x0.1}\right)^{\frac{2}{3}} = 543.2\mu\varepsilon$$

The estimated resulting strain in the top panel of the aluminum shell is 543.2με which is in the elastic range of material (up to 7087με) [ASM, 1990]. Thus, the thickness of 0.1" is fine for designing a device.

A strain gage mounted on a measuring device is connected in the form of a half-bridge circuit. This is a common arrangement for temperature compensation which is the use of a dummy gage, identical to the active gage [Window, 1989]. The dummy gage is bonded to a stress-free piece of aluminum identical to the material bonding with the active gage. Both gages are placed close to each other so that they are subjected to the same environmental conditions. The half-bridge circuit is shown in Figure 8.

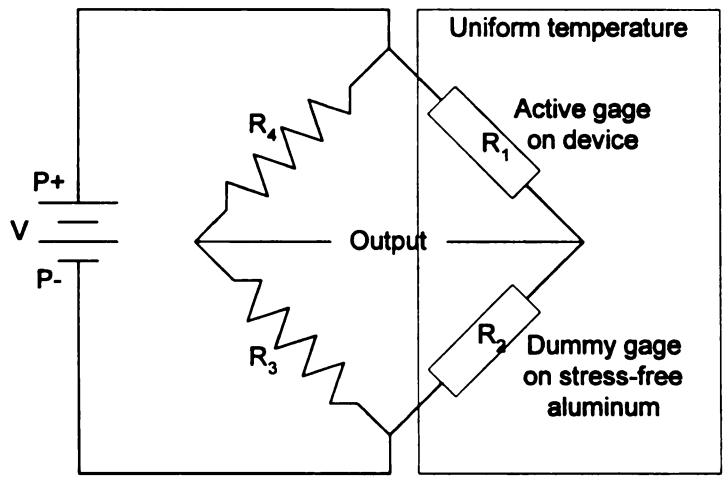

Figure 8 Temperature-Compensated Circuit (Half-Bridge)

The second design of the sealing force measuring device was used for measuring the sealing force of container-closure systems over time under

different environmental conditions. Details of construction, calibration and setup are described in the next chapter.

3.2 Theoretical Model Development

A preliminary experiment using the torque-friction model (Pisuchpen, 2000) found that the model predicted adequately only the initial sealing force from the application torque (Equation (2)). The sealing force predicted from the removal torque (Equation (3)) using the torque-friction model was overestimated. In addition, it is apparent that the equations of equilibrium for all forces acting on the system cannot describe the time dependent behaviors. This is because the torque-friction model does not account for viscoelastic properties of the materials. It was assumed that the container-closure system is a rigid body in which all parameters of the system remain constant during loading. The effects of deformation and change in shape are neglected. In fact, the mechanical behavior of the polymeric materials is strongly dependent on parameters such as time, temperature and rate of loading. This suggests that the torque-friction model is oversimplified; a more sophisticated model is necessary to study the removal torque and sealing force over time for the container-closure systems.

There has been a reasonable amount of success in using the linear viscoelastic behavior in modeling the polymeric materials. Of course, a considerable amount of experimental work and data processing has been needed to achieve this end. The theoretical model development for container-closure systems in this research deals with certain aspects of mechanical models using spring and dashpot for linear viscoelastic solids. Spring and dashpot

models are aids to visualize and develop the equations among force, deflection and time derivatives. Such models are able to explain the stress relaxation in the container-closure systems. The research employed an elementary model called Kelvin-Voight model shown in Figure 9. The reason for choosing this model to start with is that it is one of the simplest models for viscoelastic solids (Sobotka, 1984). It is composed of a spring and dashpot connected in a parallel combination and well describes some features of creep and stress relaxation in thermoplastics (Ferry, 1970). The spring is considered to represent the extension and contraction of primary bonds and angles or the entropy elasticity of randomly kinked molecules, while the dashpot represents the time-dependent sliding of main chains and flipping of side chains.

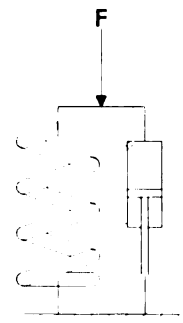

Figure 9 Kelvin-Voight Model

3.2.1 Modeling a Container-closure System

In modeling a system, distributed forces within a container-closure system were evaluated. Figure 10 shows a force diagram for the liner and threaded part of a container. In the threaded part, there are an infinite number of infinitesimal contact forces on threads which add up to force F. From the diagram, it can be simplified as forces distributed in a system. The applied sealing force F balances

with the summed forces F in which the liner arranged in series with the container neck as shown in Figure 11a. If weights and inertia of a system are ignored, the separate force diagrams are found in Figure 11b and 11c. These separate force diagrams: liner and threaded part of container neck provide flexibility in modeling the container-closure system. The liner and threaded part of container neck can be modeled separately with respect to the material properties of each part and then will be combined to a complete system later. The next parts will show modeling the liner material using different configurations of spring and dashpot.

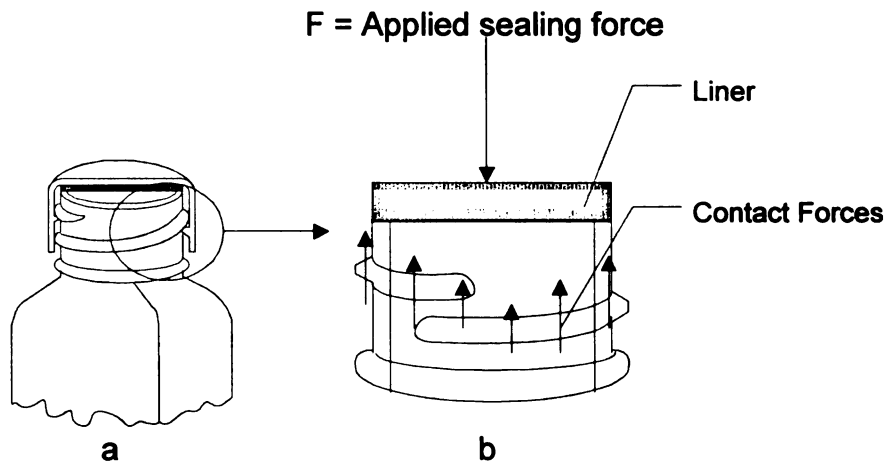

Figure 10 Force Diagram of Liner and Threaded Part of Container

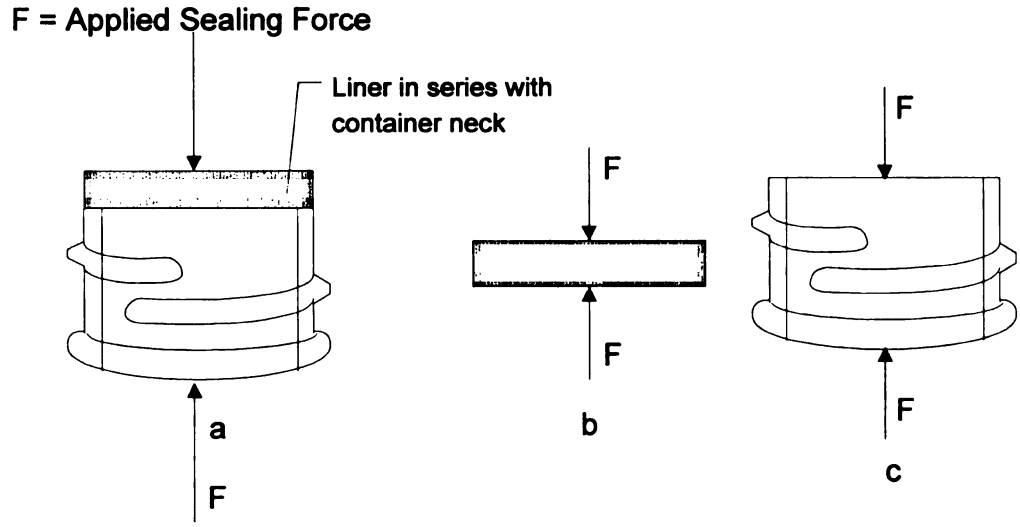

Figure 11 Separate Force Diagrams of Liner and Threaded Part of Container

3.2.2 Model A for Liner Material

The simplest model: The Kelvin-Voight model was applied for modeling the liner material as shown in Figure 12.

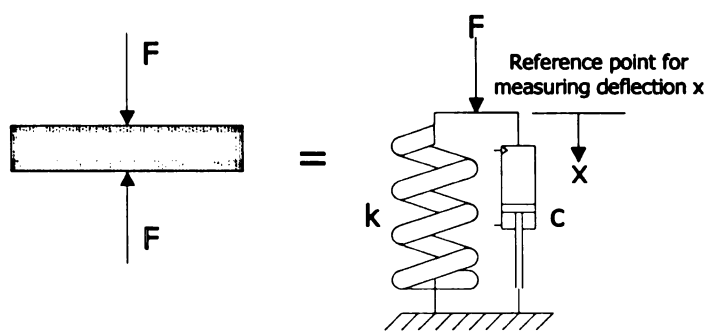

Figure 12 Liner Material in Model A (Kelvin-Voight Model)

For model A, the total force is given by

$$F = kx + c\frac{dx}{dt} \tag{18}$$

where F = Compression force or sealing force

k = Spring constant

x = Deflection

c = Damping constant

$\frac{dx}{dt}$ = Compression rate

For a liner under compression loading, there is a loading phase where the liner is compressed at a constant rate v (known). The loading phase ends at time"t_0" (also known), where the deflection is held constant at $x_0 = vt_0$ while the liner material undergoes a "relaxation phase".

Loading phase $x = vt$ at $0 \le t \le t_0$ and $\overset{o}{x} = \frac{dx}{dt} = v$

so $F = kvt + cv$ (19)

Relaxation phase $x = x_o = vt_0$ at $t_0 \le t \le \infty$ and $\overset{o}{x} = 0$

so $F = kx_0 + c(0) = kx_0 = kvt_0$ (20)

From the analysis above, a plot between force F and time t, can be generated to see the theoretical behavior of a model as shown in Figure 13.

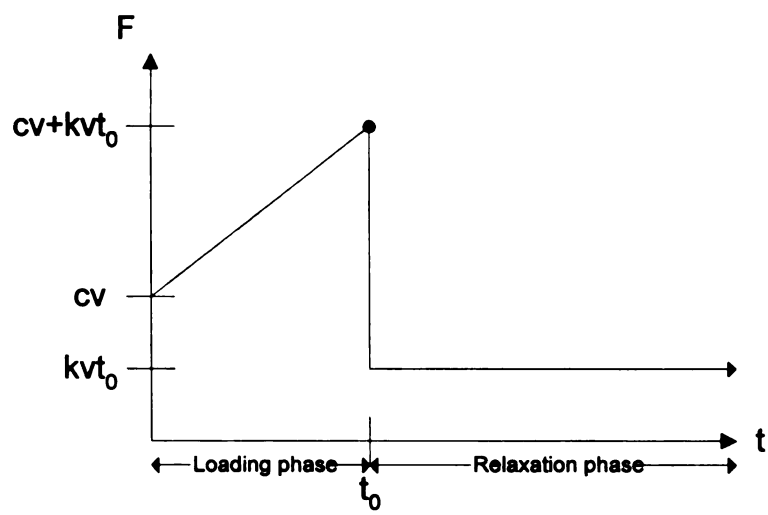

Figure 13 Plot of Force F as a Function of Time t

It is apparent that the model cannot portray the relaxation behavior. The force F drops straight down at the instant loading stops instead of coming to a gradual drop like real curves, and then remains constant at this value. However, It is important to transform force F to % force retention (P) in order to normalize the unit.

Let P = % force retention $= 100 * \left(\frac{F_{t=i}}{F_{t=0}} \right)$ and the solution is:

$$P = \frac{100}{1 + \frac{c}{kt_0}} \tag{21}$$

Equation (21) indicates that % force retention is independent of compression rate v but dependent on t_0. It means that high compression rate or low compression rate does not affect % force retention as long as a system is subjected to the same amount of time t_0.

After obtaining Equation (21), an experiment was performed to check the interpretation of the equation. The liner materials (PE foam and paper pulp) loaded at 0.1 inch/minute (in/min) were held at t_0 of 23 seconds (sec) when compression force of 130-150 pounds (lb) was reached. The decayed force after loading stopped was recorded every 30 seconds (sec) for 15 minutes (min). Relaxation curves of liner materials tested are shown in Figure 14. The experimental data from compression of PE foam and paper pulp liner on the Instron machine was then used as the input data to determine what the model explains.

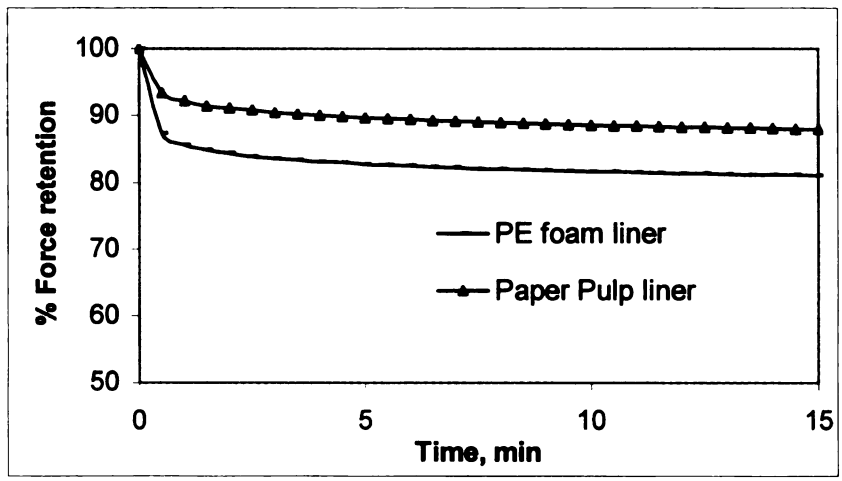

Figure 14 Plot of % Force Retention vs Time of Liners Tested on Instron

From the curves, it was found that the PE Foam and paper pulp liner reached steady state at force retention of 81% and 88% respectively, these numbers substituted in Equation (21) show:

$$81 = \frac{100}{1 + \frac{c}{kt_0}} \Rightarrow \frac{c}{kt_0} = 0.235 \quad \text{for PE foam liner}$$

$$88 = \frac{100}{1 + \frac{c}{kt_0}} \Rightarrow \frac{c}{kt_0} = 0.136 \quad \text{for paper pulp liner}$$

Apparently, model A indicates that either $c_{paper} < c_{foam}$, or $k_{paper} > k_{foam}$, or both, in order for these numbers to turn out this way. It makes sense that $k_{paper} > k_{foam}$. Thus, this model gives some insight of material properties, even though the model is incomplete to represent the relaxation process.

3.2.3 Model B for Liner Material

This model is more sophisticated than the former because it has another spring k_2 in series with dashpot, so the system has 2 degrees of freedom as shown in Figure 15.

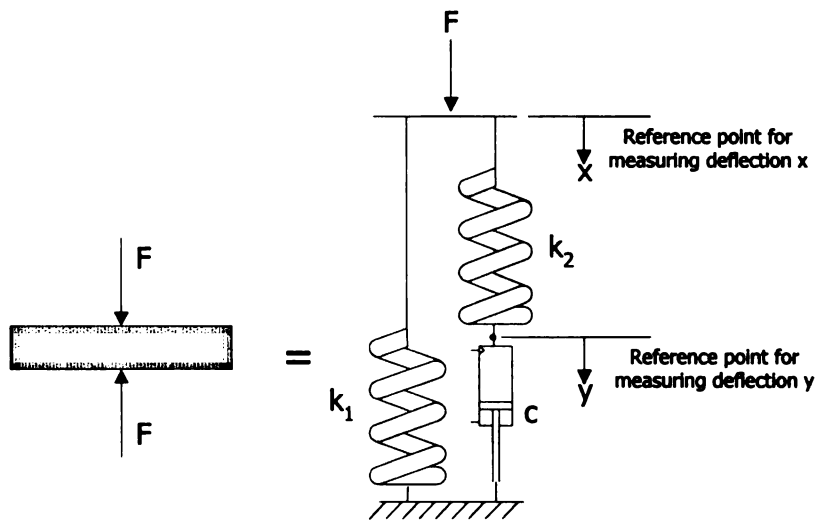

Figure 15 Liner Material in Model B

For model B, the total force is given by

$$F = k_1 x + k_2 (x - y) \tag{22}$$

and

$$k_2 (x - y) = c \dot{y} \tag{23}$$

where F = Compression force or sealing force

k_1 and k_2 = Spring constant

x and y = Deflection

c = Damping constant

$\dot{x}$ and $\dot{y}$ = Compression rate

Loading phase $x = vt$ at $0 \le t \le t_0$

Substituting x = vt into Equation (23) becomes

$$k_2(vt - y) = c\overset{o}{y}$$

Then, $$\overset{o}{y} + \frac{k_2}{c}y = \frac{k_2}{c}vt \qquad (24)$$

Equation (24) is a 1st order linear differential equation with constant coefficient in y(t).

The initial condition is y=0 at t = 0 and the solution is:

$$y(t) = vt - \frac{cv}{k_2}\left(1 - e^{-\frac{k_2 t}{c}}\right) \qquad (25)$$

Substituting Equation (25) into (22) yields:

$$\begin{aligned} F &= k_1 vt + k_2\left(vt - vt + \frac{cv}{k_2}\left(1 - e^{-\frac{k_2 t}{c}}\right)\right) \\ &= k_1 vt + cv\left(1 - e^{-\frac{k_2 t}{c}}\right) \end{aligned} \qquad (26)$$

So at t_0, $x_0 = vt_0$

and $$y_0 = vt_0 - \frac{cv}{k_2}\left(1 - e^{-\frac{k_2 t_0}{c}}\right)$$

These are the initial conditions of the relaxation phase.

<u>Relaxation phase</u> $x = fixed = x_o = vt_0$ at $t_0 \le t \le \infty$

but y will not be fixed.

Substituting x_0 = vt into Equation (23) gives

$$k_2(vt_0 - y) = c\overset{o}{y}$$

Then, $$\overset{o}{y} + \frac{k_2}{c} y = \frac{k_2}{c} v t_0 \qquad (27)$$

The initial condition is $y = y_0 = v t_0 - \frac{cv}{k_2}(1 - e^{-\frac{k_2 t_0}{c}})$ at t = 0 (at beginning of relaxation) and the solution becomes:

$$y(t) = v t_0 - \frac{cv}{k_2}\left(1 - e^{-\frac{k_2 t_0}{c}}\right) e^{-\frac{k_2 t}{c}} \qquad (28)$$

Substituting Equation (28) into (22) yields:

$$\begin{aligned} F &= k_1 v t + k_2 (v t_0 - v t_0 + \frac{cv}{k_2}(1 - e^{-\frac{k_2 t_0}{c}}) e^{-\frac{k_2 t}{c}} \\ &= k_1 v t_0 + cv (1 - e^{-\frac{k_2 t_0}{c}}) e^{-\frac{k_2 t}{c}} \end{aligned} \qquad (29)$$

Let P = % force retention $= 100 * \left(\frac{F_{t=i}}{F_{t=0}}\right)$, the following solution is obtained:

$$P = 100 * \left(\frac{1 + q e^{-\frac{k_2 t}{c}}}{1 + q}\right) \qquad (30)$$

where $$q = \frac{c}{k_1 t_0}\left(1 - e^{-\frac{k_2 t_0}{c}}\right)$$

Apparently, Equation (30) needs two parameters from the experimental results: q and $\frac{k_2}{c}$. These two parameters are material properties in test material and can be deduced from experimental data.

One way to get the value of q is by assuming that the experimental data (Figure 14) for PE foam liner and paper pulp liner reached steady state ($t \to \infty$) at the force retention of 81% and 88% respectively. These numbers substituted in Equation (30) show:

$$81 = \frac{100}{1+q} \Rightarrow q = 0.235 \quad \text{for PE foam liner}$$

$$88 = \frac{100}{1+q} \Rightarrow q = 0.136 \quad \text{for paper pulp liner}$$

Then, substituting q into Equation (30) yields:

% force retention of PE foam liner $$P = 100 * \left(\frac{1 + 0.235 e^{-\frac{k_2 t}{c}}}{1 + 0.235} \right)$$

% force retention of paper pulp liner $$P = 100 * \left(\frac{1 + 0.136 e^{-\frac{k_2 t}{c}}}{1 + 0.136} \right)$$

These equations were fitted to a curve using the experimental data (Figure 14) to get $\frac{k_2}{c}$ values. The results show that foam and paper pulp liner have $\frac{k_2}{c}$ values of 2.1 and 1.4 respectively. Although predicted curves generated in Figure 16 follow a typical relaxation curve, the predicted curve just gradually relaxes for a couple minutes and levels off over time. This indicates the limitation of this model. In addition, it is important to note that the characteristics of the predicted curve are dependent on q and $\frac{k_2}{c}$ which are material properties, but independent of compression rate v. An experimental investigation was needed

to check these characteristics; the % force retention is independent of compression rate. The result can be found in the next page. The last point to be made is that the accuracy of the prediction is based on the assumption that the experimental data used for deducing the model parameters are obtained from steady state. This is subjective and depends on the time frame.

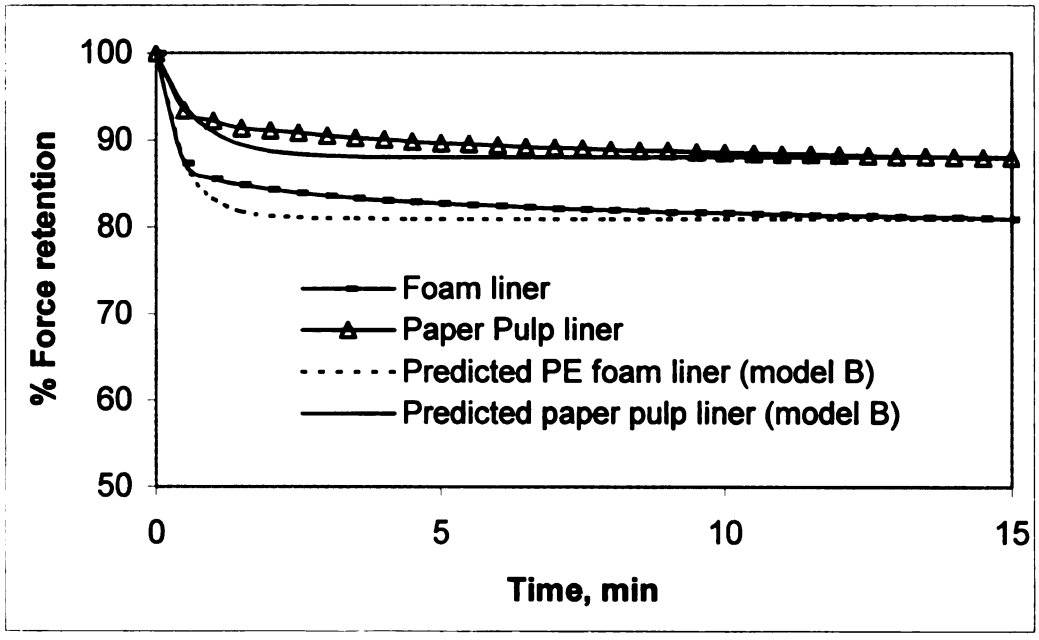

Figure 16 Comparison between Experimental and Predicted % Force Retention

One important fact follows from consideration of Models A and B. The % force retention is independent of compression rate v but dependent on t_0. Therefore, at steady state, the % force retention should depend only on how long the loading part goes on. In other words, the results depend on how long the system is loaded or how much it is compressed before starting the relaxation phase. The compression rate v is excluded from the equation; nevertheless, this result not expected because the mechanical behavior of polymeric materials is usually strongly dependent on the loading rate or compression rate v. Derivation

of the solution for spring and dashpot models shows that the compression rate v is always canceled out from the % force retention equation.

An experiment was conducted to investigate, if models A and B are correct to tell that % force retention depends on loading time alone. The PE foam liners were compressed on the Instron machine for the same loading time of 23 sec at compression rates of 0.05, 0.1 and 0.15 in/min. When they reached the desired loading time, the loading was stopped. The liner was then allowed to relax for 15 min, the retained force was recorded every 30 sec.

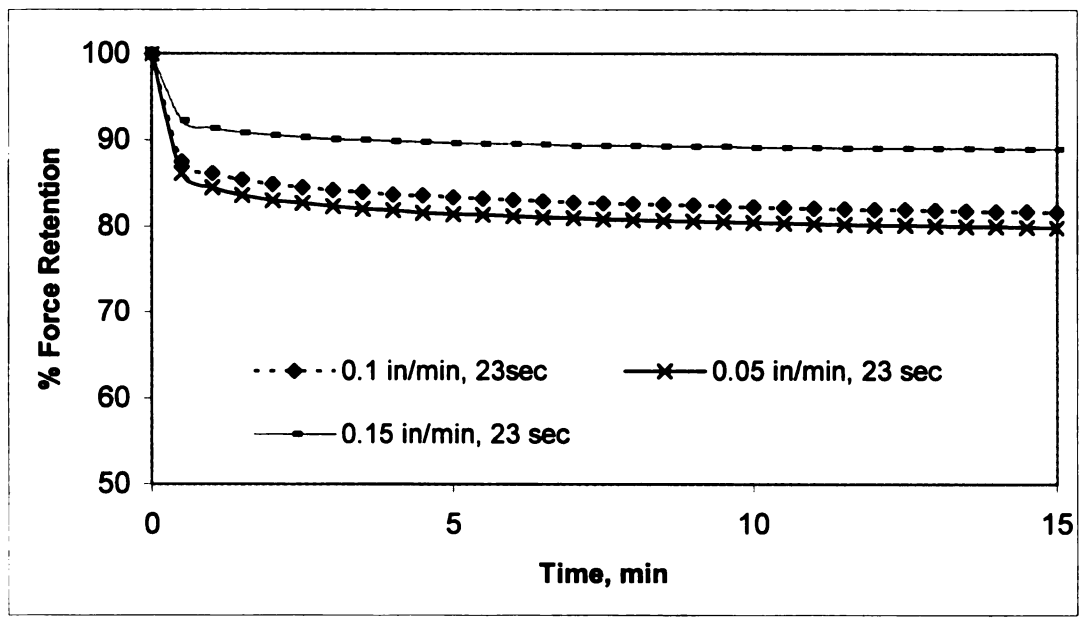

Figure 17 % Force Retention of Foam Liner as a Function of Time

The plot of experimental results in Figure 17 shows that foam liners at the same loading time have different % force retention when they are subjected to different compression rates v. The higher the compression rate, the greater the force retention at steady state. This relationship seems logical because at constant loading time t, as the compression rate v increases, the deformation x

will increase as well as the amount of load applied on the liner. Thus, it can be concluded that the % force retention of the liner material depends on loading time and compression rate.

Mechanical models using spring and dashpot for describing linear viscoelastic behavior are useful in developing qualitative thinking. However, this approach is inadequate to describe the relaxation behavior of container-closure system due to the limitations described previously. More complicated spring dashpot models can be developed to fit the actual relaxation curves but they all have similar deficits. In addition, it might turn out that the model developed is too complicated and impractical to use. As a result, it was decided to develop empirical models for predicting the relaxation behavior of the container-closure systems. Curve fitting techniques were used to fit the experimental data to the model. The details of the techniques used and the results obtained are in Chapters 4 and 5.

4. MATERIALS AND METHODS

4.1 Materials

This research focused on continuous thread closures, one of the most widely used in the food and pharmaceutical industry. The 28-400 style: 28 millimeters (mm) in major diameter and a shallow continuous thread was selected to test along with 2 different non-glued liner systems: PE foam and paper pulp liner. A description of the container-closure systems tested follows below.

Table 2 Description of Container-Closure Systems

Component	Finish size-style mm	Material	Description
Closure	28-400	PP closure/ PE foam liner	Fine rib closure, white color, non-glued, made by Owen-Illinois
	28-400	PP closure/Paper Pulp with Saran film coated	Fine rib closure, white color, non-glued, made by Owen-Illinois
Container	28-400	HDPE	White color, 60 ml volume, square shape, made by Owen-Brockway Plastics & Closures

4.2 Equipment

- Self temperature compensated bonded resistance strain gages: Measurement Group CEA-13-125-UN-120
- Direct-reading strain indicators: Measurement Group P-3500
- Flat-bed plotters: Linseis L-6012 and L-6512

- Data logger: Omega OM-500
- Manual electronic torque tester: Secure Pak
- Manual spring torque tester: Secure Pak
- Environmental chambers: EGC and Lab-line Instruments
- Universal testing machine: Instron Model 4201
- Mitutoyo digital caliper
- Mitutoyo dial caliper gage
- Bridgeport comparator

4.3 Methods

In this research, the stress relaxation study was conducted differently from the conventional technique because it was almost impossible to measure a predetermined initial strain on the actual container-closure system. The stress relaxation measurement in the actual container-closure system was studied by initiating strain of the system to a predetermined application torque or compression force using the torque meter or Instron machine. The deformation of the system was then held constant for a specific time, while a force over time was being recorded.

4.3.1 Cross-Sectional Measurement of the Container-Closure System

Five replicates of the container-closure systems: PE foam liner and paper pulp liner were measured for the dimensions. The measurement of T, E and I of the containers were made using a digital caliper and dial caliper gage. Next, a closure was applied on the container with the prescribed application torque of 14.5± 0.5 TIP using the electronic torque tester. A container-closure system was

then placed upside down into a prepared box of 3x3x1.25 inches (the inside surface of the box was covered with pressure sensitive tape). The clear casting resin and polyester catalyst were thoroughly mixed and poured into the sample and prepared box. This step was performed in the hood. The box was cured in the hood until the casting was completely dry, after which the casting was removed from the box. Finally, the casting was cross-sectioned using a band saw and polished to make a smooth clear surface. The measurements of the angles α and θ were made using an optical comparator. For the container, the T dimension is the major diameter of the container finish including the threads. The E dimension of the container is the minor outside diameter of the container finish excluding the threads. The diameter at the smallest opening inside the finish is the I dimension. The angle α is the incline angle made by the spiral of the thread in relation to the horizontal plane measured at the mean diameter of the thread interface. Likewise, the T dimension of the closure is the major inside diameter measured from one side panel to the opposite side panel and the E dimension of the closure is the minor diameter measured between threads. Finally, the angle θ is the contact angle between the closure threads and the container threads measured along the vertical axis. The illustrations of these parameters are shown in Figures 18.

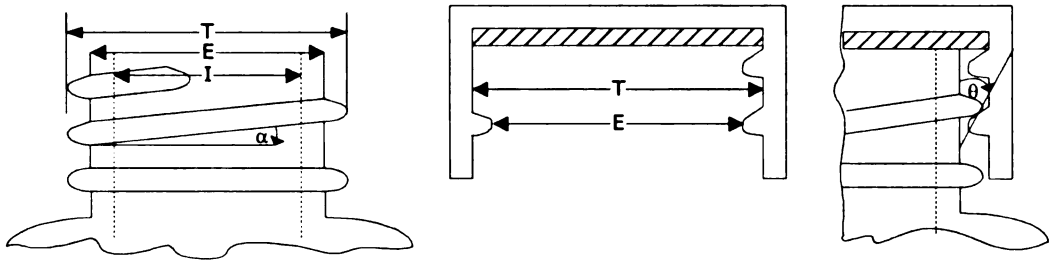

Figure 18 Dimensions of Container-Closure System

4.3.2 Sealing Force Measuring Device Fabrication Technique

The configuration of the measuring device arose from the need to measure axial force within the small space constraint of the actual container-closure system. Strain gages were utilized to produce sufficient sensitivity and accurate measurement of force over time. Strain gages and supplies used in the fabrication were obtained from Measurements Group Inc., Raleigh, NC. The bonding area of the measuring device made of 7075-T651 aluminum alloy was abraded and cleaned by water-based cleaner (MCA and MN5A) to give it the proper chemical affinity for the adhesive. The epoxy adhesive (AE-15) was then used to bond the strain gage at the center of the closed end aluminum shell. After the adhesive was completely cured, a three-conductor cable (326-DFV) with vinyl insulation was soldered on the terminals of the strain gage. Butyl rubber sealant (M-Coat F) was used to cover the strain gages in order to provide moisture protection in which the damp environmental conditions to be tested. After finishing the active gage on the measuring device, a dummy gage prepared using the same procedure was bonded on a stress-free 7075-T651 aluminum alloy disk to provide bridge completion and temperature compensation.

4.3.3 Test Method for Sealing Force Measuring Device Design Verification

The objectives of this test were to verify a "restrained" design system, which is used in the second design of the sealing force measuring device, and to propose a simple technique to study relaxation of a system on a basic testing instrument e.g. Instron. The actual situation of container-closure system after torque applied to the system can be viewed as in Figure 19 in which shaded areas are locations on a closure, liner and container where the relaxation is likely to be highest.

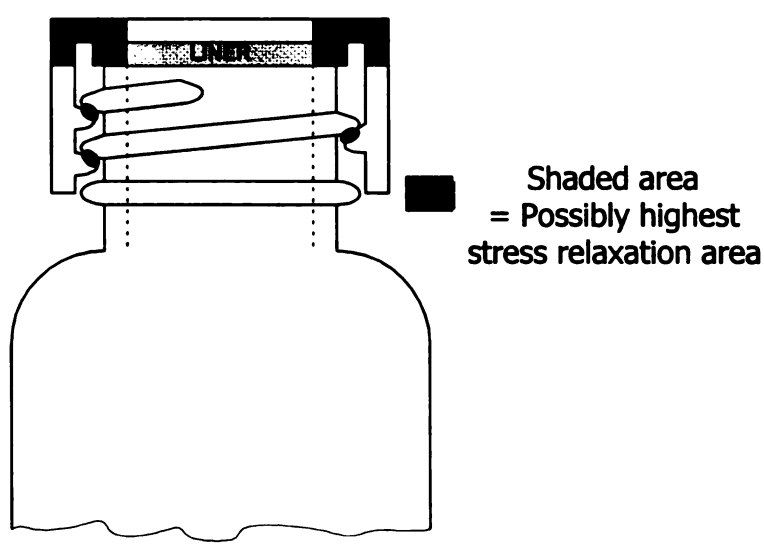

Figure 19 Actual Situation of Container-Closure System Under Loading

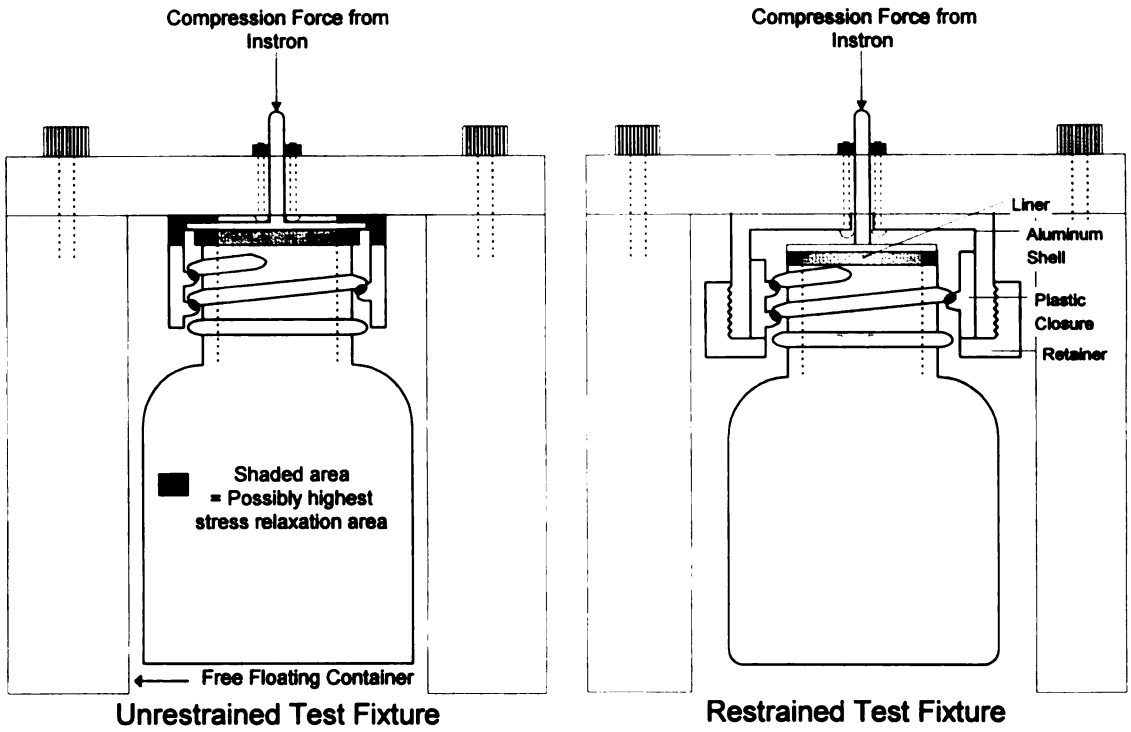

Figure 20 Test Fixtures for Design Verification

An unrestrained test fixture was developed according to the distribution of stress analysis (Figure 19) in order to simulate the actual situation when the container-closure system is under loading. Both test fixtures have the same rigid support to hold test container-closure system above the ground. But the difference is that the closure is mounted directly on an unrestrained test fixture, whereas the restrained test fixture requires a closure without top panel glued into the shell as shown in Figure 20. The restrained design assumes that the dome bending near the periphery of the dome is negligible. This design concept using a closure without its top panel is necessary for a sealing force measuring device. This is because it offers more headspace which makes a proper thread engagement and eliminates a titling effect. On the other hand, to gain more

headspace in the unstrained design, the height of the land area of test container must be cut to have enough space for inserting a plunger. Both test fixture designs shown in Figure 20 were tested at standard conditions on 28 mm PP closure with PE foam liner and HDPE container. In testing, the test container was screwed into the closure mounted on the test fixture to the same depth as the actual system applied by application torque of 14 TIP. This condition will make the threads in contact in the test fixture as close as in the actual container-closure system. The Instron machine was set at crosshead speed of 0.1 in/min and set to stop loading when the compression force of 130 lb was reached. This value is the maximum value of force which corresponded to 14 torque-inch-pounds (TIP) application torque from a preliminary study. The crosshead speed was set to achieve the same loading time as manual application torque. The deflection was maintained constant and in the mean time, the compression force over time was recorded every minute for 15 min. Five replicates were carried out in both fixtures. The comparison was then made by constructing the relaxation curves from both fixtures.

4.3.4 Test Method for Sealing Force Measuring Device Calibration

The sealing force measuring device was calibrated against a weight calibrated 1 kN load cell (Instron model 2518-806, Canton, MA) by applying loads ranging from 10 to 150 lb using Instron machine model 4201 at test speed of 0.2 in/min. A jig shown in Figure 21 made of steel was used to facilitate this process and a calibration setup is shown in Figure 22. The measuring device was placed up side down into the countersink of the jig while the Instron machine was

applying a compression force through a "bump" disk (Figure 22). The strain readings obtained from a direct-reading strain indicator were plotted against each load and the linear regression was used to fit a plot. The slope of a fit line was used as a calibration factor (με/lb) for converting strain reading to sealing force. A dummy gage was used for temperature compensation during calibration at standard conditions (73°F, 50% RH).

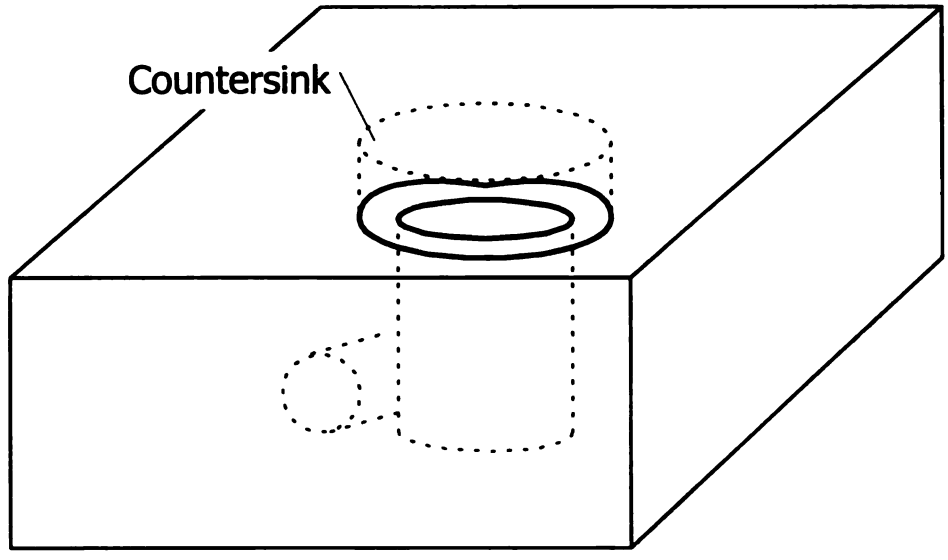

Figure 21 Calibration Jig for Sealing Force Measuring Device

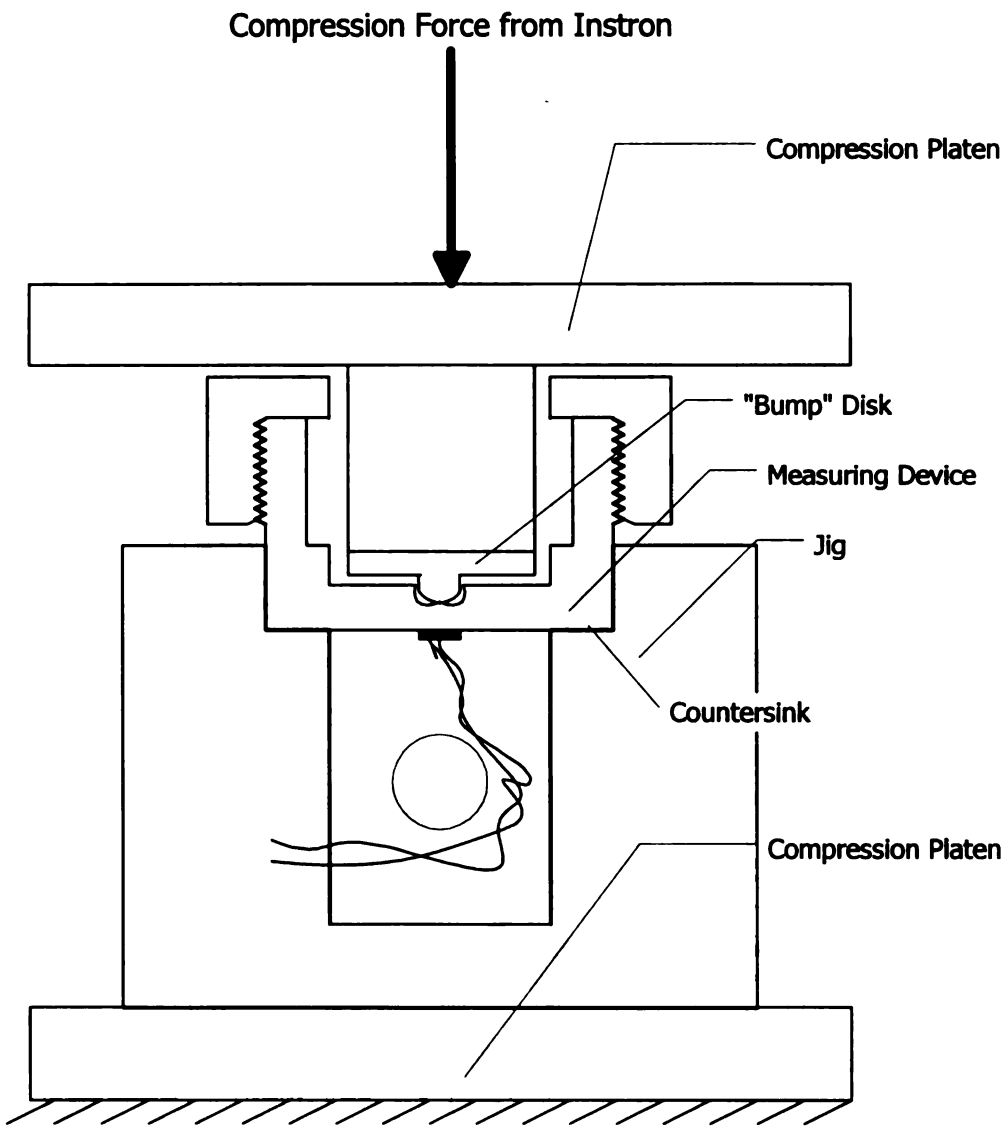

Figure 22 Calibration Setup for Sealing Force Measuring Device

The calibration result was plotted along with a fit line from linear regression as shown in Figure 23. The reason to use a direct calibration instead of shunt calibration is that the effects of a number of absolute error sources are eliminated. Calibration against a known traceable force produces readout directly related to the cause.

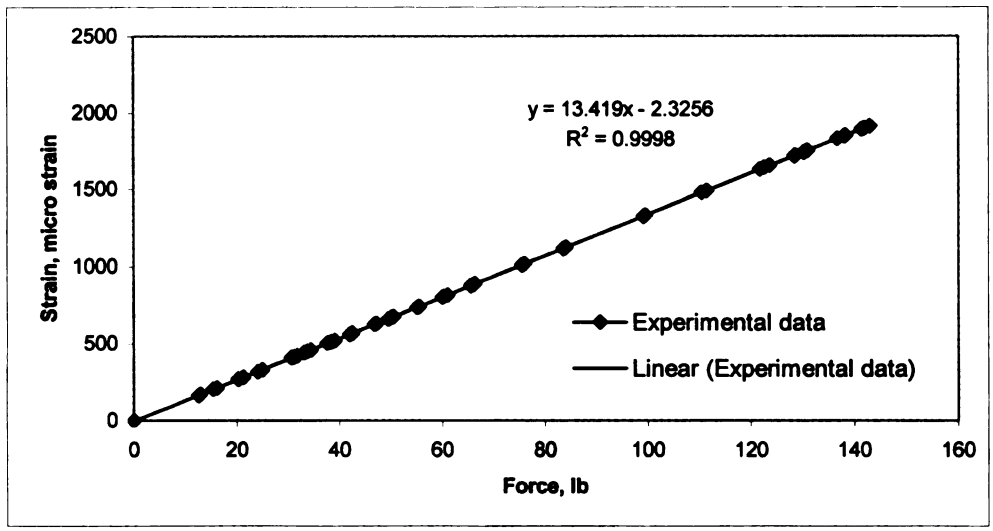

Figure 23 Calibration Curve for Sealing Force Measuring Device

Figure 23 shows the linear relationship between the applied force and strain with the coefficient of determination of 99.98% which indicates that the measuring device is nearly perfectly elastic over the service strain range. Besides, the results show that the calibration factor is 13.4 με/lb. This shows that the ability of the measuring device to detect changes in strain from the applied force is adequate for measuring the relaxation in the system studied.

4.3.5 Test Method for Temperature Compensation and Moisture Protection Verification

Since the change in resistance of the strain gage associated with strain is very small, it is necessary to consider the effect of temperature and moisture on the measuring device for two reasons. First, temperature is a major cause of non-strain induced resistance changes. Second, moisture acts to place a resistance path in parallel with the strain gage, thereby producing a change in resistance equivalent to strain. Theoretically, calibration with a known force should be carried out in a similar environment in which the device will be used. However, in practice it is very difficult to completely follow because there are many limitations of the instruments used in calibration. Temperature compensation of the measuring device is accomplished by using half-bridge configuration in which an identical gage to the active gage is mounted on an unstressed piece of the same type of material used in the measuring device. Adequate temperature compensation is an absolute necessity for accurate measurement of strains from a strain gage bonded on the measuring device. In addition, this verification also tested the effectiveness of moisture protection for the strain gage which will be subjected to very high humidity environments. For this research as described previously, the measuring device was intended for use at three environmental conditions: standard conditions (73.4±2°F, 50±2% RH), refrigerated conditions (41±4°F, 85±5% RH) and tropical conditions (104±4°F, 85±5% RH). The simplest approach to verify the effectiveness of temperature compensation and moisture protection of the measuring device is to perform a small calibration check.

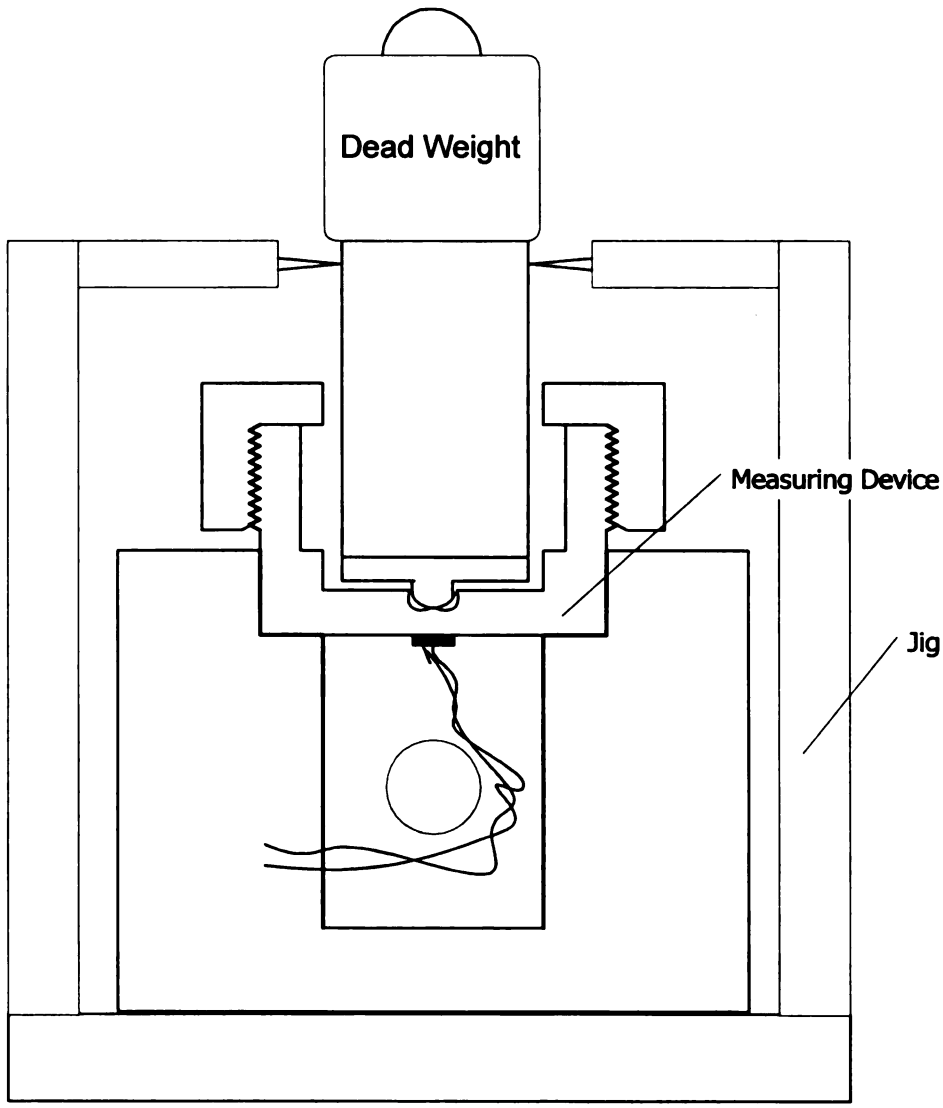

Figure 24 Setup for Verification of Temperature Compensation and Moisture Protection

This was done by using a jig and setup as shown in Figure 24 to support dead weight in the vertical position during loading. The verification method is quite similar to the calibration of the measuring device except a series of 9 different standard weights ranging from 1 to 25 lb was used for providing an increasing load for constructing a relationship between strains and the applied

loads under each test condition. The test conditions generated from the environmental chambers were 73.4±2°F, 50±2% RH, 41±4°F, 85±5% RH and 104±4°F, 85±5% RH. Finally, the applied load and strain relationships established from each test condition were then compared in a plot. The protection was considered effective if the results of the test conditions have no significant difference among them.

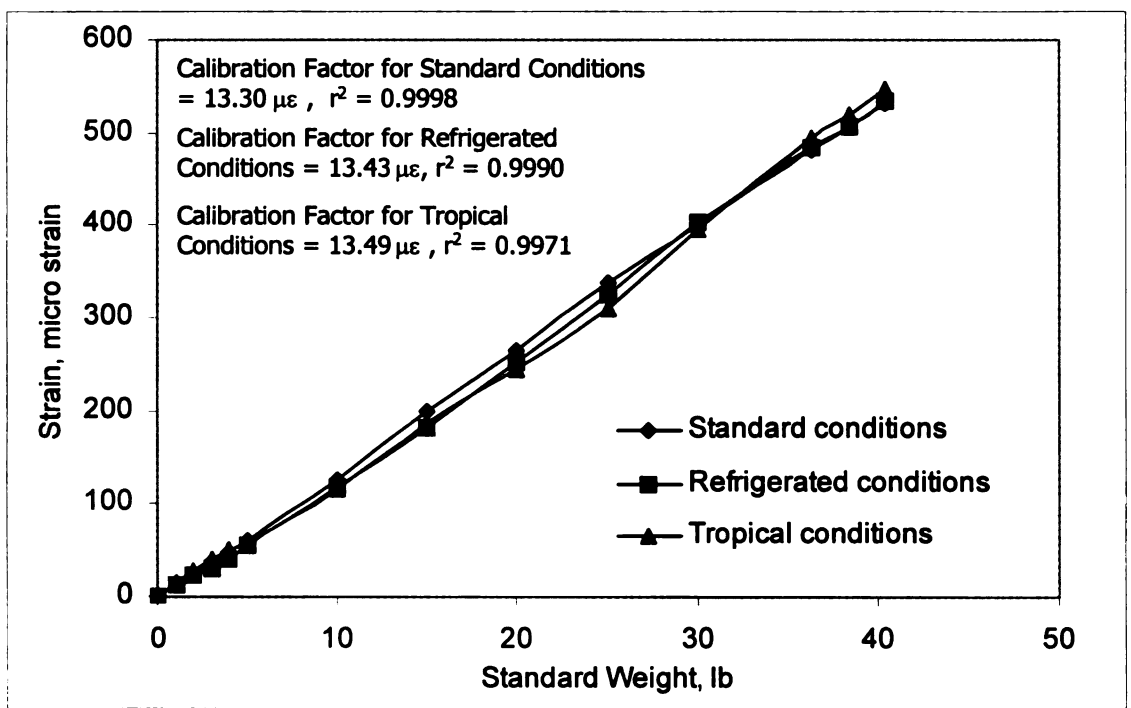

Figure 25 Strain as a Function of Standard Weight obtained from Test Conditions

Plots shown in Figure 25 indicate that the best fit of relationship between strain and standard weight would be linear for all test conditions. There is no significant difference among the three calibration factors for all test conditions. A comparison of the results among three test conditions indicates that the sealing

force measuring device can be used effectively for studying a relaxation all three conditions: standard, refrigerated, and tropical.

4.3.6 Test Method for Relaxation Study

The experimental design in Figure 26 and its procedure were established after several preliminary studies with the container-closure systems to be tested. Three different storage environments: (1) standard conditions (73.4±2 °F, 50±2% RH), (2) refrigerated conditions (41±4 °F, 85±5% RH) and (3) tropical conditions (104±4 °F, 85±5% RH) were selected for studying the relaxation of the systems. These test conditions were set in accordance with ASTM D 4332 Standard Practice for Conditioning. The experiment, which had a total of 6 treatments, ran for 10 replicates of each test condition of each container-closure system (PE foam and paper pulp). A test closure was prepared by removing the top panel of the closure from its body. Then, the closure without top panel was dotted using solder gun to increase surface area and friction before gluing in the aluminum shell by epoxy adhesive (Selleys Chemical Company, Australia), whereas a top panel of closure was glued on a "bump" disk. The closure will be replaced with a new closure every time when starting the experiment. The experimental setup is shown in Figure 27. The plastic container with a measuring device mounted on the top was inserted in holder to protect from shape distortion. Next, it was kept in the environmental chamber for 15 min to eliminate errors from the effect of instantaneous temperature change on the strain gage. The measuring device was then clamped in an electronic torque tester and pre-applied slowly on the container until the nose of "bump" disk just touched the inside top panel of

aluminum shell. The application torque of 14.5± 0.5 TIP was manually applied on the system at test conditions with the loading time of 5 sec. The electronic torque tester was used for measuring the application torque at standard conditions; for the other two test conditions, the spring torque tester was employed. This is because the electronic torque tester was not designed for use at high humidity environment. After applying the application torque, the signal response generated by unbalancing of the half bridge was indicated on the display of strain indicator. The signal response was also recorded by the data logger and plotter every 30 sec for the first hour and every hour for 5 days. At the end of day-5, the container-closure system with a measuring device mounted on the top was taken from the environmental chamber to measure the removal torque by using the electronic torque tester. In addition to the sealing force measuring test set, six sets of the actual container-closure system were also stored at the same environments. The closures were slowly applied on the containers until the liners just touched the land area of containers. This ensured proper placement to provide the consistent results and deformation of all container-closure systems. The application torque and loading time similar to the measuring device were then manually applied. The actual container-closure systems were taken in a set of five replicates from the test environments to measure the removal torque after the first 15 min storage and then every day until reaching five-day storage. The data of sealing force during storage time from the measuring device and removal torque during storage time from the

actual container-closure systems were used to calculate the % force retention (FRT) and % torque retention (TRT) respectively.

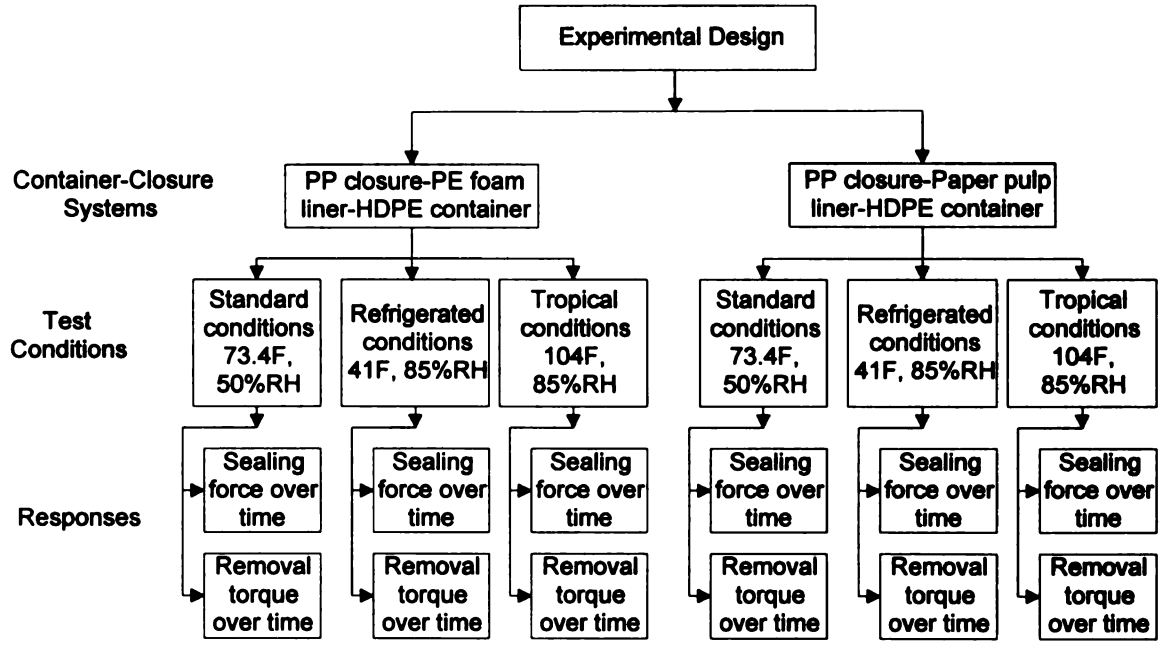

Figure 26 Experimental Design for Relaxation Study

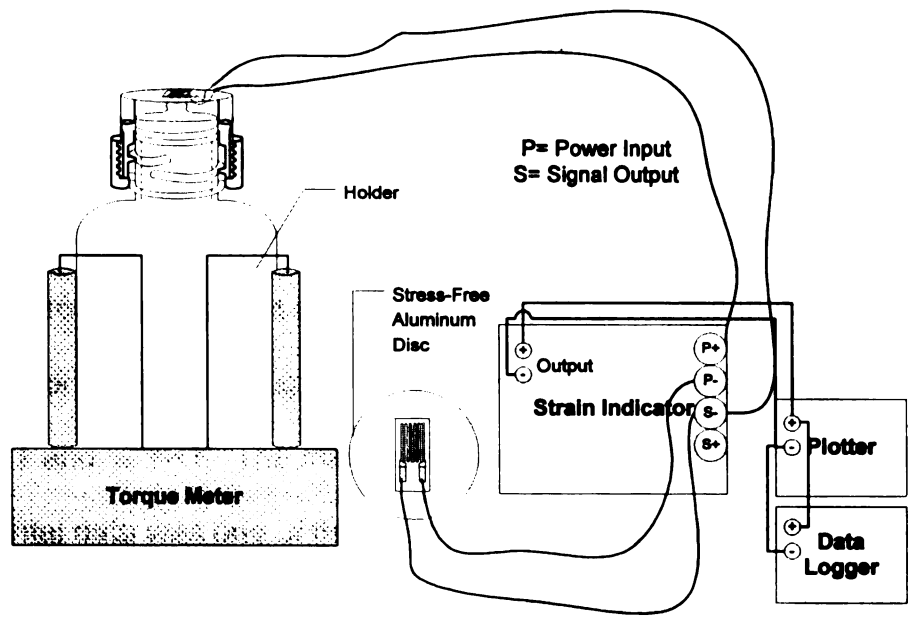

Figure 27 Experimental Setup for Relaxation Study

4.3.7 Data Analysis

The collected data were generally organized into 2 categories: (1) the sealing force over time data and (2) the removal torque over time data. Both categories contained data of 6 treatments from 2 factors studied: (1) the container-closure systems and (2) the environmental conditions. The data of two categories were normalized to the % force retention (FRT) and % torque retention (TRT) using the following equations:

$$\%FRT = \frac{F_t \times 100}{F_i} \tag{31}$$

$$\%TRT = \frac{RT_t \times 100}{AT} \tag{32}$$

where F_t = Sealing force at time t, lb

F_i = Initial sealing force, lb

RT_t = Removal torque at time t, TIP

AT = Application torque, TIP

The % FRT and TRT data were used as the input data for developing the empirical models for each treatment. Generally, many physical processes such as the relaxation follow an exponential decay rule. Several models and algorithms from the simplest exponential function to the rational fraction that have this characteristic were brought in to examine the fit of the experimental data of the % FRT and % TRT. The maximum error calculated from the predicted and experimental data was one of the criteria for selecting the best fit model along with practicality and easy to use. After examining, It was found that there are

three models that can properly represent the relaxation characteristic of the test container-closure systems (Figure 28).

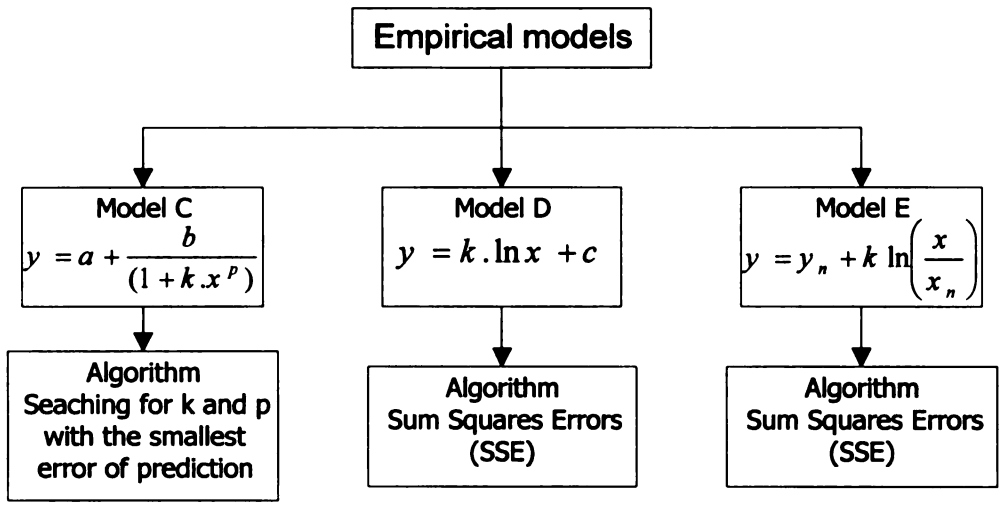

Figure 28 Empirical Models for Relaxation Data of % FRT and % TRT

Model C

Model C derived from the general form of the exponential function can be expressed as

$$y = a + \frac{b}{(1 + kx^p)} \qquad (33)$$

where $a = y_n - \frac{100 - y_n}{kx_n^p}$

$b = 100 - a$

x and y = Time (min) and % FRT or % TRT

x_n and y_n = last data point of time (min) and % FRT or % TRT

k and p = Coefficients of the equation

The concept of this model is that the model is forced to fit through the first data point: (0, 100%) and the last data point at 5 days: (7200, y_n). The condition

on fitting through the first and last data point will ensure that the predicted relaxation curve will follow the experimental relaxation curve as close as possible. This is expected to give a good prediction of the % FRT and % TRT after the five-day experiment. The coefficient k and p in the equation are determined from developing a computer program in BASIC to search for the coefficients that provide the minimum error of prediction. This approach is basically searching for the coefficients (k and p) that offer the best fit. This was done by arbitrarily trying some range of number for k and p first and then the range for these two coefficients is narrow down until finding the optimum number for k and p. This is only possible done by using the computer. In computer program, after choosing the range of number, the number in that range is changed in small step and the error between the predicted data and experimental data is calculated for every number in that range. The reason for choosing this algorithm over the sum square error is that it gives a better fit solution for a non-linear form. The adequacy of the fit can be determined from the max error obtained from calculating the difference between the experimental data and predicted data.

Model D

A previous investigation found that the characteristics of the relaxation curves are non-linear and a simple exponential model ($y = a + b.e^{-k.x}$) is incomplete to describe the behavior. The semi-log model (model D) was then selected to model the behavior since its simple form holds the decay characteristics. The model can be expressed mathematically as:

$$y = k.\ln x + c \tag{34}$$

where x and y = Time (min) and % FRT or % TRT

k and c = Coefficients of the equation

The curve-fitting criterion of this model is that the sum of the squares of the errors (SSE) be minimized. Then, the derivative of the SSE equation with respect to each coefficient is set the result to zero. This is the customary approach to minimize the error between the calculated value and actual value and it returns the resulting equations for finding the coefficients as follows:

$$k = \frac{n.\sum_{i=1}^{n}(\ln x_i.y_i) - \sum_{i=1}^{n}\ln x_i.\sum_{i=1}^{n}y_i}{n.\sum_{i=1}^{n}(\ln x_i)^2 - (\sum_{i=1}^{n}\ln x_i)^2} \tag{35}$$

and

$$c = \frac{\sum_{i=1}^{n}y_i.\sum_{i=1}^{n}(\ln x_i)^2 - \sum_{i=1}^{n}\ln x_i.\sum_{i=1}^{n}(\ln x_i.y_i)}{n.\sum_{i=1}^{n}(\ln x_i)^2 - (\sum_{i=1}^{n}\ln x_i)^2} \tag{36}$$

Note that n = number of experimental data points from i=1 to n

After the coefficients are established, one frequently wishes to know how well the predicted line fits the experimental data. The measure of the best-fit is the correlation coefficient r and the equation is:

$$r = \frac{n.\sum_{i=1}^{n}(\ln x_i.y_i) - \sum_{i=1}^{n}\ln x_i.\sum_{i=1}^{n}y_i}{\left\{\left[n.\sum_{i=1}^{n}(\ln x_i)^2 - (\sum_{i=1}^{n}\ln x_i)^2\right].\left[n.\sum_{i=1}^{n}y_i^2 - (\sum_{i=1}^{n}y_i)^2\right]\right\}^{1/2}} \tag{37}$$

Model E

Model E is actually a special case of the semi-log model D in which the model is forced to fit through the last data point (x_n,y_n). The reason to force fit the last data point is that the model is aimed to predict long term response. It is better to extrapolate the predicted results by focusing on the latest information. In addition, the last data point is least sensitive to the experimental errors made in the beginning of the experiment. The model relaxes logarithmically with time and is given by

$$y = y_n + k.\ln\left(\frac{x}{x_n}\right) \tag{38}$$

where x and y = Time (min) and % FRT or % TRT

x_n and y_n = Last data point of time (min) and % FRT or % TRT

k = Coefficient of the equation

The sum of the squares of the errors (SSE) algorithm was used to derive the coefficient k which can be shown the resulting equation as follows:

$$k = \frac{\sum_{i=1}^{n}\left[(y_i - y_n).\ln\left(\frac{x_i}{x_n}\right)\right]}{\sum_{i=1}^{n}\left[\ln\left(\frac{x_i}{x_n}\right)\right]^2} \tag{39}$$

The adequacy of the fit is measured by using the correlation coefficient r in the following equation:

$$r = \sqrt{1 - \frac{\sum_{i=1}^{n}(y_i - y_{ic})^2}{\sum_{i=1}^{n}(y_i - \bar{y})^2}} \qquad (40)$$

Note that y_{ic} = predicted y from the model and $\bar{y}$ is the average of y from experimental data.

All proposed models in this section were used to fit with the test data (6 treatments) and the fit results can be found in Chapter 5. The empirical models developed in this chapter were planned to be incorporated with the torque-friction model (Pisuchpen, 2000) derived from the force diagram. The integration of these models was expected to improve the accuracy and usefulness of the torque-friction model. The results of integration of the models are also shown in Chapter 5.

5. RESULTS AND DISCUSSION

5.1 Cross-Sectional Measurement of the Container-Closure Systems.

A summary of cross-sectional measurement results is shown below.

Table 3 Summary of Container-Closure Systems Dimensions

Parameter	28 mm Container-Closure System			
	HDPE Container-PP Closure-Foam Liner		HDPE Container-PP Closure-Paper Pulp Coated Liner	
	Closure	Container	Closure	Container
T, in	1.0895	1.0745	1.0895	1.0745
E, in	1.0050	0.9777	1.0050	0.9777
l , in	-	0.8360	-	0.8360
p, in	0.167	0.167	0.167	0.167
α, degree	2.96	2.96	2.96	2.96
$\overline{r_i}$, in	-	0.5131	-	0.5131
$\overline{r_s}$, in	-	0.4534	-	0.4534
θ, degree	42.07		41.12	

Note: Dimensions are the average of maximum value and the value measured at 90° away from this.

The results in Table 3 were compared with voluntary standards of closure and container design developed by the Closure Manufacturers Association and Plastic Bottle Institute. It was found that the dimensions of samples fall within the range of the standard recommended. Thus, it is confident to conclude that the closures used in this research are compatible with the containers. It is necessary for this research area to start with the dimensions measurement because the ability of the closure to be retained on a container by threads that engage corresponding threads of the container depends on the compatibility of

dimensions. The use of incompatible container-closure system will adversely affect the closure performance in providing seal integrity. The buttress thread profiles "M" Style and "P" Style were obtained from containers and closures respectively. The only difference between both profiles is that the "P" Style has a full nose radius instead of a modified buttress nose profile. The results also show that the closure threads made contact with the container threads with the contact angle around 40 degrees. This is fairly typical contact angle value obtained from plastic systems. In theory, a closure thread profile shows the greatest holding power when three conditions are satisfied. Firstly, the shape of container threads and closure thread must match each other as closely as possible. Secondly, the engagement of threads made on two adjacent threads of the container finish must fully contact. Lastly, both container and closure threads must have pressure angles approaching the horizontal. However, in practice, this consideration of optimum holding power is rarely achieved because of variations in mold, design and dimensions, and the material used in manufacturing. The results found from this part were used in modeling and verifying the container-closure systems models.

5.2 Verification of the Design of Sealing Force Measuring Device.

There are two designs proposed in Chapter 3: unrestrained design and restrained design. The restrained design was used as a basis for developing the sealing force measuring device. The analysis using a force diagram indicated that both designs have the distributed stresses all around the test unit from loading similar to the actual container-closure system. The restrained design was chosen over the unrestrained design because it is easier and has fewer preparation steps when implemented in the measuring device. In addition, in practice, using the restrained design is less likely to produce a tilting problem and the problem of non-uniform distribution of forces. Test fixtures were developed to verify both designs conducted on the Instron machine at standard conditions for the relaxation test. The compression force was applied on the container-closure system mounted on the test fixture with the loading time of 5 sec until reaching 130 lb force (the maximum force obtained from an application torque of 14 TIP). The average and range of force over time obtained from each design during relaxation phase were plotted as shown in Figures 29 and 30.

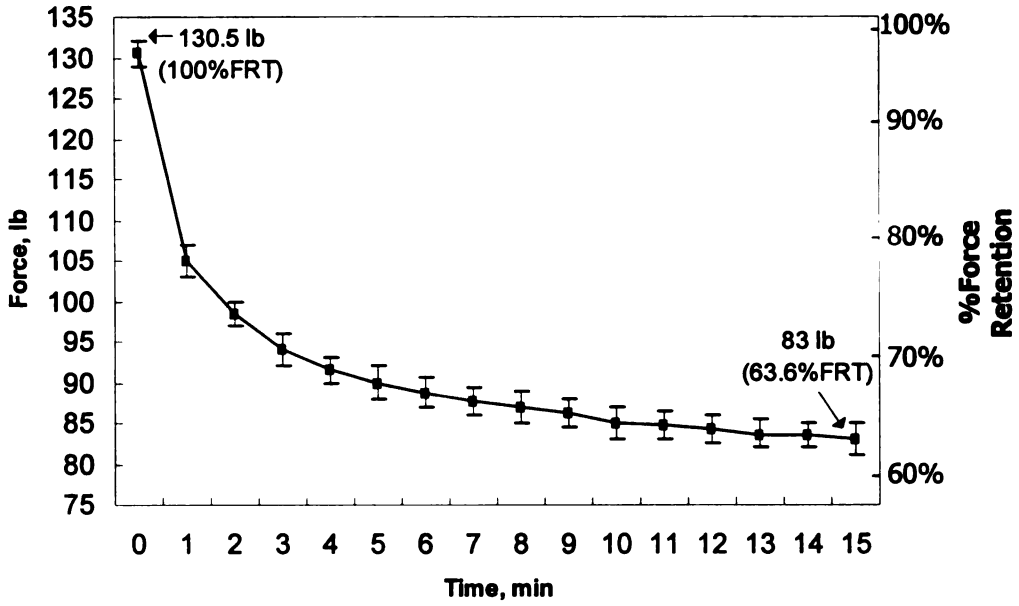

Figure 29 Force as a Function of Time obtained from Unrestrained Fixture

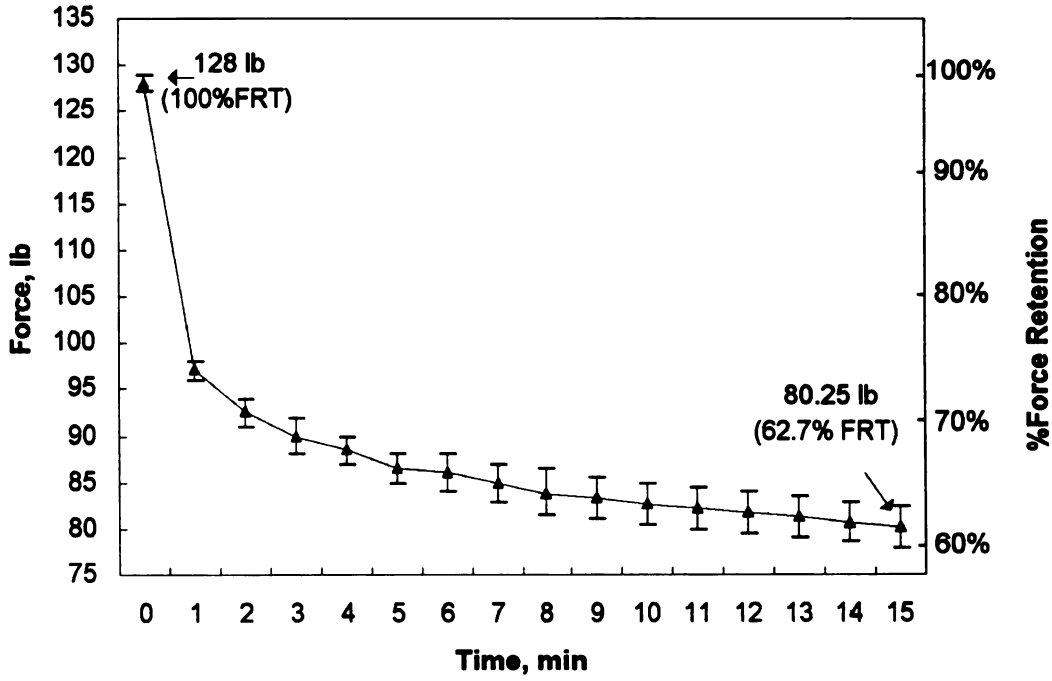

Figure 30 Force as a Function of Time obtained from Restrained Fixture

In general, both designs provide typical relaxation curves with only small variations of force over time. The applied force rapidly dropped as soon as loading force stopped and then continued to gradually drop down until stopping the test at 15 min. For the unrestrained design, the initial applied force of 130.5 lb or 100% force retention (% FRT) relaxed to 83.0 lb or 63.6 % FRT as much. Likewise at the end of the test, the applied force of 80.25 lb or 62.7% FRT was retained in the system when using the restrained design. It can be concluded that there is no difference between the designs in the results of the relaxation study. The results support the use of the restrained design in developing the measuring device. The only restriction of using the unrestrained fixture is that the height of the land area of test container is needed to be precisely cut before screwing into the closure mounted on the fixture. This is done in order to obtain the similar condition of the thread engagement when the actual system was applied by application torque of 14 TIP. The test fixtures are inexpensive to fabricate and require only a basic testing instrument (e.g. Instron) for applying the prescribed compression force. This offers the simplest technique for a direct study of the force relaxation in the container-closure systems.

5.3 Relaxation of Container-Closure Systems

It is important to note that the relaxation of the container-closure systems was investigated by initiating strain of a system to a prescribed application torque (14.5 ± 0.5 TIP). The system was subjected to constant strain at test conditions and the decay of sealing force during storage was observed over time. The sealing force over time data was analyzed in % FRT and compared to the % TRT

from the actual systems. The analysis was based on the theory that the removal torque is proportional to the sealing force. Therefore, the removal torque relaxes in proportional to the sealing force. In other words, the % FRT must be the same as the % TRT. The experimental results are summarized in Table 4.

Table 4 Summary of % FRT and % TRT of Container-Closure Systems

Time	Parameters	Test Conditions					
		Refrigerated		Standard		Tropical	
		PE Foam	Paper Pulp	PE Foam	Paper Pulp	PE Foam	Paper Pulp
0	AT, TIP	14.8	14.6	14.5	14.5	14.7	14.5
		(0.4)	(0.4)	(0.4)	(0.3)	(0.4)	(0.4)
	Sealing force, lb	92.3	94.8	96.9	97.6	97.8	94.9
		(9.8)	(12.4)	(10.9)	(13.1)	(7.9)	(9.7)
15 min	% FRT	58.3	55.6	61.5	56.0	55.5	49.2
		(2.7)	(2.8)	(1.0)	(1.6)	(2.0)	(1.8)
	% TRT	65.0	72.6	63.3	67.6	60.2	63.6
		(4.0)	(4.4)	(3.9)	(3.7)	(3.8)	(5.6)
	% TRT/% FRT	1.21	1.31	1.05	1.21	1.14	1.29
1 day	% FRT	45.9	42.3	47.5	43.8	43.1	35.4
		(1.6)	(2.2)	(1.9)	(1.4)	(2.2)	(2.2)
(1440 min)	% TRT	61.9	71.0	53.7	59.0	42.2	38.3
		(2.2)	(4.8)	(4.0)	(2.8)	(5.5)	(3.2)
	% TRT/% FRT	1.43	1.68	1.22	1.35	1.04	1.08
2 days	% FRT	44.4	41.1	45.8	42.3	41.6	33.3
		(1.6)	(2.1)	(1.9)	(1.5)	(2.1)	(2.2)
(2880 min)	% TRT	61.0	67.9	51.8	55.6	38.2	37.8
		(3.7)	(3.1)	(3.4)	(2.7)	(3.5)	(4.7)
	% TRT/% FRT	1.47	1.65	1.21	1.31	0.97	1.14
3 days	% FRT	43.6	40.2	44.9	41.4	40.9	31.9
		(1.5)	(2.0)	(1.8)	(1.5)	(2.2)	(2.2)
(4320 min)	% TRT	60.3	59.8	49.5	55.2	36.9	35.9
		(4.4)	(3.5)	(3.2)	(4.0)	(2.3)	(3.9)
	% TRT/% FRT	1.48	1.49	1.18	1.33	0.96	1.13
4 days	% FRT	43.0	39.6	44.2	40.8	40.3	31.0
		(1.5)	(2.0)	(1.8)	(1.5)	(2.3)	(2.2)
(5760 min)	% TRT	58.0	58.0	50.1	53.3	35.9	34.9
		(3.4)	(5.3)	(3.6)	(2.3)	(3.7)	(2.5)
	% TRT/% FRT	1.44	1.47	1.21	1.31	0.95	1.13
5 days	% FRT	42.6	39.0	43.8	40.4	39.9	30.2
		(1.5)	(2.1)	(1.8)	(1.5)	(2.4)	(2.3)
(7200 min)	% TRT	56.2	58.2	49.3	50.7	34.3	35.2
		(3.3)	(4.6)	(4.3)	(3.5)	(3.0)	(2.9)
	% TRT/% FRT	1.41	1.49	1.21	1.26	0.92	1.16

Note: Average (Sd) from 10 runs

Table 4 shows that a sealing force of 92 to 98 lb is obtained from the application torque of 14.5 ± 0.5 TIP. Overall the % TRT is higher than the % FRT. The system of PE foam liner at tropical conditions shows that the % TRT is slightly lower than the % FRT from 1 day relaxation until the end at 5 days.

The results of the relaxation study are presented graphically in Figure 31 and 32, where the % FRT and % TRT of container-closure systems stored at refrigerated, standard and tropical conditions are plotted against time. The relaxation profile curves using the % FRT and % TRT as the indicator appear to follow the typical relaxation behavior. For the % FRT in Figure 31, the sealing force of the systems drops rapidly from 100% to around 80% as soon as loading stopped and then the rate of drop diminishes continually. Although a similar relaxation profile is found when using the % TRT as the indicator, large variation of % TRT over time is noticed. This indicates that the results from the % TRT are less consistent than the % FRT. This is because the relaxation study using the removal torque measurement is required to change the system studied over a period of time. After the removal torque is measured, the container-closure system is no longer use. Deviation of the removal torque from one measure to another is usually fairly large causing large variation of the results.

The relaxation data from the five-day experiment shows that on day 5 the system of PE foam liner at standard conditions has the highest % FRT at 43.8% and the system of paper pulp liner at tropical conditions has the lowest % FRT at 30.2%. For the % TRT, the system of paper pulp liner at refrigerated conditions has the highest % TRT at 58.2% and the system of PE foam liner at tropical

conditions has the lowest % TRT at 34.3%. It is also evident that the relaxation of the container-closure system is time dependent and it is enhanced by storage conditions especially at tropical conditions (104±4°F, 85±5% RH). The time dependent properties are characteristic of long chain structures and can be explained by the polymer structures. For instance, an entangled linear polymer is held at constant elongation. The force applied instantly to obtain the given elongation is that needed to uncoil the chains; it is equivalent to the elastic restoring force. But as the system is held at the given elongation, the chains will have time to flow past each other, allowing them to recoil and relax the stress. After a long enough time, no load will be required to maintain the deformation.

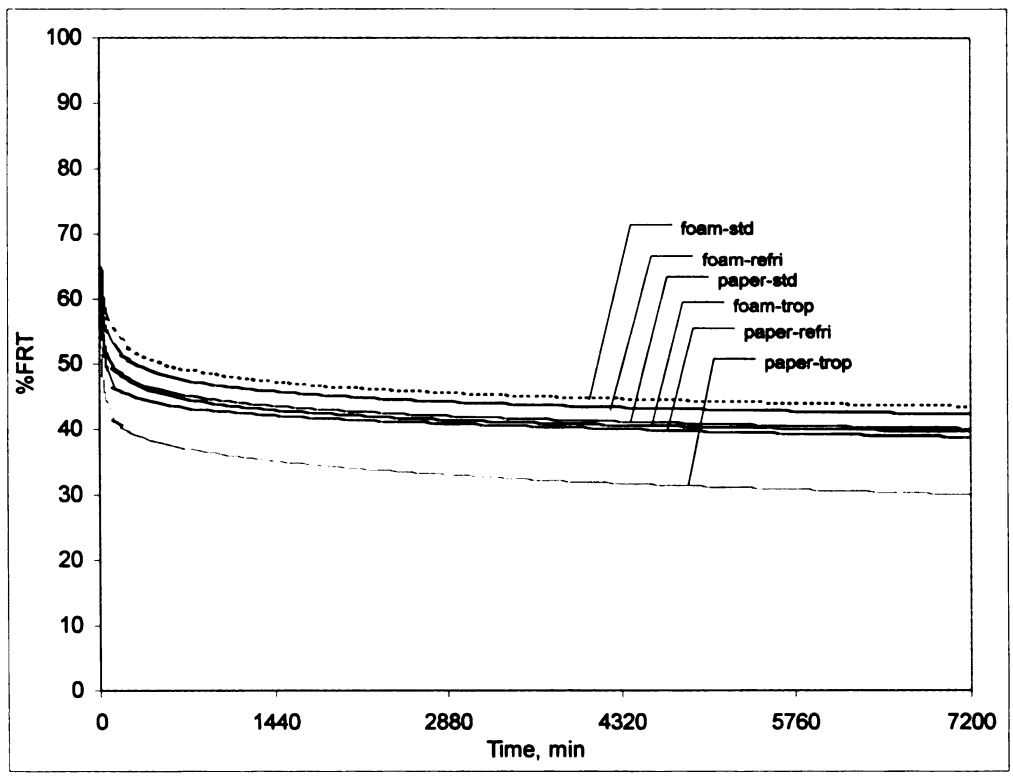

Figure 31 Plot of % FRT as a Function of Time for All Treatments

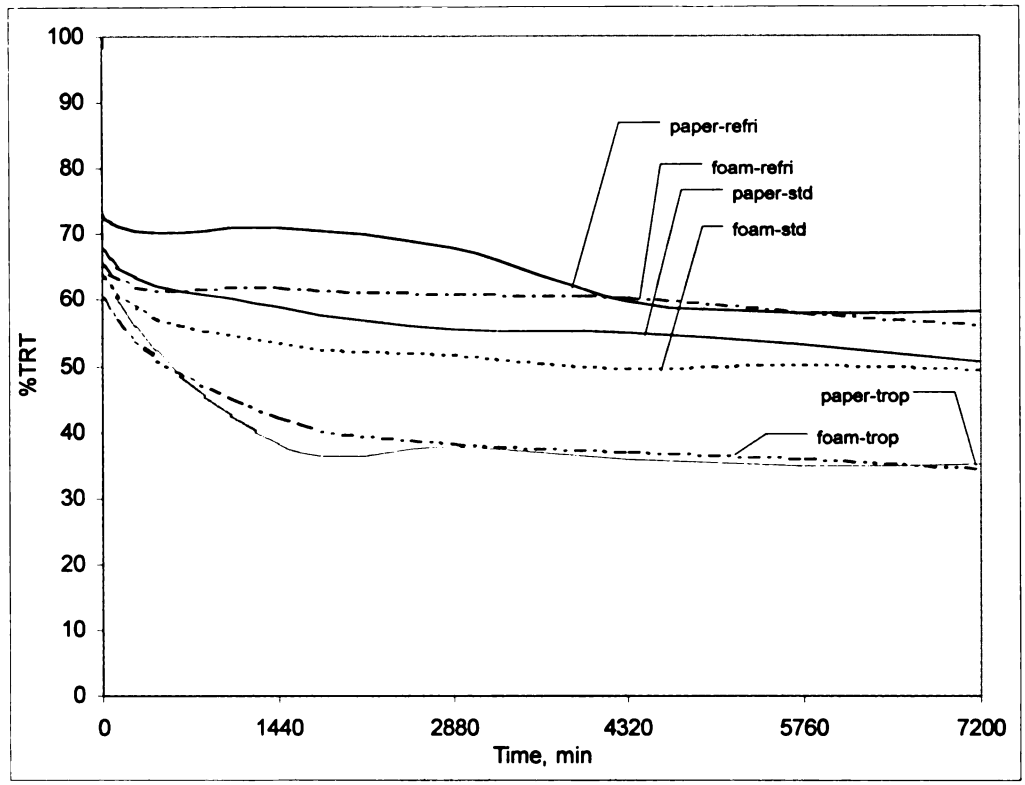

Figure 32 Plot of % TRT as a Function of Time for All Treatments

5.4 Effect of Environmental Conditions on the % FRT and % TRT

In order to analyze the effect of temperature and relative humidity on the % FRT and % TRT of container-closure systems (PE foam and paper pulp liner), a plot of the % FRT and % TRT for each liner system in test conditions was generated. From the plots of the % FRT (Figures 33 and 34), the % FRT of PE foam systems in the three test conditions was distributed over the narrow range from 40% to 44% after 5-day relaxation. The environmental conditions did not have a significant effect on the % FRT of PE foam systems. The effect on the % FRT of paper pulp systems was similarly limited except for the system at tropical conditions in which it was subjected to high temperature of 104°F and high relative humidity of 85%. The % FRT of the paper pulp system at this conditions

was significantly lower (10%) than the other two conditions. This is because high temperature and high relative humidity in storage conditions. Paper is a hygroscopic material; the mechanical properties especially the elasticity that is associated with the % FRT varies as a function of the moisture content of the material. As the moisture content increases, the elasticity of the paper pulp will decrease; as a result decreasing the % FRT over time. In addition, since the moisture content in paper is also related to the amount of moisture in the air, a psychrometric chart can be used to provide supportive information to the explanation. The amount of moisture in the air at refrigerated, standard and tropical conditions was 32.1, 61.2 and 287.5 grains/ lb of dry air respectively. Apparently, the tropical conditions show the highest moisture content in the air. Therefore it may conclude that the highest temperature and highest moisture content in the air at tropical conditions leads to the lowest % FRT of the paper pulp system.

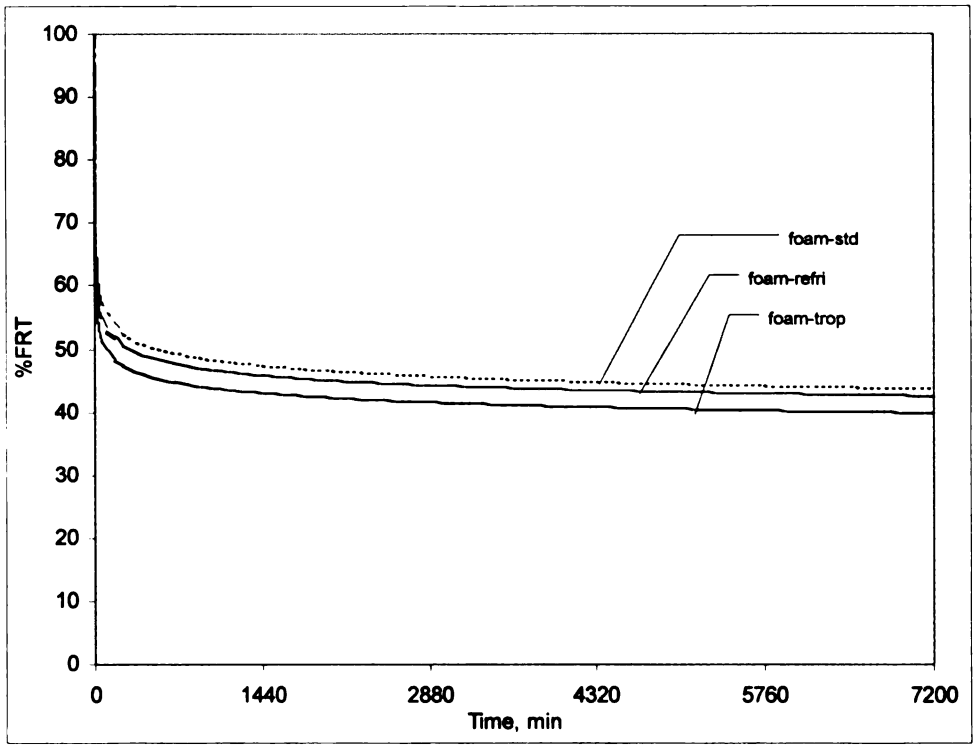

Figure 33 Plot of % FRT as a Function of Time for PE Foam Liner

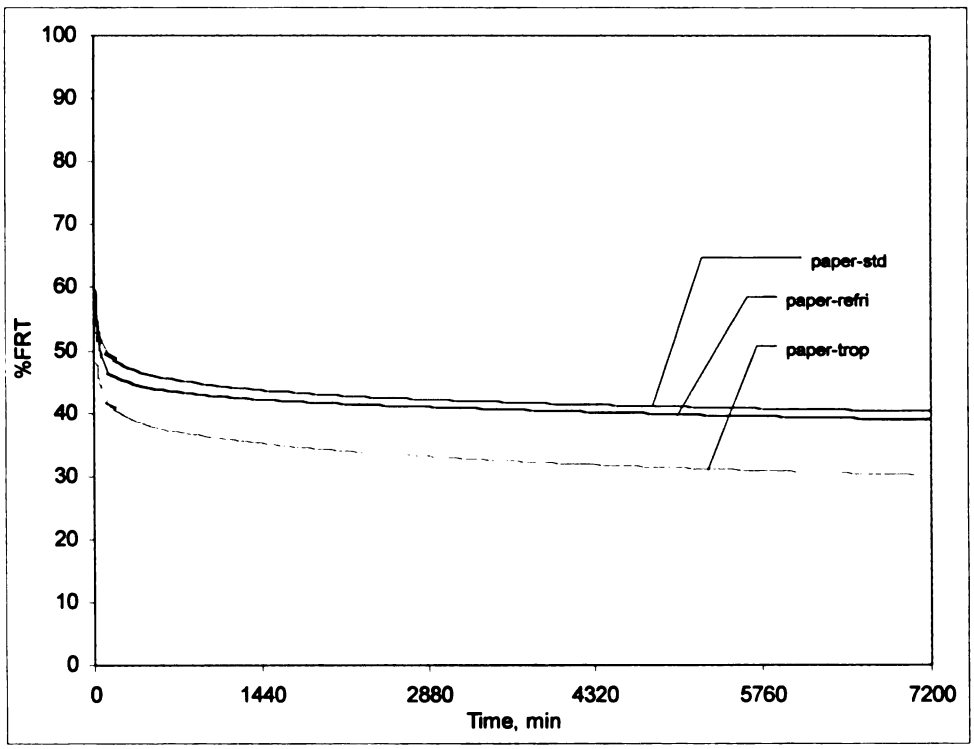

Figure 34 Plot of % FRT as a Function of Time for Paper Pulp Liner

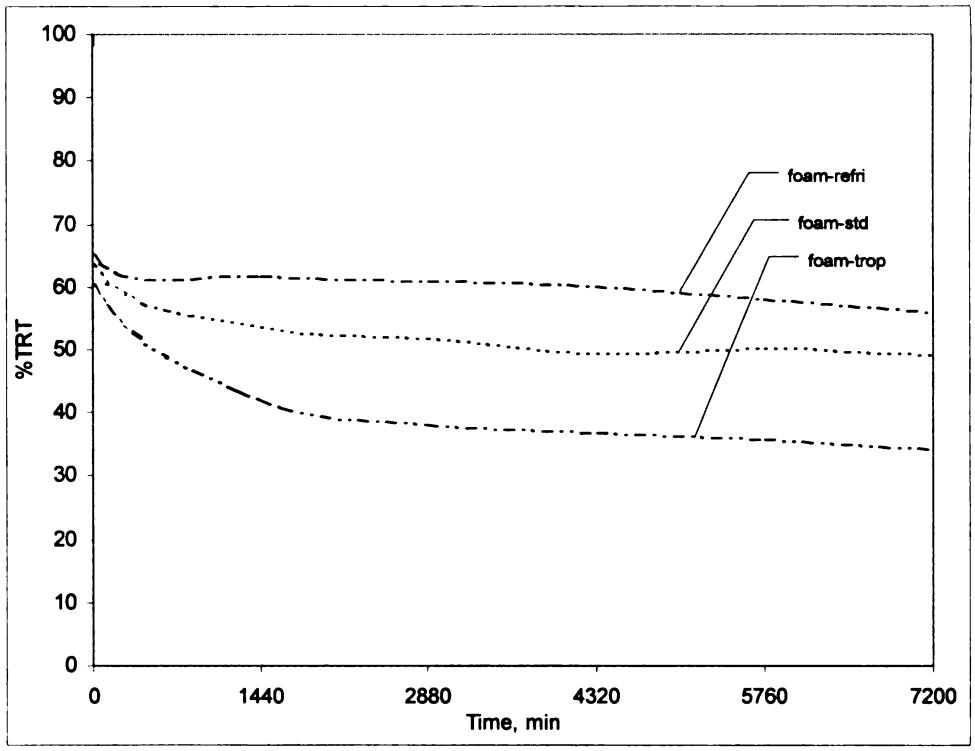

Figure 35 Plot of % TRT as a Function of Time for PE Foam Liner

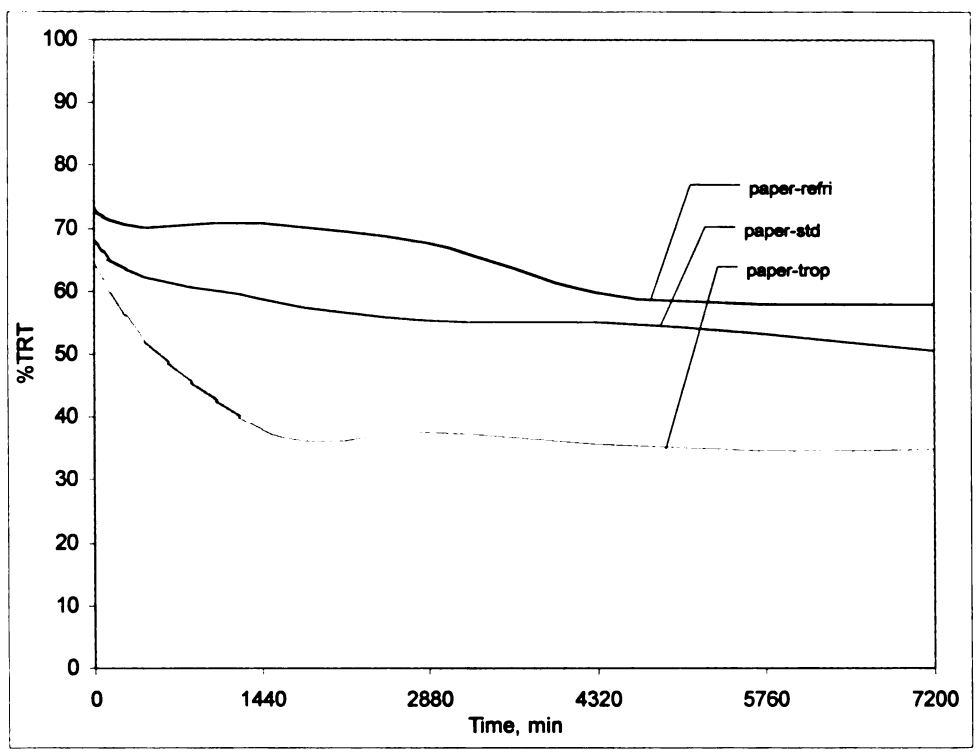

Figure 36 Plot of % TRT as a Function of Time for Paper Pulp Liner

In contrast to the % FRT, the % TRT of both systems in Figures 35 and 36 shows fluctuations over time due to the nature of measurement of removal torque and the significant effect of the environmental conditions on the % TRT of all test conditions is noticeable. The PE foam and paper pulp systems responded to the test conditions in the same way; the % TRT ranged from high to the low are the systems at refrigerated, standard, and tropical conditions. The systems stored at tropical conditions always have the lowest % TRT and % FRT. This is exactly the sort of behavior that could occur if a container-closure system was stored at tropical conditions. The mechanical properties of polymers are generally very sensitive to high temperature. The modulus of polymer decreases with increasing temperature. In this case, the storage temperatures are higher than the glass transition temperatures (T_g) of PP, HDPE and PE foam which induce some form of molecular motion causing a relaxation process. In general, as the temperature is increased, the modulus decreases and the polymer becomes more ductile as a result in increasing the relaxation process. Therefore, the lowest % TRT and % FRT were found in storage at tropical conditions. Besides, it must be realized that the coefficients of friction at thread interface and liner interface play a significant role in the torque retention of the container-closure systems. These coefficient values are greatly decreased when a lubricant (moisture) is present in between the interface layers. The reason for this may be related to the amount of moisture in the air. It is believed that this factor may be used to explain the significant effect of environmental conditions on the % TRT. This is because the moisture in the air behaves like a lubricant. However, the

experimental data is not available to support this statement yet. The observation on the systems stored at tropical conditions found that they showed tiny water drops around the container neck at the end of day 5. The higher the amount of moisture in the air, the higher the lubricating effect which causes a lower % TRT. This explanation supports the results that the highest temperature and amount of moisture in the air (using psychrometric chart) yield the lowest % TRT and vice versa.

5.5 Characteristics of the % FRT and % TRT

As discussed earlier, the removal torque or % TRT is generally used as the mechanical seal indicator for the container-closure systems throughout the industry. However, there has been dissatisfaction with accuracy and precision of this indicator. The % FRT was proposed in this research as an alternative indicator. In this part, Figure 37 was deduced from the experimental results in order to investigate the characteristics of the % FRT and % TRT. The curves of % TRT were higher than the curves of % FRT except for the PE foam system at tropical conditions; this indicated that the % TRT is always higher than the % FRT indicating less relaxation of torque than of force. The difference between these two parameters becomes smaller when the temperature and amount of moisture in the air increase. The % TRT curves dropped down more when either the PE foam system or paper pulp system was subjected to storage conditions having the higher temperature and amount of moisture in the air. This indicates that the % TRT is more sensitive to the change of temperature and moisture in the air than the % FRT if the system is in the same storage conditions. The

correlation between both indicators is also of interest since the theory points out that the removal torque is proportional to the sealing force. In other words, theoretically, the TRT is equal to the %FRT. The results show that the average of this ratio for five days distributed from 1 to 1.44 which disagree with the theory. The systems at refrigerated conditions show the highest ratio of TRT to FRT, whereas the lowest ratio was obtained from the systems at tropical conditions. This is because of the effect of time dependent properties and temperature on the relaxation of viscoelastic materials. The theory derived from the assumption of a rigid body cannot completely describe these complicated properties of viscoelastic materials. Although the correlation between the % TRT and the % FRT seems to be linear, the linear regression was not employed in this analysis. The % TRT data over time were too crude in comparison to the % FRT data, which contributed to the large error when using the linear regression. Thus, the average ratio of % TRT to % FRT was chosen to describe this correlation. The application of both parameters in describing the seal integrity must be considered carefully because the result from one parameter might conflict with the result from another.

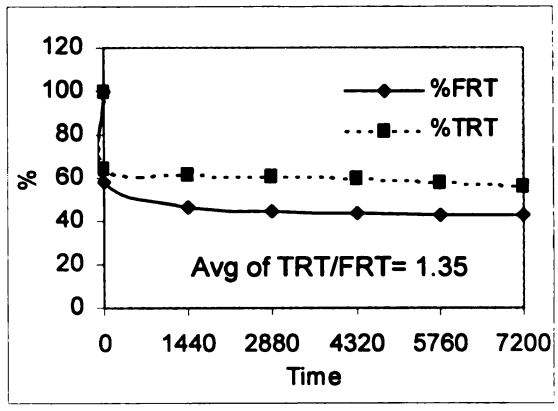

Foam refri

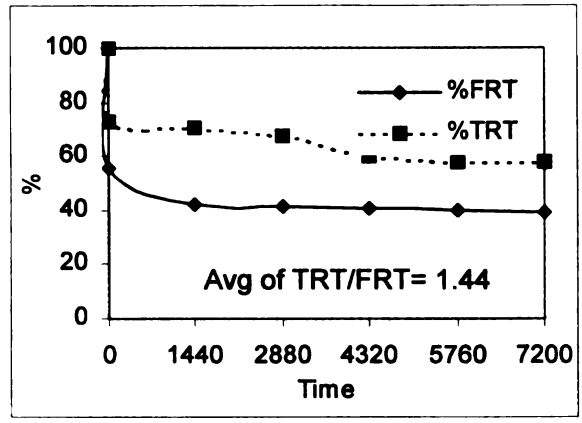

Paper refri

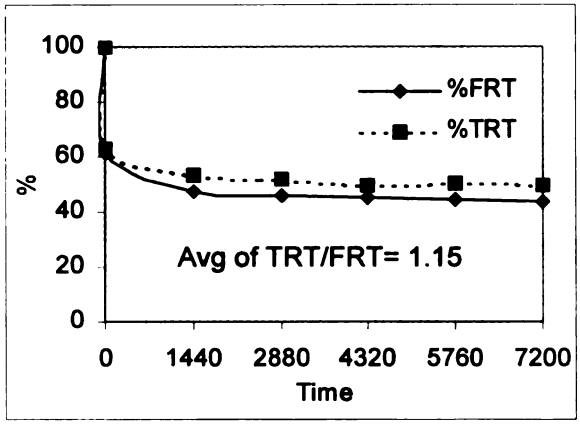

Foam std

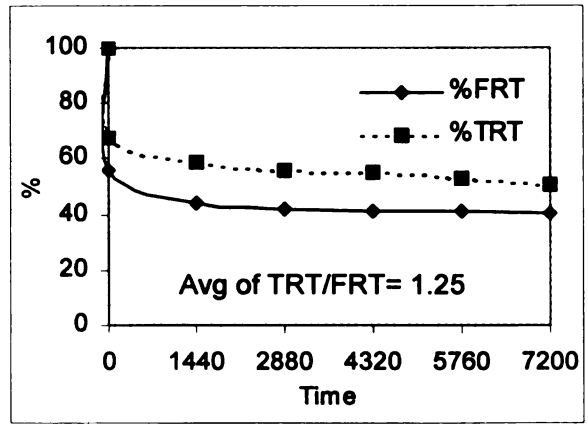

Paper std

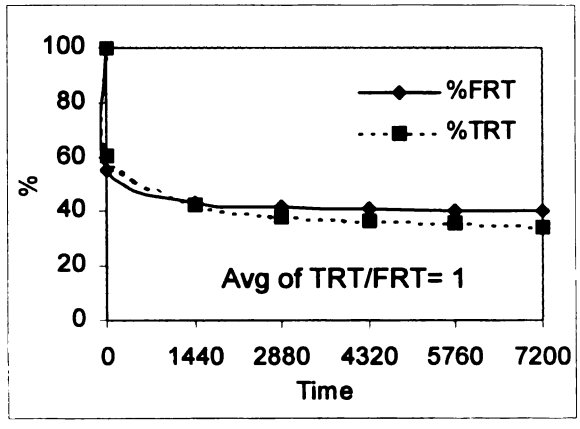

Foam trop

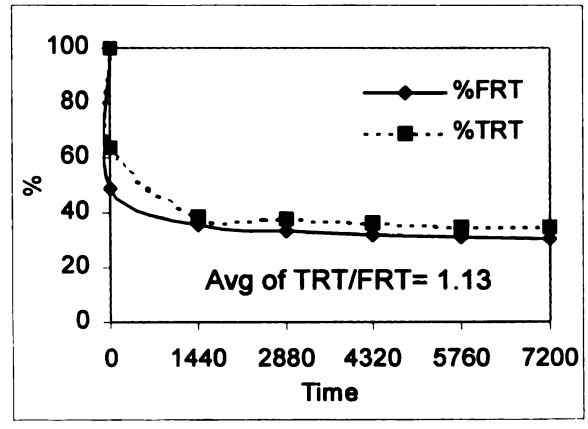

Paper trop

Figure 37 Comparing % FRT and % TRT of Systems at Test Conditions

The practical application: at standard conditions, after relaxation for 15 min which corresponds to the conditions for measuring the immediate removal torque, was chosen as the example. A comparison of seal integrity between the paper pulp system and the PE foam system is shown in Figure 38. Note that 1a and 1b are the % TRT of the paper pulp system and of the PE foam system, and 2a and 2b are the % FRT of the paper pulp system and of the PE foam system. It shows that % TRT-1a of the paper pulp is higher than % TRT-1b of the PE foam. Using % TRT as the indicator, one might conclude that the paper pulp system is better than the PE foam system. This is incorrect because the sealing force retained in the paper pulp system (% FRT-2a) is actually lower than the PE foam liner (% FRT-2b). Therefore, using the % TRT as the indicator may be misleading interpretation of the seal integrity. The results disagree with each other because the removal torque is a complex indicator; other factors not related to the seal integrity can affect the removal torque. This finding would be one reason that in some cases; the container-closure systems having high removal torque still shows leakage problem.

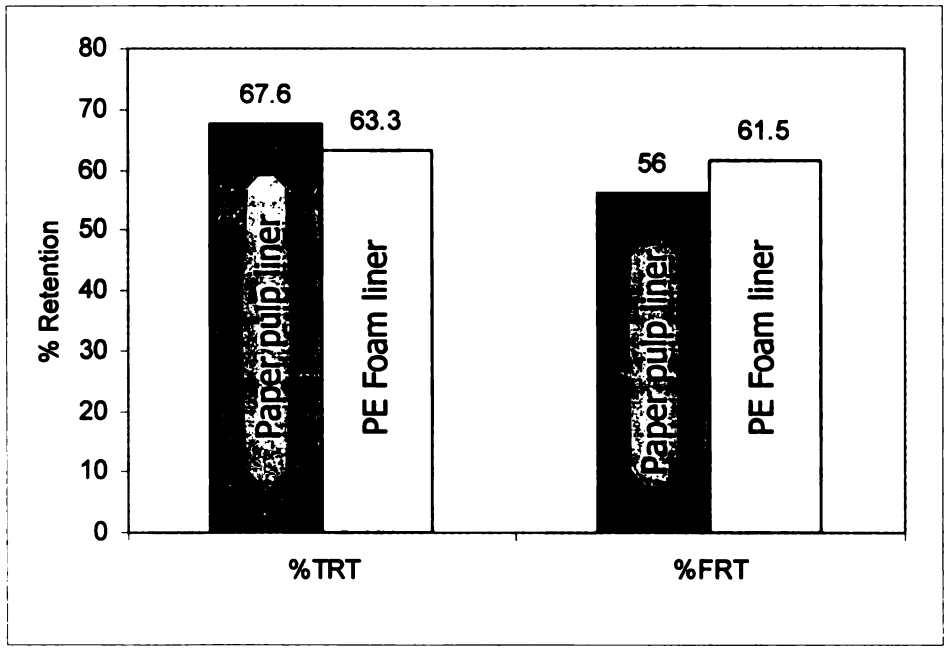

Figure 38 % FRT and % TRT of Systems at Standard Conditions at the End of 15 Minutes

5.6 Modeling the Relaxation Behavior of Container-Closure Systems

Determination of the seal integrity of container-closure systems during required shelf life is, in many cases, an essential part of packaging evaluations. Running actual storage tests (keeping the container-closure systems under actual or simulated environmental conditions) is an expensive and time consuming process. Often it is impossible to perform complete storage tests since the shelf life of packaged products is often more than a year. To reduce time and the amount of experimentation necessary to finish the long-term storage test, mathematical modeling is commonly used. Principally, the entire history of the stress relaxation of the polymer can be reconstructed by adding the stress histories that correspond to individual bits of a strain history (Matsuoka, 1992). Modeling the % FRT and % TRT of the systems is then based on the assumption

that if the model fits very well with the experimental data during 5-day relaxation, the reasonably predicted results beyond the experimental data can be obtained by extrapolating the model. In building the theoretical models, the effect of environmental conditions was excluded from the independent variable because there is no simple theory to explain this effect on the relaxation. It was found that the theoretical models derived from mechanical model using spring and dashpot are unsuccessful to describe the relaxation characteristics of the container-closure systems. The relaxation behavior obtained from the theoretical model levels off over time. In fact, the actual behavior of the systems continues to relax indefinitely. This is because the strain energy is continuously dissipated through the rearrangement of molecules into a lower free energy state causing the relaxation behavior to approach a nearly constant strain rate. Thus, the relaxation behavior is a continuous process. The spring and dashpot can mimic material behavior only under limited sets of conditions because the relaxation rate is only formulated by a first-order equation. In addition, if a model derived from spring and dashpot is made to fit a set of real relaxation data, it cannot fit the creep data for the same material. This shows that a model of springs and dashpots has a serious deficiency because a valid mathematical model must fit all experimental data without changing the values of the parameters. More complicated models can be derived from combinations of numbers of springs and dashpots but none of those can satisfy this simple requirement.

The relaxation of the container-closure systems is so far very complex behavior; more sophisticated theory is needed to model this behavior which may

not promise a success in modeling the relaxation behavior of the system and also may reduce simplicity of use in the application. In considering practical applications, an alternative approach using curve fitting techniques on the empirical model was then introduced to fit the experimental data of % FRT and % TRT as a function of one variable: time. The reason for choosing only one variable is the limitation of the experimental design which did not include the study of temperature and % relative humidity factors individually. Therefore, the effect of environmental conditions on the % FRT and % TRT cannot isolate the effect of temperature and % relative humidity from each other because they are confounded with each other. It may be that both temperature and % relative humidity contributed to a combined effect on the relaxation in this study. In this research, the form of the empirical model was decided according to these criteria:

a. Low error between the experimental and predicted values.
b. Simplicity of the model from a computational point of view.
c. The model should satisfy conditions at the extreme of independent variable.
d. The model should have no discontinuities in the range of practical values of the independent variable.

The coefficients of empirical models were then determined by using the curve fitting techniques presented in Chapter 4 and they are listed in Table 5. In addition, the predicted values of the % FRT and % TRT during storage over time

at three test conditions were calculated according to the coefficients of the models and plotted in comparison with the experimental data in Figures 39 to 50.

Table 5 Empirical Models for % FRT and % TRT of Container-Closure Systems

Model	System	Relaxation Indicator	Parameters	Adequacy of Fit
Model C $y = a + \frac{b}{(1 + k.x^{p})}$	Foam-refri	% FRT	a=37.74, b=62.26, k=0.89, p=0.28	Max error = 1.40%
		% TRT	a=-7.28, b=107.28, k=0.33, p=0.079	Max error = 3.12%
	Foam-std	% FRT	a=37.62, b=62.38, k=0.72, p=0.28	Max error = 1.16%
		% TRT	a=32.79, b=67.21, k=0.73, p=0.16	Max error = 0.90%
	Foam-trop	% FRT	a=34.99, b=65.01, k=0.94, p=0.29	Max error = 1.30%
		% TRT	a=-391.56, b=491.56, k=0.069, p=0.088	Max error = 0.54%
	Paper-refri	% FRT	a=35.14, b=64.86, k=0.91, p=0.32	Max error = 1.40%
		% TRT	a=-1458.33, b=1558.33, k=0.01, p=0.11	Max error = 6.12%
	Paper-std	% FRT	a=35.15, b=64.85, k=0.86, p=0.30	Max error = 1.63%
		% TRT	a=-319.95, b=419.95, k=0.051, p=0.088	Max error = 2.59%
	Paper-trop	% FRT	a=19.54, b=80.46, k=0.85, p=0.23	Max error = 1.97%
		% TRT	a=30.86, b=69.14, k=0.35, p=0.42	Max error = 0.71%
Model D $y = k.\ln x + c$	Foam-refri	% FRT	k=-2.76, c=66.41	r = 0.9911
		% TRT	k=-1.13, c=68.70	r = 0.8586
	Foam-std	% FRT	k=-3.03, c=69.90	r = 0.9949
		% TRT	k=-2.28, p=69.59	r = 0.9941
	Foam-trop	% FRT	k=-2.70, p=63.07	r = 0.9874
		%TRT	k=-4.14, p=71.55	r = 0.9989
	Paper-refri	% FRT	k=-2.73, c=62.34	r = 0.9749
		% TRT	k=-2.19, c=80.60	r = 0.7602
	Paper-std	% FRT	k=-2.70, c=63.60	r = 0.9824
		% TRT	k=-2.46, p=74.88	r = 0.9674
	Paper-trop	% FRT	k=-3.13, p=57.78	r = 0.9912
		% TRT	k=-4.77, p=75.85	r = 0.9908

Table 5 (cont'd).

Model	System	Relaxation Indicator	Parameters	Adequacy of Fit
Model E $y = y_n + k.\ln\left(\frac{x}{x_n}\right)$	Foam-refri	% FRT	k=-2.55, y_n=43, x_n=7200	r = 0.9865
		% TRT	k=-1.69, y_n=56, x_n=7200	r = 0.4880
	Foam-std	% FRT	k=-2.84, y_n=44, x_n=7200	r = 0.9342
		% TRT	k=-2.28, y_n=49, x_n=7200	r = 0.9941
	Foam-trop	% FRT	k=-2.53, y_n=40, x_n=7200	r = 0.9844
		% TRT	k=-4.25, y_n=34, x_n=7200	r = 0.6524
	Paper-refri	% FRT	k=-2.56, y_n=39, x_n=7200	r = 0.9865
		% TRT	k=-2.86, y_n=58, x_n=7200	r = 0.6524
	Paper-std	% FRT	k=-2.63, y_n=40, x_n=7200	r = 0.9819
		% TRT	k=-2.99, y_n=51, x_n=7200	r = 0.9016
	Paper-trop	% FRT	k=-3.13, y_n=30, x_n=7200	r = 0.9912
		% TRT	k=-4.39, y_n=35, x_n=7200	r = 0.9106

Notes: y = % FRT or % TRT and x = Time (min)

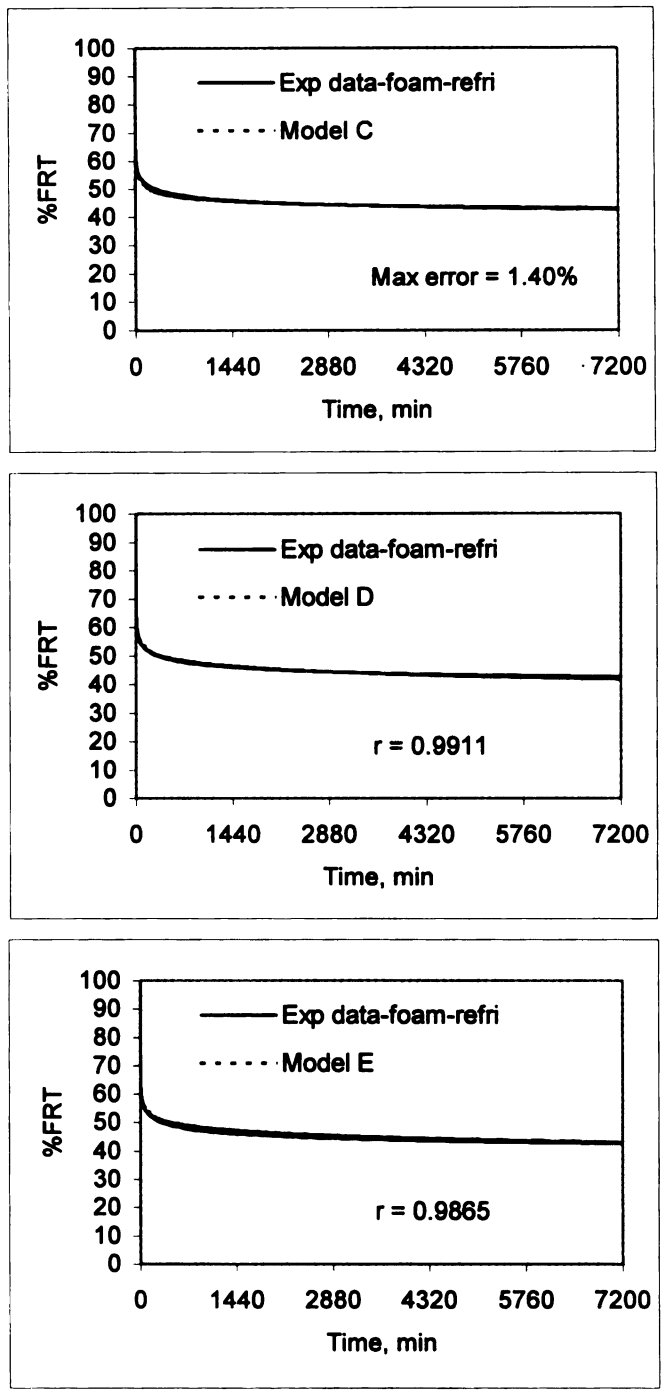

Figure 39 Comparison of Experimental and Predicted % FRT of PE Foam Liner at Refrigerated Conditions (Short-Term Prediction 5 Days)

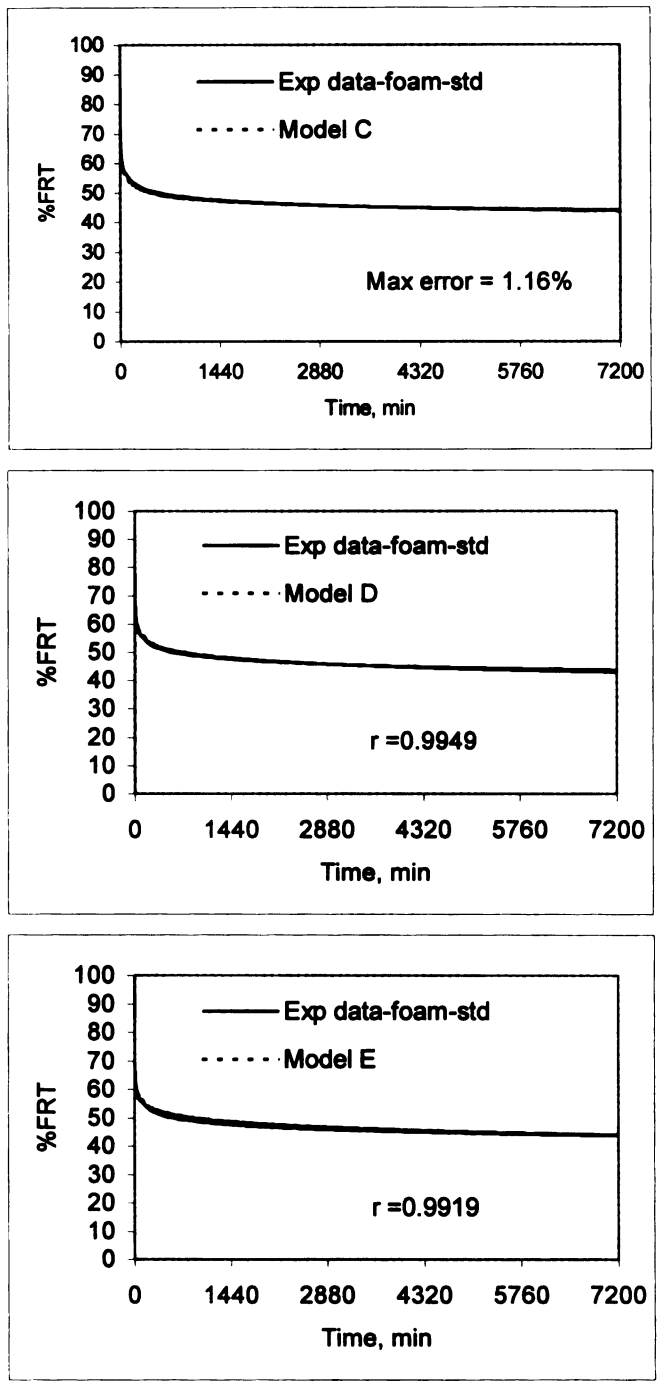

Figure 40 Comparison of Experimental and Predicted % FRT of PE Foam Liner at Standard Conditions (Short-Term Prediction 5 Days)

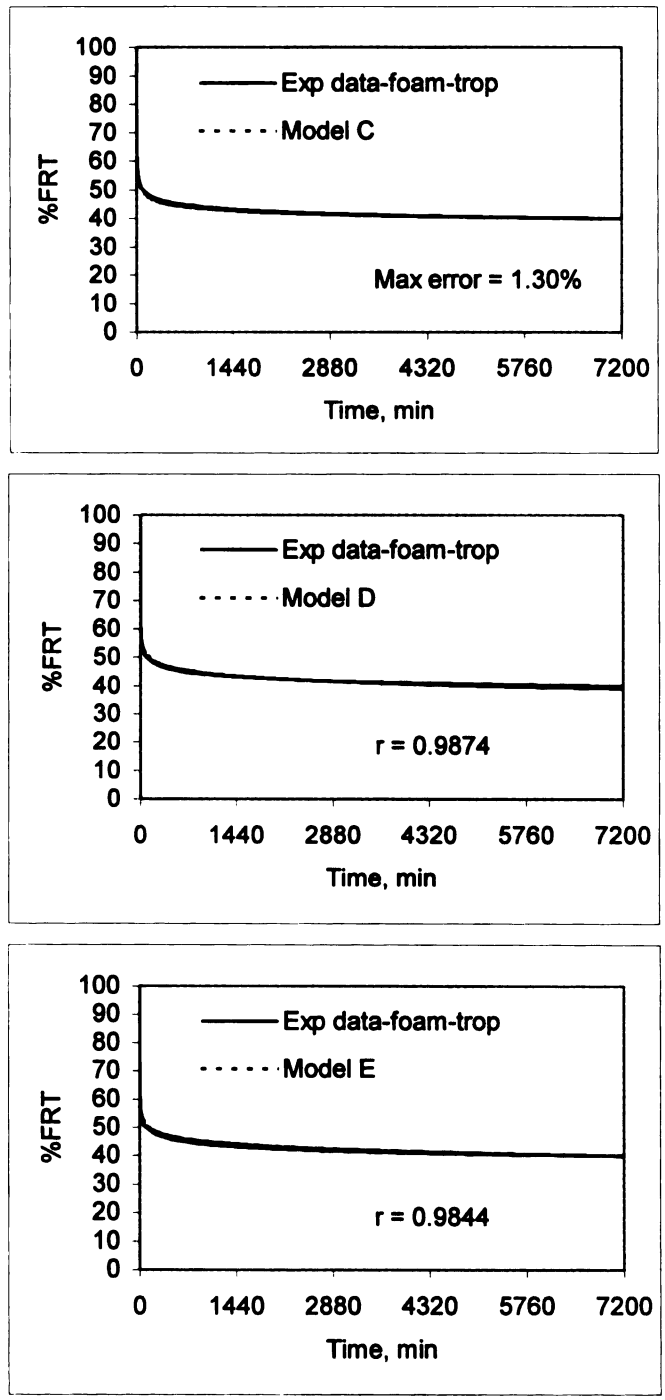

Figure 41 Comparison of Experimental and Predicted % FRT of PE Foam Liner at Tropical Conditions (short-term prediction 5 Days)

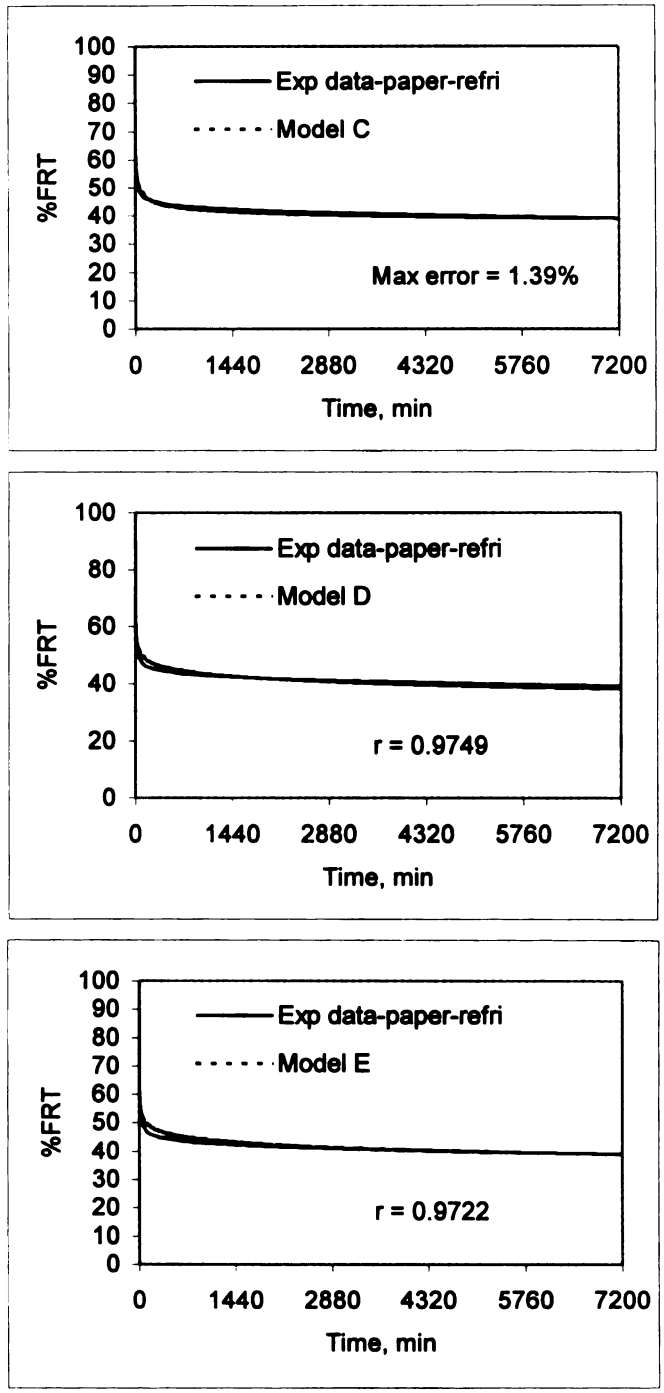

Figure 42 Comparison of Experimental and Predicted % FRT of Paper Pulp Liner at Refrigerated Conditions (Short-Term Prediction 5 Days)

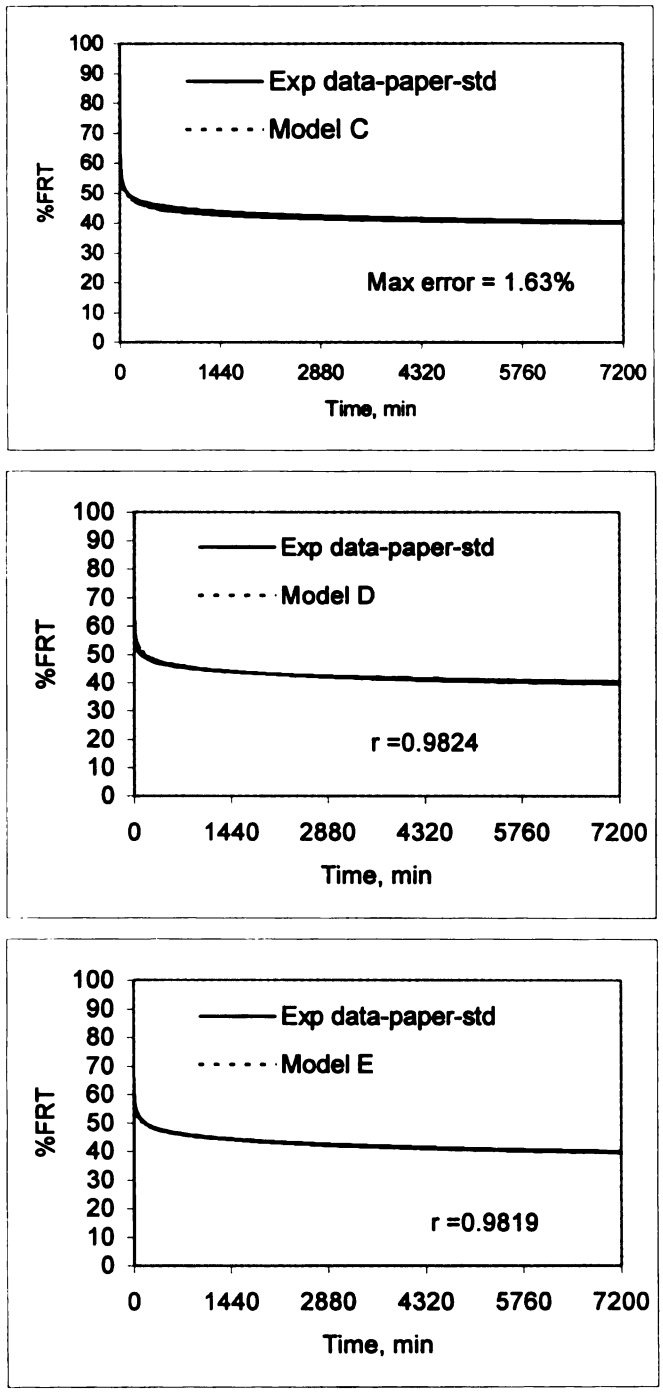

Figure 43 Comparison of Experimental and Predicted % FRT of Paper Pulp Liner at Standard Conditions (Short-Term Prediction 5 Days)

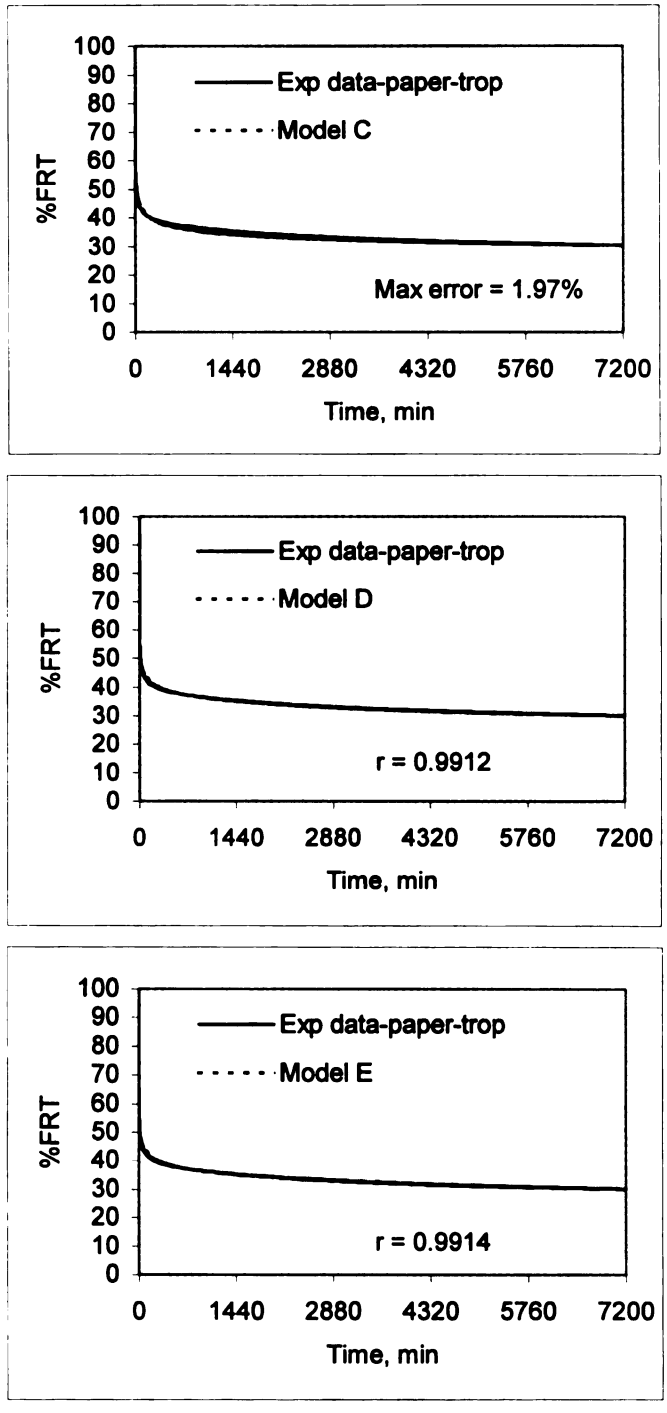

Figure 44 Comparison of Experimental and Predicted % FRT of Paper Pulp Liner at Tropical Conditions (Short-Term Prediction 5 Days)

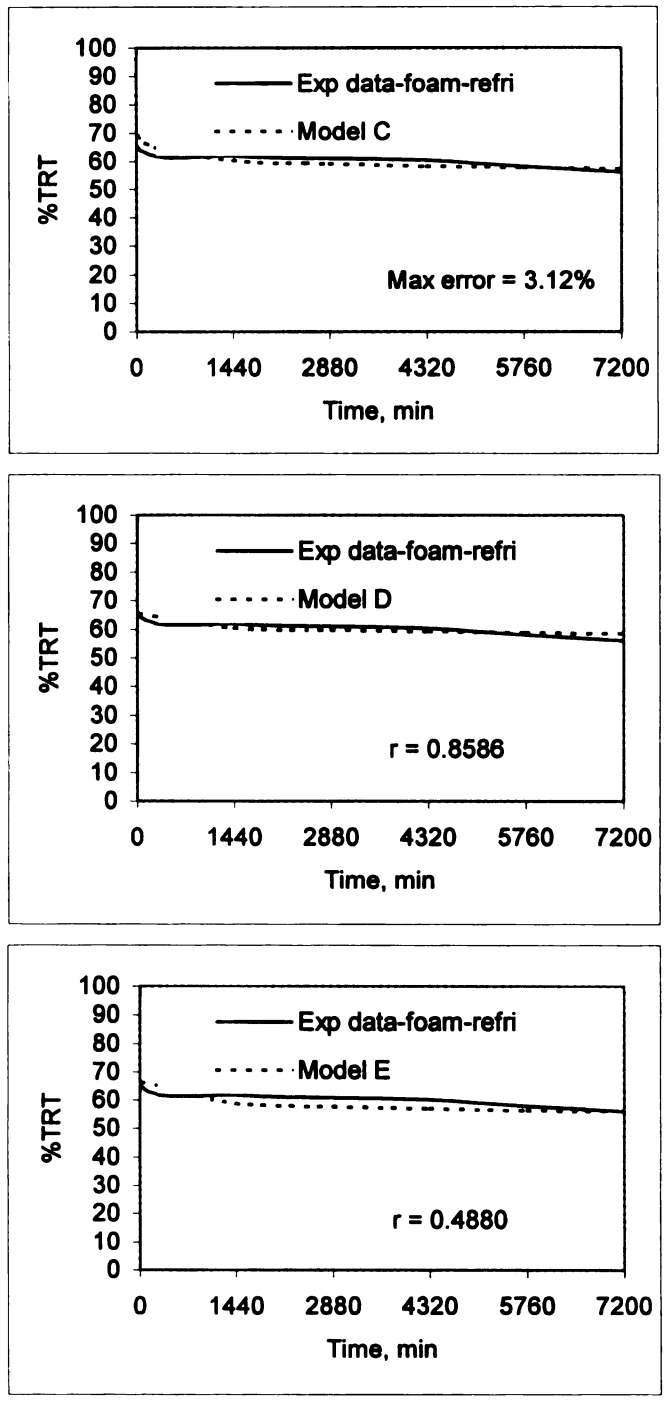

Figure 45 Comparison between Experimental and Predicted % TRT of PE Foam Liner at Refrigerated Conditions (Short-Term Prediction 5 Days)

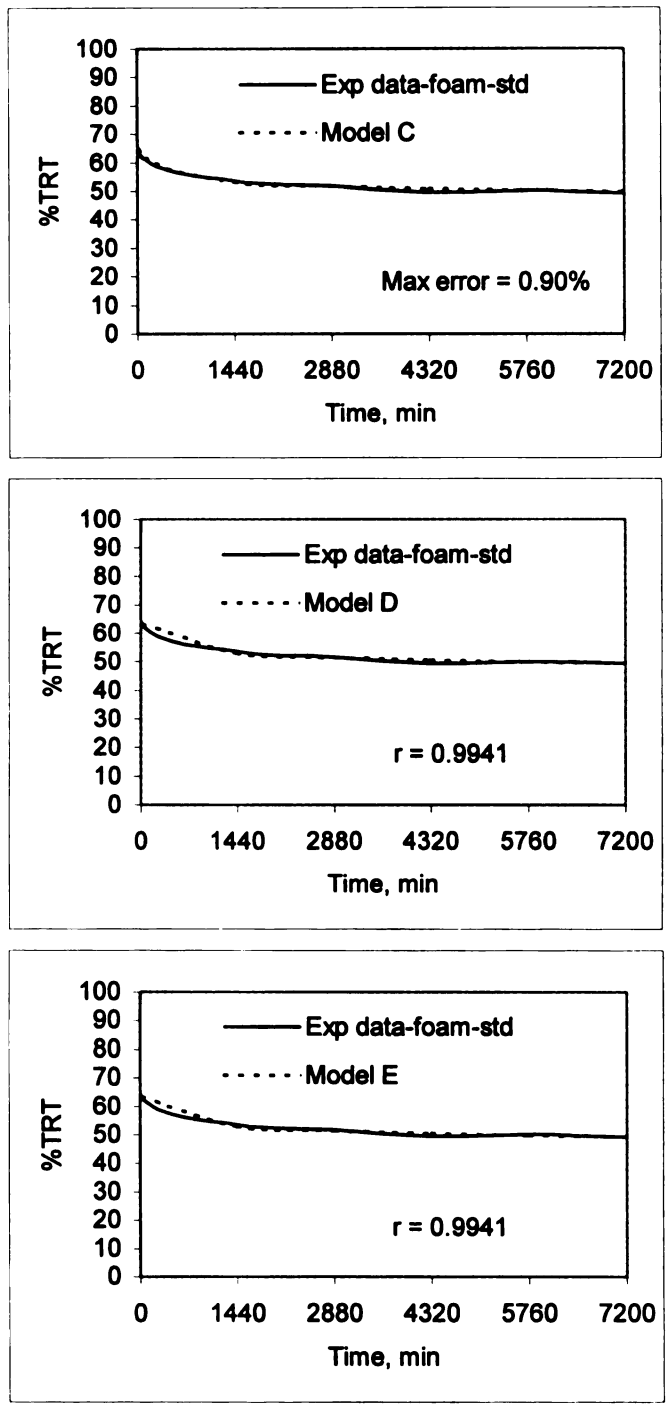

Figure 46 Comparison between Experimental and Predicted % TRT of PE Foam Liner at Standard Conditions (Short-Term Prediction 5 Days)

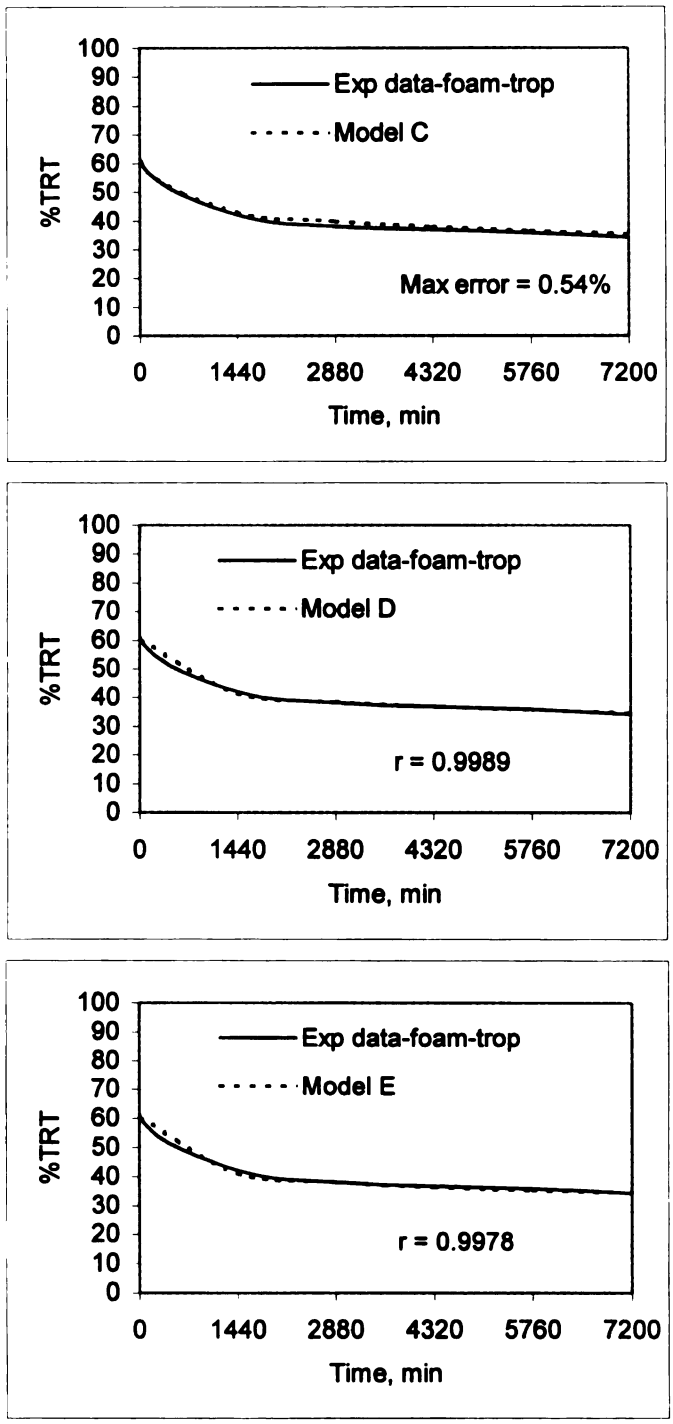

Figure 47 Comparison between Experimental and Predicted % TRT of PE Foam Liner at Tropical Conditions (Short-Term Prediction 5 Days)

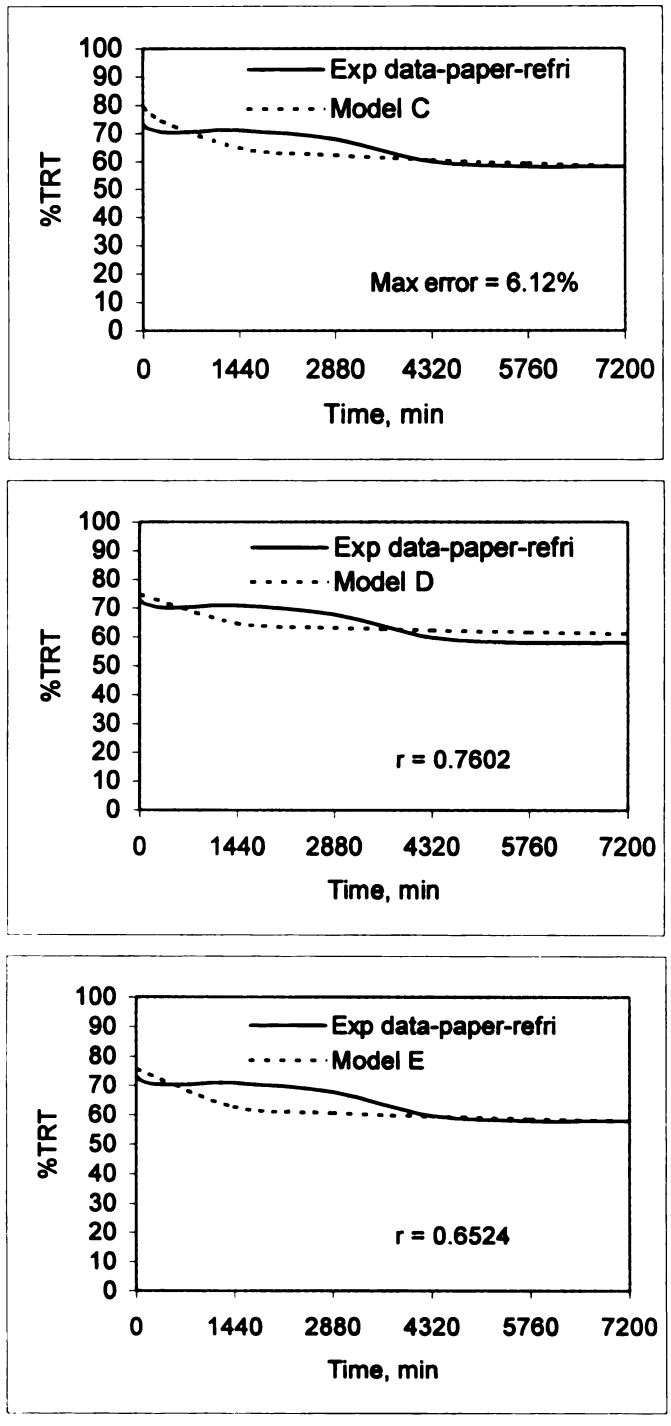

Figure 48 Comparison between Experimental and Predicted % TRT of Paper Pulp Liner at Refrigerated Conditions (Short-Term Prediction 5 Days)

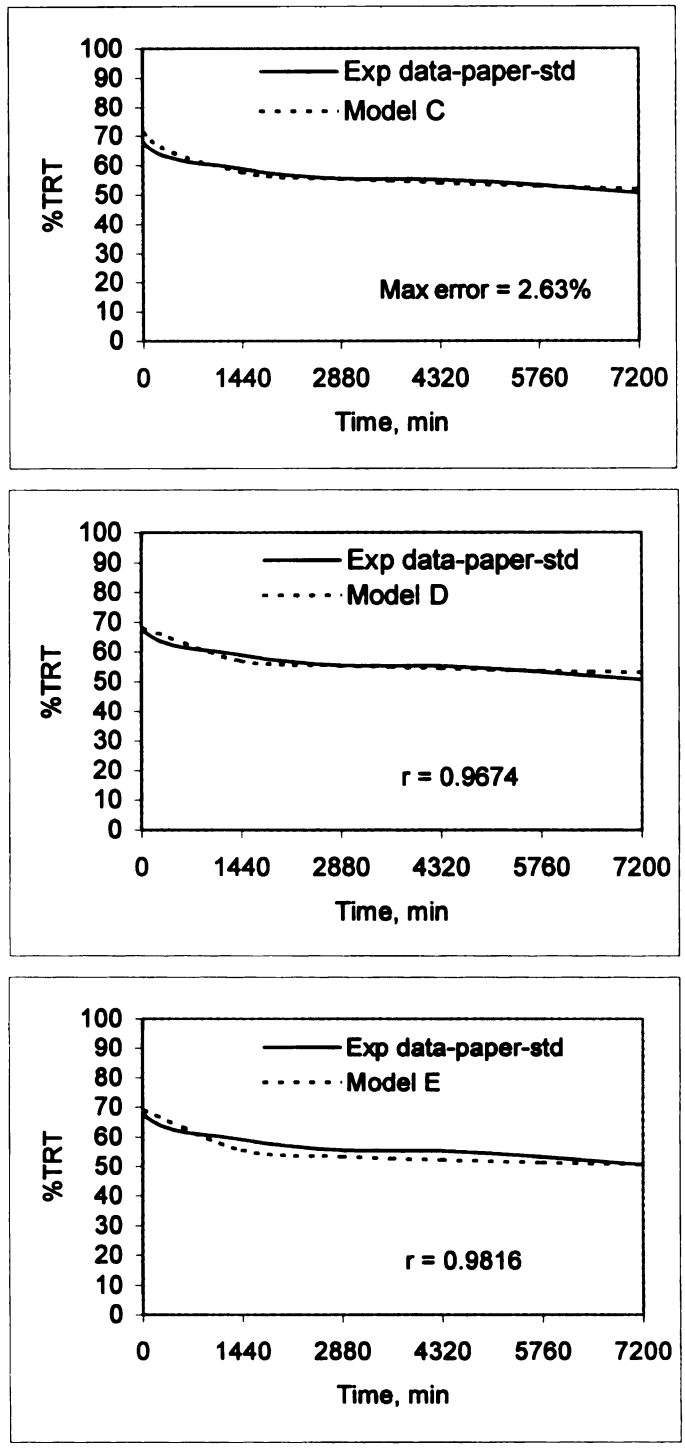

Figure 49 Comparison between Experimental and Predicted % TRT of Paper Pulp Liner at Standard Conditions (Short-Term Prediction 5 Days)

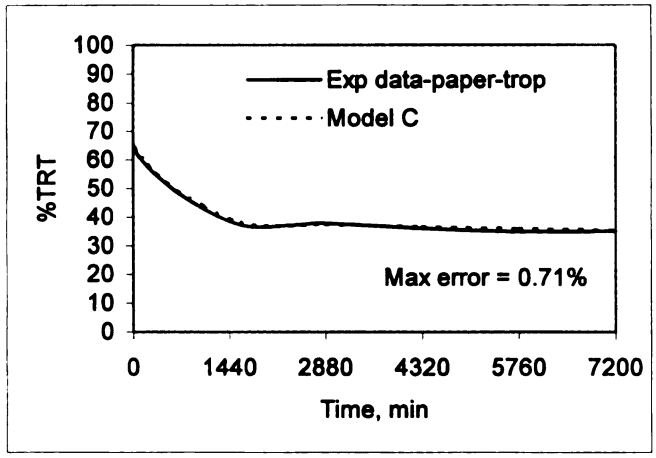

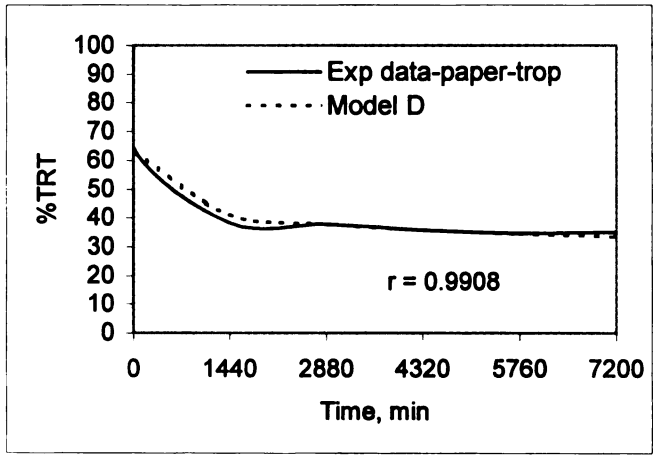

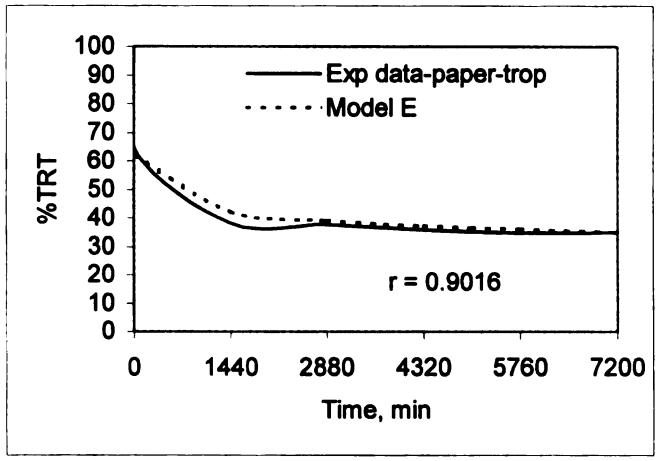

Figure 50 Comparison between Experimental and Predicted % TRT of Paper Pulp Liner at Tropical Conditions (Short-Term Prediction 5 Days)

In comparing the experimental and predicted values of % FRT and % TRT over time at test conditions, it can be seen that generally, the predicted results of % FRT obtained from all three models are in excellent agreement with those determined experimentally. Even so, the models show a poorer fit when used to predict the % TRT over time especially for the systems stored at refrigerated conditions. This is because the % TRT data from one point to the next point fluctuated during the first 3 days and dropped down quickly later. A possible explanation is that the amount of moisture in the air at refrigerated conditions is low which will take a longer time for the moisture passing through the container-closure systems to reach equilibrium stage compared with other conditions. This moisture affects the static coefficients of friction of the systems which contribute to the removal torque. Hence, during the first 3 days, the amount of moisture in the systems might not reach the equilibrium yet, thus causing the fluctuations of the measuring results. In addition, regarding the limitation of the measuring technique, the removal torque was measured on different container-closure systems every time; this would contribute to high variability as well. However, based on the adequacy of fit, the models proposed are still acceptable for predicting the % TRT over time. Overall, the comparisons suggest that the empirical model provides the best fit for modeling the relaxation behavior of the container-closure systems.

It is important to note that the empirical models of % FRT and % TRT are proposed for predicting long term response; thus, it makes sense to focus on the last data point which is least sensitive to the error made at the beginning such as

experimental error. This can be done by forcing fit through the last data point and these forced fit models are expected to provide a better extrapolated long term response. This is the philosophy behind model C and E. It is also worthwhile to continue a discussion on model D and E which are semi-log models. These were primarily initiated from examination of the relaxation curves of the container-closure systems which indicated that the % FRT and the % TRT decrease rapidly during the first fifteen minutes and then continue to drop down at slower rate indefinitely. Thus, it is logical to formulate a simple linear model by using a logarithmic time scale which is the basis for model D and E. Plots of the % FRT and % TRT on a logarithmic time scale in Figures 51 and 52 substantiate this concept. A linear relationship is observed from Figure 51; the container-closure systems response at all test conditions is simple linear regression, therefore. It is also obvious that these % FRT curves have almost similar shape to each other, which is theoretically possible to apply a superposition principle for developing a master curve of the container-closure systems at test conditions. This would be an interesting area for future researches. There was a possible source of error that lies in using the linear regression for modeling the systems. The rate of % FRT change in log of time is averaged out of the set of data as indicated in the slope of the equation, whereas the actual curves show that the actual rate of % FRT change slowly changes over time. This may introduce an error in long term prediction of the % FRT and % TRT.

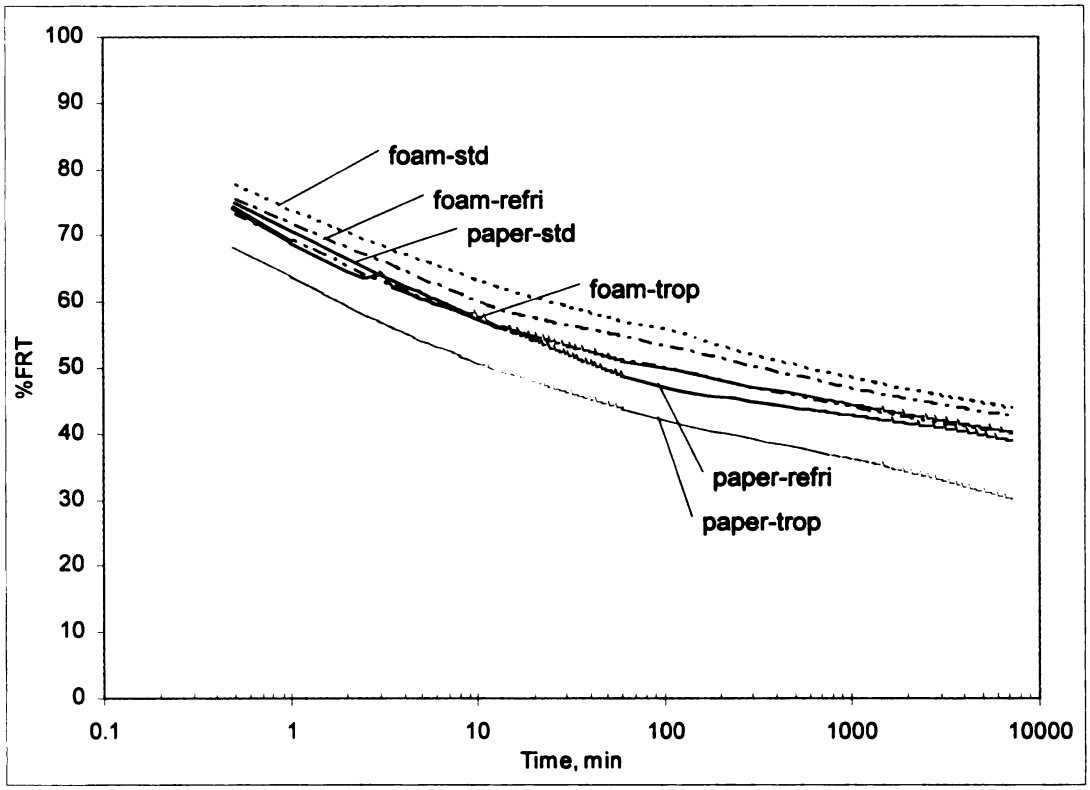

Figure 51 % Experimental FRT as a Function of Logarithmic Time

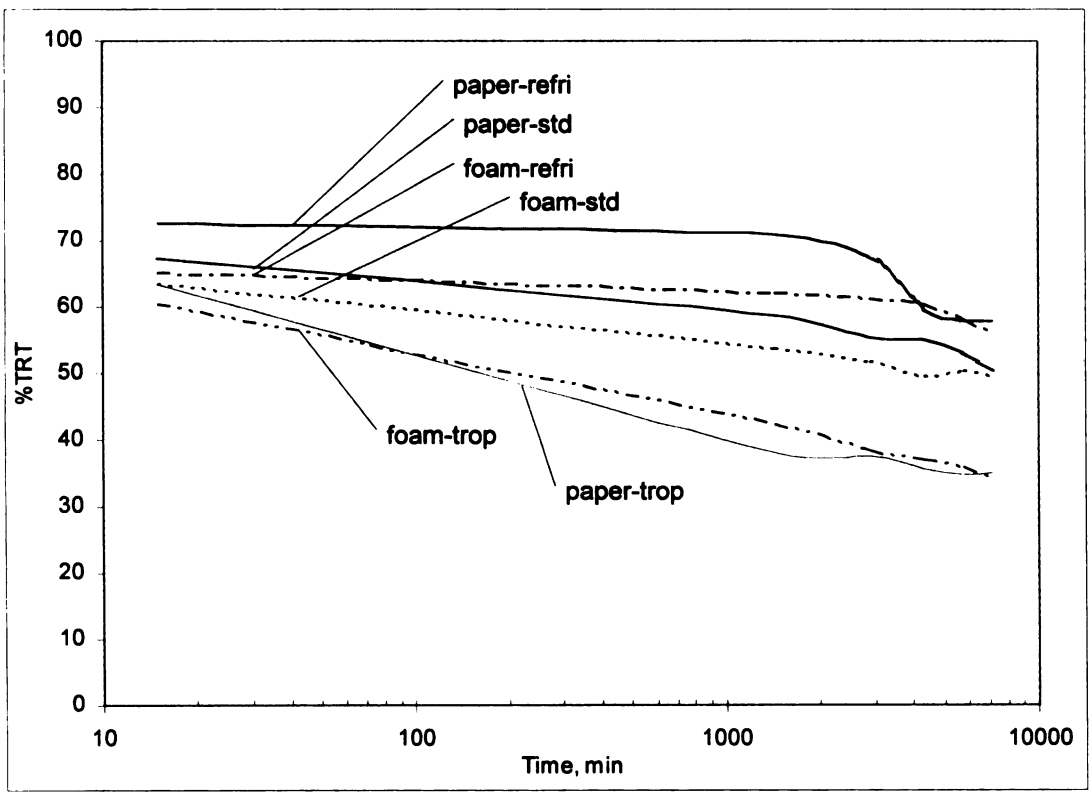

Figure 52 % Experimental TRT as a Function of Logarithmic Time

Regarding to the excellent short-term prediction results from the models, it is confident to use the models developed for long-term prediction of % FRT and % TRT. The predicted results of 3-year prediction were tabulated in Table 6 and plotted in Figures 53 to 56.

Table 6 Predicted Values of % FRT and % TRT for Long-term Prediction

Relaxation indicator	System	Model	Predicted Value					
			15 min.	5 days	30 days	1 year	2 years	3years
% FRT	Foam-refri	C	59.1	43.0	41.0	39.4	39.1	39.0
		D	58.9	41.9	36.9	30.0	28.1	27.0
		E	58.8	43.0	38.4	32.1	30.3	29.3
	Paper-refri	C	55.6	39.0	37.4	36.2	36.0	35.9
		D	55.0	38.1	33.2	26.4	24.5	23.4
		E	54.8	39.0	34.4	28.0	26.2	25.2
	Foam-std	C	62.2	44.0	41.7	39.7	39.3	39.2
		D	61.7	43.0	37.6	30.0	27.9	26.7
		E	61.5	44.0	38.9	31.8	29.8	28.7
	Paper-std	C	57.3	40.0	38.1	36.6	36.3	36.2
		D	56.3	39.6	34.7	28.0	26.1	25.0
		E	56.2	40.0	35.3	28.7	26.9	25.8
	Foam-trop	C	56.4	40.0	38.1	36.5	36.3	36.1
		D	55.8	39.1	34.2	27.5	25.6	24.5
		E	55.6	40.0	35.5	29.1	27.4	26.4
	Paper-trop	C	50.7	30.2	26.9	23.9	23.3	23.0
		D	49.3	30.0	24.4	16.6	14.4	13.1
		E	49.3	30.0	24.4	16.6	14.4	13.1
% TRT	Foam-refri	C	68.9	57.2	53.5	48.3	46.8	46.0
		D	65.6	58.6	56.6	53.7	53.0	52.5
		E	66.4	56.0	53.0	48.7	47.6	46.9
	Paper-refri	C	78.8	58.2	49.2	33.5	28.3	25.2
		D	74.7	61.1	57.2	51.7	50.2	49.3
		E	75.7	58.0	52.9	45.7	43.7	42.6
	Foam-std	C	64.4	49.7	46.3	42.6	41.7	41.2
		D	63.4	49.4	45.3	39.6	38.0	37.1
		E	63.1	49.0	44.9	39.2	37.6	36.7
	Paper-std	C	71.1	52.1	45.0	34.0	30.7	28.8
		D	68.2	53.0	48.6	42.5	40.8	39.8
		E	69.5	51.0	45.6	38.2	36.1	34.9
	Foam-trop	C	60.4	35.5	26.1	11.2	6.7	3.9
		D	60.3	34.8	27.4	17.0	14.2	12.5
		E	60.3	34.0	26.4	15.8	12.8	11.1
	Paper-trop	C	64.1	35.5	33.1	31.7	31.5	31.4
		D	62.9	33.5	24.9	13.0	9.7	7.7
		E	62.1	35.0	27.1	16.2	13.1	11.4

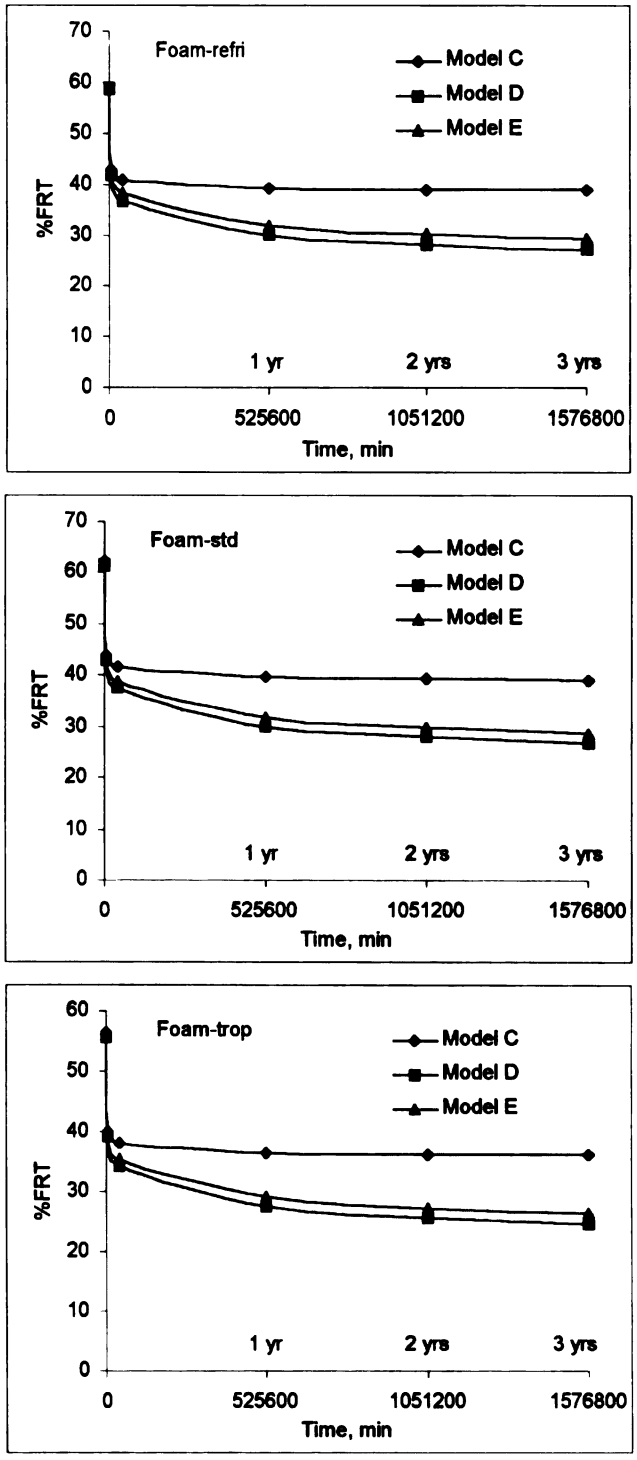

Figure 53 Long-Term Prediction of % FRT Values for PE Foam Liner

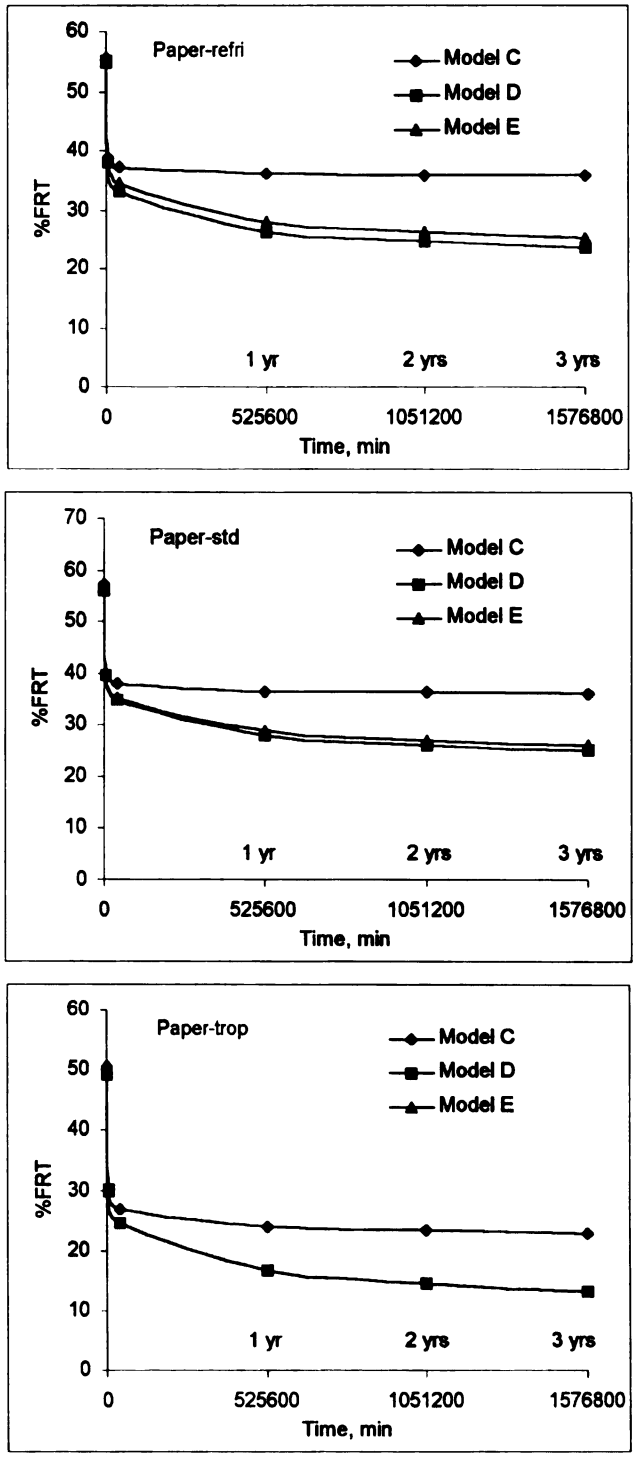

Figure 54 Long-Term Prediction of % FRT Values for Paper Pulp Liner

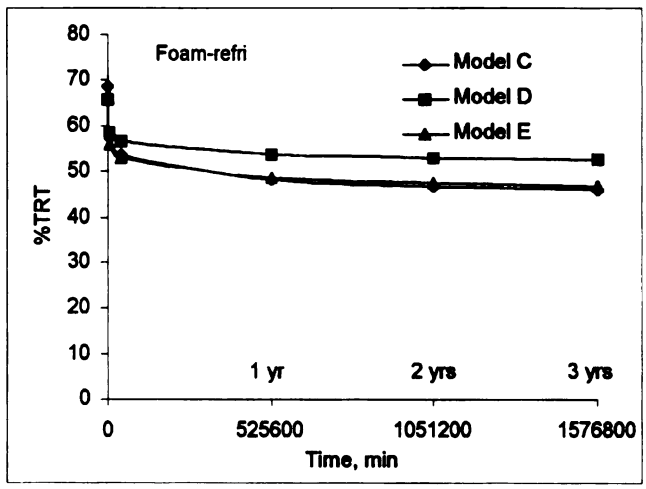

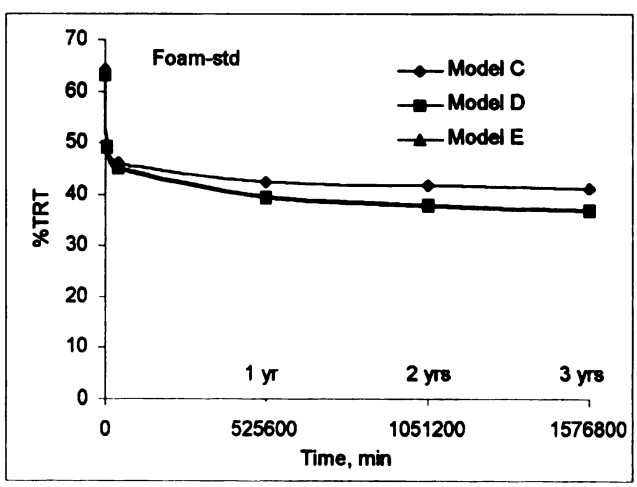

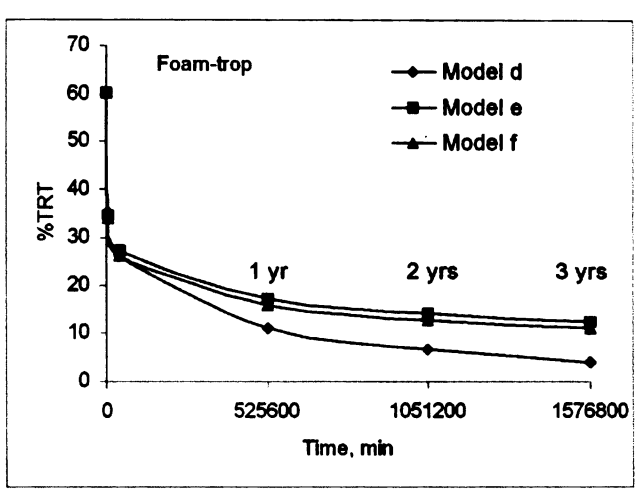

Figure 55 Long-Term Prediction of % TRT Values for PE Foam Liner

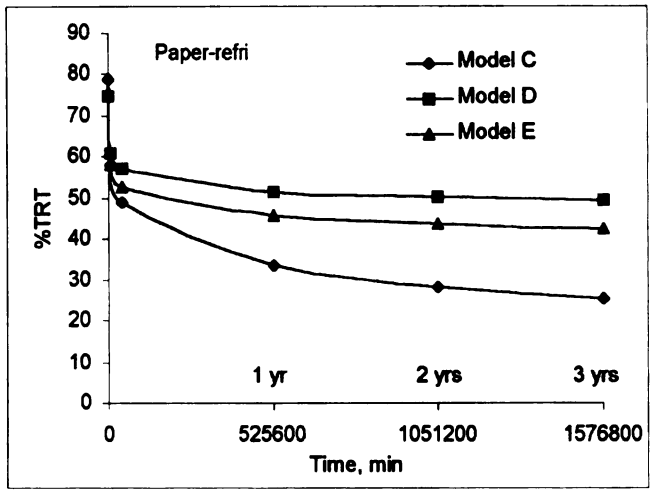

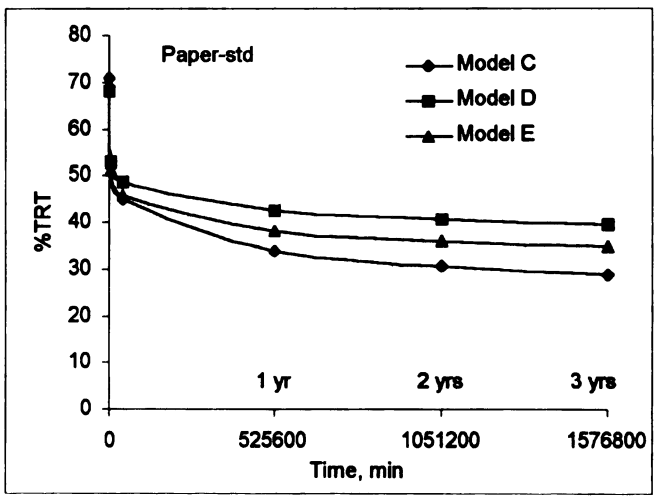

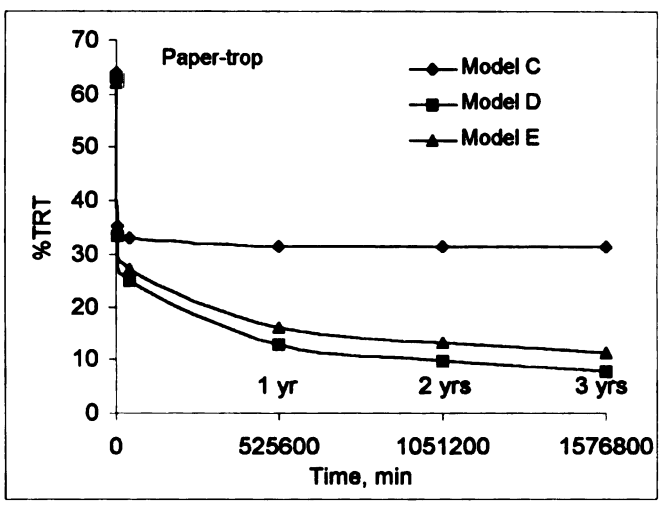

Figure 56 Long-Term Prediction of % TRT Values for Paper Pulp Liner

The predicted results in Table 6 (page 97) show that the % FRT obtained from models C, D and E agree with each other. There is no significant difference of predicted % FRT values among the systems at test conditions except for the paper pulp system at tropical conditions which shows a significantly lower value; the results agree with the experimental results of 5-day relaxation which indicates the consistency of the predictive models. It was found that the models (C, D and E) show excellent agreement of the results for short time prediction (less than 30 days). Then, as the prediction period is longer, the algorithms of models C, D and E appear to show the effect on the predicted % FRT values. This is because the accumulation of deviation of the predicted results among the models over time. The predicted results from model C tend to be higher than the semi-log models (D and E) around 10% at the end of year 3. The predicted result is still in the acceptable range for agreement among the models. However, the experimental data to support the predicted results for long-term prediction is not available. The validity of the long-term prediction must be conducted in the future research.

The quality of the input data from relaxation experiment affects the accuracy and agreement of the predicted results obtained from models C, D and E. This can be noticed in the predicted % TRT values in Table 6. The predicted values show fairly high variation from model to model up to 24% especially between model C and models D and E. This is the result of fluctuations of input % TRT data which can be explained by the nature of removal torque measurement. A general conclusion can be drawn from the predicted values that

at 3-year relaxation, the systems stored at refrigerated conditions have the highest % TRT value whereas the systems stored at tropical conditions retain the lowest % TRT value. This conclusion also corresponds to the experimental results of 5-day relaxation (short-term prediction).

The analysis of predicted values from models C, D and E was performed further to compare between the % FRT and % TRT at 3-year relaxation. The results of each model were plotted as bar graphs as shown in Figures 57, 58 and 59. The predicted values obtained from model C indicate that there is not much difference between the predicted % FRT and % TRT values except for the PE foam system at tropical conditions. On the other hand, the predicted values obtained from models D and E show that overall, the % TRT is higher than the % FRT except for the systems at tropical conditions. Therefore, it can be concluded that for long-term storage at standard conditions, for the same container-closure system the % TRT tends to be higher than the % FRT. There is not much difference when comparing between the % FRT of PE foam liner and % FRT of paper pulp liner. The same result also found when comparing between the % TRT of PE foam liner and %TRT of paper pulp liner.

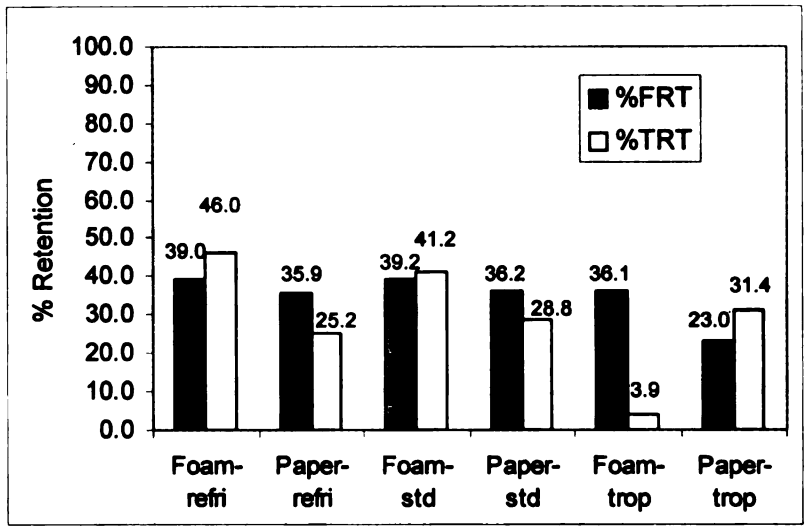

Figure 57 Comparison of Predicted % FRT and % TRT at 3 years using Model C

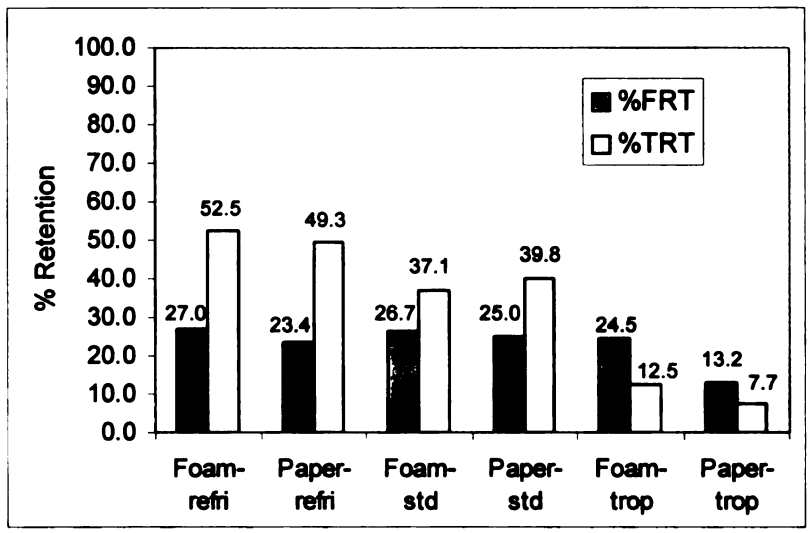

Figure 58 Comparison of Predicted % FRT and % TRT at 3 years using Model D

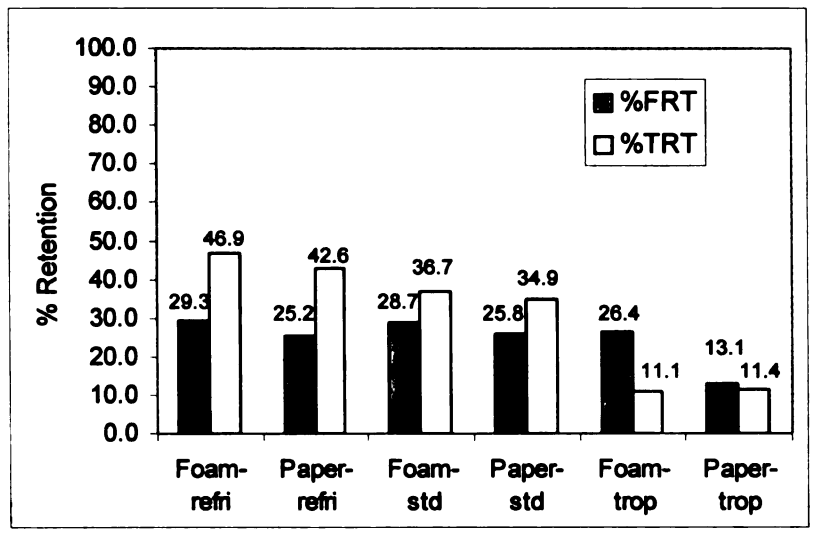

Figure 59 Comparison of Predicted % FRT and % TRT at 3 years using Model E

Modeling of relaxation behavior of container-closure systems was then extended to improve the torque-friction model (Equations 2 and 3). The idea of improvement is to combine this theoretical model based on the equations of equilibrium which is inadequate to describe the relaxation behavior with the empirical model of the coefficients of friction at thread interface and liner interface. According to the torque-friction model (Equations (2) and (3), the time dependent and nonlinear terms are not included in the original equation. These terms were planned to impose on the coefficients of friction terms in Equations (2) and (3). To do this, it is necessary to acquire and check the data of both coefficients over time from the experimental results before modifying the model. Data for coefficient of friction at the thread interface were deduced from the torque-friction model by using the input data of sealing force during storage over time from the measuring device and removal torque over time during storage from the actual system as shown in Figure 60. It was found that the coefficient increased over time from 0.33 at 15 min to 0.431 at day 5 and the coefficient obtained from this method is a lot higher than using the method developed from a previous study (Pisuchpen, 2000).

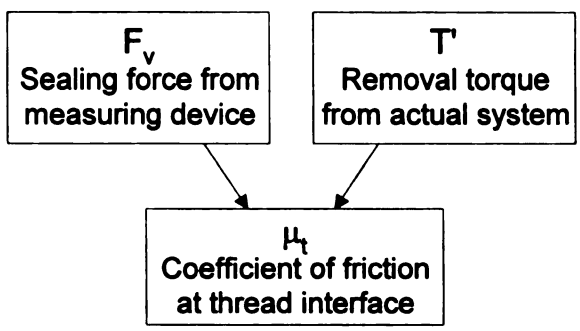

Figure 60 Coefficient of Friction at Thread Interface determined from Sealing Force Measuring Device and Actual System

Data of the coefficient of friction at liner interface were also deduced from the torque-friction model but using the input data of removal torque over time from the actual system and coefficient of friction at thread interface and sealing force over time from the measuring device as shown in Figure 61. Verification of the data shows that negative values of coefficient of friction at the liner interface were found.

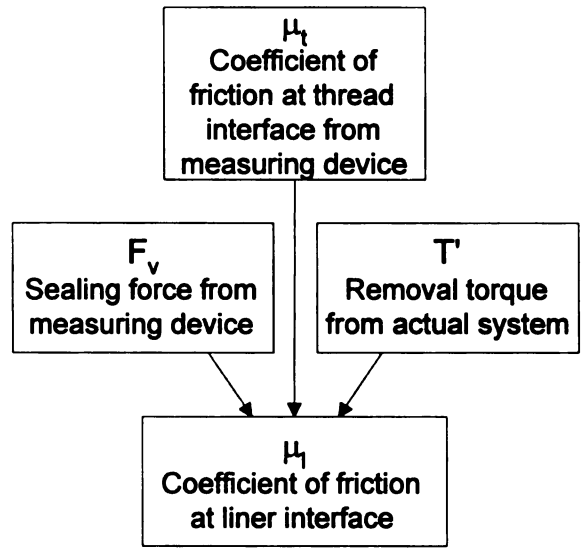

Figure 61 Coefficient of Friction at Liner Interface determined from Sealing Force Measuring Device and Actual System

In doing this, we tried to add every part of the input energy applied in the torque-friction model to end up as friction loss. This is because the equations have only the coefficients of friction term that contributes to the loss of input energy. The negative values of the coefficient were attributed to the error from either the method to deduce the data or the torque-friction model itself. This suggests that the simple modification as described on the torque-friction model is unable to provide a satisfactory. Elaboration on the time dependent properties of

the torque-friction model with other approaches is needed in order to make the model showed relaxation behavior.

6. CONCLUSIONS, RECOMMENDATIONS AND FUTURE WORKS

This new technique for measuring sealing force of container-closure systems using a strain gage based transducer offers an alternative way to measure and verify the mechanical seal integrity of the systems. Although the removal torque is widely used through out the industry, it sometimes provides high variation results in some container-closure systems. On the other hand, the sealing force shows the consistent results and is considered as a direct indicator compared to the removal torque. The technique developed in this research can be applied to other types of container-closure systems; in addition, the test fixtures were also proposed as a simple technique for study of the relaxation behavior of container-closure systems. The sealing force measuring device in combination with a torque meter was employed in this research to study the effect of environmental conditions on the relaxation behavior of container-closure systems. The responses over time from both devices transformed to the % force retention (FRT) and % torque retention (TRT) were used to analyze the effect of environmental conditions.

The results of this investigation show that only the relaxation (% FRT and % TRT) of the systems stored at tropical conditions especially the paper pulp system was significantly higher than the relaxation of other conditions. The high temperature and high relative humidity of the environment play a significant role in the relaxation behavior of the systems. The % TRT data were less consistent than the % FRT data. Comparing between the % FRT and % TRT, the relaxation results obtained from the % TRT were less than the % FRT which disagrees with

the theory based on the equations of equilibrium (Pisuchpen, 2000). Therefore, using the removal torque or % TRT may be misleading in the interpretation of the seal integrity of the container-closure systems. This finding may explain in some cases, the leakage problem found in container-closure systems having high removal torque.

In attempting to predict a long-term relaxation of container-closure systems based on mathematical models, it was found that the theoretical models derived from spring and dashpot are not applicable. The empirical models using curve fitting techniques were then suggested for modeling the relaxation behavior of the systems. Excellent fits were obtained from % FRT and % TRT of short-term prediction (5 days). The results were extended to long-term prediction by extrapolating the same models to 3 years. The predicted results were found in the acceptable range. However, the experimental data to support the long-term prediction from the models is not available. Future research must be done in order to verify the predicted results. From simplicity of the mathematical operation, the semi-log model: model D was suggested to use in general applications to the relaxation behavior of the systems. Despite the benefit of modeling in long-term prediction, it must be realized that accuracy of the predicted results relies on the accuracy of the input data of the models. Thus, the errors from experimentation and human should be minimized and controlled. The concept of modeling in this research can be applied to other cases which undergo the relaxation behavior.

Recommendations and Future Works

Implication of the technique developed in this research is immense since it introduces a new concept in monitoring the mechanical seal integrity of the container-closure systems. The concept of this technique can be applied to develop the sealing force measuring device for other types of closure-container system. It is important to note that the sealing force measuring device is designed only to measure the sum of all forces acting at the thread and liner interface. Hence, uniformity of the distributed sealing forces around the contact area should be measured additionally by other techniques in order to have complete information about seal integrity of the systems. It should be emphasized that the present investigation was based on limited data sets and types of container-closure system; more research is needed to check the validity of the models and to investigate their precision. More input data over time would probably increase the precision and make the models suitable for a large range of prediction. The future growth expected in this area will be the combination of this technique with other analytical methods such as permeation test and package leak detection in which the results can be used to correlate the physical parameter (% FRT) and the product-package parameters (permeability and leak rate). Further refinement on the modeling of long-term relaxation behavior will be also needed. Appropriate solutions to combine the theoretical model with the empirical model are needed in order to develop standard parameters for material used in the container-closure systems. Another crucial area that will demand attention is to generate master curves of relaxation behavior of container-closure

systems which will provide useful information for estimating the seal integrity of the container-closure systems during service time.

APPENDIX

THE COMPUTER PROGRAM FOR MODEL C

```
10 REM: FITS  Y=A+B/(1+K*X^P)  TO N (X,Y)'s
20 REM: CREEP/RELAXATION MODEL: Y goes from 100 to F as X goes from 0
to infinity
30 READ N,F : DIM X(N),Y(N) 'open arrays X and Y for data
40 FOR I=1 TO N : READ X(I),Y(I) : NEXT I 'read N data
50 DATA N, F 'number of data (N), value of the last data point (F%) for fit
60 DATA X, Y 'user inputs data: x = time, y = %FRT or %TRT, for example x, y is
0, 100
70 MIN=10000 'search for fit with smallest maximum error for all P,K
80 FOR K=.703 TO .705 STEP .0001 : FOR P=.172 TO .174 STEP .0001 'user
varies K and P in desired step in order to minimize the error between actual
value of y and calculated value of y.
90 BIG=0 : FOR I=1 TO N 'BIG is largest error for a given K,P
100 A=F-(100-F)/(K*X(N)^P) : B=100-A
110 ER=ABS(Y(I)-A-B/(1+K*X(I)^P)) 'error at Ith data point
120 IF ER>BIG THEN BIG=ER 'call "BIG" the largest error for given K,P
130 NEXT I
140 IF BIG>=MIN THEN 160 'compare BIG's for every possible K,P
150 MIN=BIG : K0=K : P0=P 'remember the K and P with smallest BIG
160 NEXT P : NEXT K
170 PRINT "   k=";K0;"     p=";P0;"     max error=";MIN
180 'LIST 80
```

```
190 GOTO 280
200 FOR J=1 TO N/20 : INPUT Z 'meaningless input to slow down printout
210 PRINT " I          X          given Y      fitted Y      error"
220 FOR I=20*(J-1)+1 TO 20*J
230 A=F-(100-F)/(K*X(N)^P) : B=100-A
240 YI=A+B/(1+K0*X(I)^P0)
250 PRINT I,X(I),Y(I),YI,YI-Y(I)
260 NEXT I
270 NEXT J
280 PRINT "A=";A";    B=";B;"    K0*X(N)^P=";K0*X(N)^P0
290 INPUT "give a time in days";XX
300 XX=XX*24*60 : YI=A+B/(1+K0*XX^P0) : PRINT "Y=";YI
310 GOTO 290
```

THE COMPUTER PROGRAM FOR MODEL D

```
10 REM: FITS Y=K*LNX+C, TO N (X,Y)'s
20 REM: user makes changes to line 60
30 READ N : DIM X(N),Y(N) 'open arrays X and Y for data
40 FOR I=1 TO N : READ X(I),Y(I) : NEXT I 'read N data
50 DATA N ' user inputs number of data
60 DATA   X, Y 'user inputs data: x = time, y = %FRT or %TRT, for example x, y
is 0, 100
70 SX=0 : SY=0 : SXX=0 : SXY=0 : SYY=0 : SSE=0 'initialize sums
80 FOR I=1 TO N 'form sums
90 SX=SX+LOG(X(I))/N : SY=SY+Y(I)/N : SXY=SXY+LOG(X(I))*Y(I)/N
100 SXX=SXX+LOG(X(I))*LOG(X(I))/N : SYY=SYY+Y(I)*Y(I)/N
110 NEXT I
120 K=(SXY-SX*SY)/(SXX-SX*SX) : C=SY-M*SX 'slope, y-intercept
130 R=ABS(M)*SQR((SXX-SX*SX)/(SYY-SY*SY)) 'correlation coefficient
140 FOR I=1 TO N : SSE=SSE+(Y(I)-M*LOG(X(I))-B)^2 : NEXT I 'sum of
squares of errors
150 PRINT "   y=k*lnx+c    fit to";N;"data"
160 PRINT : PRINT "   k=";K;"     c=";C
170 PRINT : PRINT " x          given y      predicted y=k*lnx+c"
180 FOR I=1 TO N : PRINT X(I),Y(I),K*LOG(X(I))+C : NEXT I
190 PRINT : PRINT "  correlation coefficient R=";R
200 PRINT "  sum of squares of errors SSE=";SSE
```

```
210 PRINT "  rms error = sqr(SSE/N)=";SQR(SSE/N)
220 END
```

THE COMPUTER PROGRAM FOR MODEL E

```
10 REM: FITS  Y=Yn+K*LN(X/Xn) TO N (X,Y)'s
20 N=6 : DIM X(N),Y(N) 'open arrays X and Y for data
30 FOR I=1 TO N : READ X(I),Y(I) : NEXT I
40 DATA X, Y 'user inputs data: x = time, y = %FRT or %TRT, for example x, y is
0, 100
50 S1=0 : S2=0 : FOR I=1 TO N
60 S1=S1+(Y(I)-Y(N))*LOG(X(I)/X(N))
70 S2=S2+LOG(X(I)/X(N))^2
80 NEXT I
90 K=S1/S2
100 PRINT "   fit   y=yN+k*ln(x/xN)   to";N;"data"
110 PRINT : PRINT "   k=";K
120 PRINT : PRINT "        x       given y    fitted y"
130 S3=0 : S4=0 : S5=0
140 FOR I=1 TO N
150 S3=S3+Y(I)
160 YI=Y(N)+K*LOG(X(I)/X(N))
170 S5=S5+(Y(I)-YI)^2
180 PRINT USING"   ####.####";X(I),Y(I),YI
190 NEXT I
200 M=S3/N
210 FOR I =1 TO N
```

```
220 S4=S4+(Y(I)-M)^2 : NEXT I
230 R=SQR(1-S5/S4) : PRINT "   correlation coeff=";R
240 'PRINT : INPUT "time in days";T
250 'T=T*24*60 : YI=Y(N)+K*LOG(T/X(N)) : PRINT "y=";YI
260 'GOTO 240
```

REFERENCES

REFERENCES

1. Aklonis, John J., MacKnight William J.,and Shen, Mitchel (1972), Introduction to Polymer Viscoelasticity.

2. Arridge, R.G.C. (1985), An Introduction to Polymer Mechanics, Taylor & Francis.

3. ASM Metals Handbook, Vol 2 (1990), ASM International, Ohio.

4. Closure Guides (1993), Closure Manufacturers Association.

5. Dally, James W., Riley, William F., McConnell, Kenneth G. (1993), Instrumentation for Engineering Measurements, John Wiley & Sons.

6. Dowling, Norman E. (1993), Mechanical Behavior of Materials, Prentice Hall.

7. Ferry, John D. (1970), Viscoelastic Properties of Polymers, John Willey & Sons.

8. Greenway, Gerald, A Short-Term Study of Cap Torque Decay, Packaging Technology & Engineering, May 1993, p38, 39 and 61.

9. Lai, Ching-Sung and Greenway, Gerald, The Effect of Time on Cap Removal Torque, Packaging Technology & Engineering, June 1999, p34-36.

10. Lockhart, Hugh, Determination of Torque Loss for a 28 mm Metal Closure on Plastic Bottle, School of Packaging, Michigan State University, Unpublished, August 1992.

11. Matsuoka, Shiro (1992), Relaxation Phenomena in Polymers, Oxford University Press.

12. McCarthy, Robert V. (1956), Performance of Plastic Screw Thread Attachment. M.S. Thesis, Franklin and Marshall College, Lancaster, Pennsylvania.

13. Pisuchpen, Supachai (2000), Model for Predicting Application Torque and Removal Torque of a Continuous Thread Closure, M.S. Thesis, School of Packaging, Michigan State University.

14. Rosan, Stephen L. (1993), Fundamental Principles of Polymeric Materials, John Wiley & Sons.

15. Sobotka, Z. (1992), Rheology of Materials and Engineering Structures, Elsevier Science Publishers.

16. Window, A.L. (1989), Strain Gauge Technology, Elsevier Science Publishers.